LOW COMPLEXITY WIDEBAND CDMA RECEIVER DESIGNS FOR NEXT GENERATION CDMA SYSTEMS

by

Bin Dong

A thesis submitted to the

Department of Electrical and Computer Engineering

in conformity with the requirements

for the degree of Master of Science (Engineering)

Queen's University

Kingston, Ontario, Canada

2002

Abstract

The demand for higher data rate and multimedia service in wireless communication systems has recently seen unprecedented growth. To support the multimedia services, wideband direct sequence code division multiple access (WCDMA) is emerging as the predominant wireless technology for future wireless multimedia application. Wider bandwidth allocation results in more resolvable multipath available at the receiver, therefore more multipath diversity gain could be achieved. In principle, an optimal RAKE could combine all the multipath components by maximal ratio combining (MRC). Due to the prohibitive complexity of the optimal RAKE receiver, in this thesis, we propose a sub-optimal low complexity RAKE receiver where code acquisition, RAKE combining and channel estimation are combined together.

In this thesis, a parallel PN code acquisition algorithm based on the concept of code tree-structure within one bit duration is studied. Assuming knowledge of users' spreading sequences, we formulate code acquisition in terms of multiple hypothesis testing for all the possible shifts of all PN codes. The receiver employs truncated sequential decision-making as well as tree structured joint hypothesis testing. To include the code cross-correlation property between different users and paths, the test is

modified to be a delayed "SPRT". The performance of the proposed code acquisition scheme in multipath channel is analytically determined. We quantify the complexity saving in multipath channel by concatenatedly labeling the code tree according to the multipath signals. A close-form of signal combining loss is also declared. To make the numerical calculation practical, a tight lower bound of signal combining loss is also provided to approximate the signal detection performance. Through analysis and simulation, we quantified the complexity saving and signal-combining loss in comparison to a full chip-matched filter implementation. For example, in a system with 10 users, 4 signal paths per user and 5 dB SNR, a computation savings of more than 97% can be achieved at a cost of only a 1.1 dB signal combining loss.

In a practical wideband CDMA communication systems, channel state information(CSI) is not available at the receiver. As an extention of the above delay estimation, we also study channel estimation. Here, we address pilot symbol aided weighted multislot averaging (PSA-WMSA) technique to estimate channel tap weights. The experimental results has shown only a slight loss due to channel estimation error in comparison to receiver with perfect channel knowledge. All the above work is also extended to data block scenario where a block of bits are available for multipath delay profile estimation.

Acknowledgements

First, I would like to express my deepest appreciation and gratitude to Professor Steven Blostein, my thesis advisor, for his guidance, encouragement and enthusiasm throughout the course of my graduate research. For his judgement and trust that made my admission to Queen's University possible and introduced me such an interesting field I have been fortunate in being able to benefit from his experiences.

I would also like to thank my committee members for carefully reviewing my thesis and providing useful suggestions. I would also like to thank all the members of IPCL, especially who have been very helpful to my studies.

Finally, a sincere word of thanks goes to my parents and other family members for their support and encouragement throughout my life.

This work was supported by Canada Institute of Telecommunication and Research and School of Graduate Studies and Research at Queen's University.

Contents

List of Tables

List of Figures

Symbols and Abbreviations

a_G	decision threshold for deciding if a signal is present or not
A	upper threshold in Wald's approximation
A_n	upper threshold at stage n in multistage hypothesis test
A_{N_t}	the threshold at truncation stage N_t
ADC	analog to digital converter
AWGN	additive white Guassian noise
ASN	average sample size
$b_i(n)$	the data bit transmitted for user i at time n
B	lower threshold in Wald's approximation
BER	bit error rate
B_n	lower threshold at stage n in multistage hypothesis test
BPSK	binary phase shift keying
CDMA	code division multiple access
C	code book C,containing all the possible shifts of PN code of all the user

C_1	code book which contains all the shifts of PN code of all the user contained in the multi-path signal
c_1	mixing constant of multistage hypothesis test
c_2	mixing constant of multistage hypothesis test
C_C	channelization code for pilot channel
CDF	cumulative distribution function
C_D	channelization code for data channel
C_i	PN code for user i
CSI	channel state information
$C_i(n-\tau_{ij})$	PN code for user i after a circular shift τ_{ij}
CSI	channel state information
df	the array to recorded the detected paths
$d_i(n)$	data symbol transmitted from user i in time n
DA	data aided
DD	dicision directed
DSSS	direct sequence spread spectrum
EGC	equal gain combining
FDD	frequency division duplex
FS	full search
FSS	fixed sample size
G	number of chips per symbol or processing gain
$h_i(n)$	channel impulse response of user i at time n

H_0	hypotheses that denote signal is not present
H_1	hypotheses that denote signal is present
IN_{ij}	interference plus noise for the i^{th} path of user i for uplink
LOS	line of sight
L	number of paths of each user
L_d	multipath delay spread region
IPI	interpath interference
LFSR	linear feedback shift registers
m_1	modified m-sequence to generate the orthogonal Gold code
m_2	modified m-sequence to generate the orthogonal Gold code
M	number of samples in FSS test
MADs	multiplication and additions
MAI	multiple access interference
MC-CDMA	multi-carrier code division multiple access
MF	matched filter
MHT	multistage hypothesis testing
MIP	multipath intensity profile
MRC	maximal ratio combining
n	time index
$n(k)$	the k^{th} white guassian noise sample at chip matched filter output
$N(\theta, \sigma^2)$	normal distribution with mean θ and variance σ^2
NDA	non data-aided

N_t	truncation stage
K	number of paths of each user
N_p	number of pilot symbols in one slot in time multiplexed pilot channel structure
P	total number of path types
P_D	probability of detection
OVSF	orthogonal variable spreading factor
P_M	probability of missed detection
P_F	probability of false alarm
PN	pseudo noise
PSA	pilot symbol aided
QoS	quality of service
$r(n)$	received discrete-time signal
RMS	root mean square
SC	seletion combining
SINR	signal to interference noise ratio
SNR	signal-to-noise-ratio
SPRT	sequential probability ratio test
T_0	code tree of code book C, containing all the possible shifts of PN code of all the user
$\tilde{T}$	hypotheses labeled code tree
θ	signal mean

θ_1	signal mean under H_1
T_c	chip period
TDD	time division duplex
TDL	tapped delay line
TOA	time of arrival
TPC	transmit power control
TSPRT	truncated sequential probability ratio test
w_i	RAKE combining weights at the i^{th} matched filter output
w_{ij}	RAKE combining weights for user i at the j^{th} matched filter output
$WC(d_i(n))$	Walsh code corresponding to the data bit $d_i(n)$
WCDMA	wideband code division multiple access
WLAN	wireless local area networks
WMSA	weighted multi-slot averaging
$\mathbf{Y}$	Gaussian random sequence
Y_i	Gaussian random variable at time index i
Z_{ij}	time domain correlation statistic for the j^{th} path of the i^{th} user
$ZF_{i,j}$	test statistics of the father node input to tree node (i,j)
α	nominal probability of false alarm
β	nominal probability of missed detection
β_{ij}	scalar attenuation experienced by the j^{th} path of the i^{th} user
ω_{ij}	RAKE combining weight of branch j for user i
Σ	summation

$\int$	integral
Φ	the standard (normalized) Gaussian distribution function
Φ^{-1}	the inverse of Φ
$r_i(\theta)$	probability that MHT reaches stage i conditioned on signal strength θ
$\gamma_i(\theta)$	probability that H_1 is accepted at stage i conditioned on signal strength θ
$\xi_i(\theta)$	probability that H_0 is accepted at stage i conditioned on signal strength θ
π	constant
σ^2	variance in Gaussian distribution
σ_t^2	thermal noise variance
$\sigma_{i,j}^2$	both interference and additive thermal noise experience by the j^{th} path of i^{th} user
τ	truncation threshold
τ_{ij}	integer chip time delay in respective to to first arriving component for j^{th} path of i^{th} user

Chapter 1

Introduction

1.1 Motivation

In the wireless world, the demand for advanced wireless communications services is growing at an explosive rate. Voice and low-rate data services that the second-generation mobile systems provide are insufficient in the new millennium where high-speed Internet access and video/high-quality images transmission are taken for granted. The trend is toward global information networks that offer flexible multimedia information services to users on demand, anywhere, anytime. The need to support bandwidth-intensive multimedia services places new and challenging demands on cellular systems and networks. The third-generation (3G) mobile systems (called IMT-2000) are being designed to support wideband services, at data rates as high as 2 Mb/s, with the same quality as fixed networks [9, 10, 45, 61]. It is everyone's wish that wireless could act like a wired connection. To realize future wireless multimedia

communication systems, a new wideband wireless access technology incorporating as many recent technology developments as possible is necessary.

Wideband direct sequence code division multiple access (wideband CDMA) is emerging as the predominant wireless technology for the 3G and beyond systems, and is being developed throughout the world. Wideband CDMA is designed to flexibly offer wideband services, such as wireless Internet services (i.e. peak rate of 384 kb/s to download information from the Web) and video transmission (data rate up to 2Mb/s). Wideband is essentially about data rate. The physical limitations and impairments to radio channels (bandwidth constraints, multipath fading, noise, and interference) present fundamental technical challenges to the goal of reliable high data rate communications [17, 26, 27, 45, 63, 65].

To combat the multipath fading, RAKE receive is used to coherently combine multipath components in wideband CDMA systems. Theoretically, we could use an adaptive RAKE receiver with unlimited resources and instant adaptability so that it could combine all the resolvable multipath signals. Unfortunately, it is impractical due to prohibitive complexity. Here, designing a low complexity wideband CDMA receiver is a completely open problem.

1.2 Summary of Contributions

The contributions of this thesis are:

- Propose a novel parallel code acquisition scheme with tree search, where multistage sequential hypothesis testing is employed to prune the code tree.

- Delay the decision of multistage hypothesis testing (MHT) so that the effect of cross-correlation of PN codes of different users are mitigated.

- Performance analysis of the proposed code acquisition scheme by truncated sequential analysis in single path case. The performance are quantified by steady-state computational complexity savings and signal combining loss.

- Analysis of complexity savings in multipath channels by labelling code tree with hypotheses and classify the paths according to the different concatenation of the sequence of hypotheses.

- Obtain analytical result of signal combining loss in multipath channels by enumerating the signal power of all the possible multipath detection results weighted by the corresponding probability of detection. The complexity of analysis is greatly reduced by applying De Caen's union bound.

- Study the channel estimation problem for practical wideband CDMA receivers. We estimate the channel tap weights by pilot symbol aided (PSA)-weighted multislot averaging (WMSA) filter in both single pilot and multiple pilot symbols scenarios.

1.3 Thesis Outline

In the following chapters, we propose a new low-complexity receiver architecture for wideband CDMA communications systems, where code acquisition, channel estimation and RAKE combining are incorporated. The goal of this study is to achieve the low complexity of the receiver while introducing a moderate signal detection performance trade-off.

We begin our development in Chapter 2 with a survey of the wideband CDMA system and receiver architecture. A brief introduction of CDMA concepts, its advantages and disadvantages in contrast to the traditional FDMA and TDMA systems is followed by the new technical features of wideband CDMA systems and receiver structure. Following this, we formulate the problem to be solved in this thesis work and the corresponding system environment.

In Chapter 3, we move into the realm of signal detection theory, beginning with a fixed sample size (FSS) test. Follow this, truncated sequential hypothesis test and its advantages over FSS are presented. The chapter concludes with a description of multistage hypothesis test (MHT), a modified form of TSPRT along with its performance analysis.

Code acquisition is an important aspect in any wideband CDMA receiver designs. The emphasis shifts in chapter 4 toward tree structured sequential detection based code acquisition algorithm. First, the definition of code acquisition as well as different approaches according to different classification criteria in literature are presented

followed by some researcher's recent work. The idea of applying MHT to multipath detection is described and tree structured temporal search algorithm is presented. Its performance in single path channels is obtained both by Monte Carlo simulation and numerical calculation.

The performance analysis of code acquisition in multipath channels is the subject of chapter 5. Beginning with the characteristic description of wideband CDMA multipath channels, the discussion progresses through generalization of analysis of steady-state computation complexity savings and signal combining loss in single path channels to that in multipath channels. As an extension, practical RAKE receiver with channel tap weight estimation is also investigated. A general pilot symbol aided-weighted multislot averaging (PSA-WMSA) channel estimation approach is presented to estimate channel tap coefficients both in single pilot symbol and multiple pilot symbols scenario. It concludes with experimental results of the above analysis and Monte Carlo simulation.

Chapter 6 summarizes the conclusions of this thesis and present topics for future research.

Chapter 2

Background of Wideband CDMA Receiver

2.1 Introduction

A spread spectrum CDMA scheme is one in which the transmitted signal is spread over a wide frequency band, much wider than the minimum bandwidth required to transmit the information being sent [65]. It employs a waveform that for all purpose appears random to anyone but the intended receiver of the transmitter wave form. Actually, for ease of both generation and synchronization by the receiver, the waveform is pseudo-random, meaning that it can be generated by mathematically precise rules, but statistically it nearly satisfies the requirement of a truly random sequence.

A CDMA system has several advantages over narrowband TDMA or FDMA systems including universal one-cell frequency reuse, inherent resistant to multipath fading, narrow band interference rejection, soft capacity, soft hand-off, simplification of channel allocation problem, ability to exploit silent periods in speech voice activity, inherent message privacy and low probability of interception [35, 36, 37, 38, 39]. While CDMA promises all the above merits, there are still many technical issues that need to be solved. Synchronization to PN sequences is still a difficult task for a receiver with Doppler and multipath effects further complicating the issue [28]. Fast power control is essential for combating near-far effect on reverse channels. The near-far problem occurs when a transmitter close to the basestation swamps out the weaker signals from more distant mobiles. Hence, the power levels must be adjusted so that the basestation receives the same power from each of the mobile users. Multiple access interference (MAI) is a main factor that limits the capacity and performance of DS-CDMA systems. This type of interference is the result of the random offsets between multipath signals of different users, which makes it impossible to design the code waveforms to be completely orthogonal. In [58, 59, 62], multi-user detection (MUD) techniques are proposed to cancel the multiple access interference, therefore provide significant performance improvement at the expense of high implementation complexity of the receiver. Thus, for real-time implementation in realistic communication systems the low complexity receiver architecture is expected to trade performance for complexity.

In wideband CDMA communications systems, it is often desirable to allow the

subscriber to send simultaneously information to the base station while receiving information from the base station, which is termed duplexing. Duplexing may be done using frequency or time domain techniques [45]. The term downlink or forward link refers to transmission from the base station (fixed network side) to the mobile terminal (user equipment) and the term uplink or reverse link refers to transmission from the mobile terminal to the base station. Frequency division duplexing (FDD) provides two distinct bands of frequencies for every user, i.e., forward band (downlink) and reverse band (uplink). In FDD, any duplex channel is actually composed of two simplex channels, and a device called duplexer is employed inside each subscriber unit and base station to allow simultaneous radio transmission and reception on the duplex channel pair. Regardless of the particular channel being used, the frequency split between the forward and reverse channel is constant throughout the system [27]. Time division duplexing (TDD) uses the same frequency band but alternates the transmission direction in time. If the time split between the forward and reverse time slot is small, then the transmission and reception of data appears simultaneous to the user. Figure 2.1 illustrates the operating principles of the FDD and TDD modes in WCDMA systems. TDD allows communication on a single channel, and simplifies the subscriber equipment by omitting duplexer, and, therefore, reduce the size of the terminals.

There are several factors worth considering when choosing FDD mode or TDD mode. FDD is targeted at radio communication systems that provide individual radio frequency for each user. Because each transceiver simultaneously transmits and

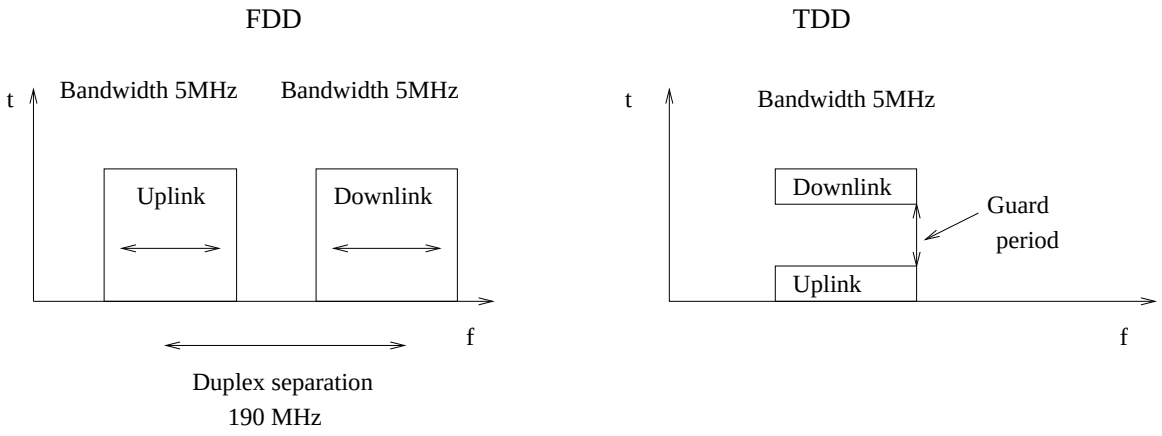

Figure 2.1: Principle of FDD and TDD operation

receives radio signals which vary more than 100 dB [27], the frequency allocation used for the forward and reverse channels must be carefully coordinated with out-of-band users that occupy spectrum between these two paths. Moreover, the frequency separation must be chosen so that the inexpensive RF technology could be utilized. In contrast, TDD eliminates the need for separate forward and reverse frequency bands because bi-directional communication occurs in a single frequency band. However, receiver latency cannot be avoided due to the fact that communication is not full duplex in more strict sense.

2.2 New Technical Features in Wideband CDMA

In wideband CDMA systems, there are several new requirements: high spectral efficiency, high data rate, inter-system handover and multimedia communications with

different transmission quality of multiplexed voice, data, image and video and different delay requirements from delay sensitive real-time traffic to delay flexible packet data.

To meet the new service requirement, more sophisticated signal processing and communications techniques are proposed in [9, 24, 60, 61]. These new techniques include: short scrambling codes concatenated by orthogonal variable spreading factor (OVSF) channelization codes [24] [45], time multiplexed pilot channel structure and I/Q code-multiplexed pilot channel structure [21], fast transmit power control (TPC) [45], pilot symbol aided (PSA)-coherent delay lock loop (CDLL), PSA coherent code acquisition, coherent RAKE combining, fast cell search under asynchronous operation, soft and softer handover, inter-frequency handover, blind bit rate detection, transmit diversity, multiuser detection, turbo coding and smart antennas [2, 63].

2.2.1 Spreading Codes

In CDMA communication systems, the spreading codes is classified into short codes and long codes according to the code length. A short spreading code has a period equal to the symbol duration, while the period of long code is much larger than the symbol duration. In a long code system, the correlation between the users changes from bit to bit and the multiple access interference (MAI) therefore appears to be random in time, causing the performance for different users to be (more or less) identical and determined by the average interference level. Short codes, on the other

hand, have cross-correlations that remain unchanged over time, and an unfortunate user might be trapped in an inferior performance scenario.

In wideband CDMA systems, multiple spreading techniques are used where the data is first spread by a short orthogonal code followed by a spreading by a PN sequences, which is cell-specific but common to all users of that cell in the forward link and user-specific in the reverse link. The short orthogonal codes are called channelization codes and PN codes are called scrambling codes. Hence, each transmission channel code is distinguished by the combination of a channelization code and a scrambling code. For example, in IS-95 systems, a walsh orthogonal sequences of length 64 is used as a channelization code in the forward link and different offsets of a common long m-sequence is used as scrambling code. To support multi-rate and variable rate data transmission, a variable-length orthogonal sequence is used as the channelization code in both forward link and reverse link. The two-layered spreading code allocation provides flexible system deployment and operation [9] [24].

2.2.2 Fast Transmit Power Control (TPC)

In wideband CDMA systems, fast transmit power control (TPC) is used so that all signals transmitted from different mobile terminals are received with almost equal power at the basestation receiver which reduces the multiple access interference (MAI) caused by the large differences in received signal powers resulting from the well-known near/far problem and fast fading. There are two kinds of power control mechanisms,

namely, open-loop and closed-loop power control. In reverse link, for example, if open-loop power control is used, the higher the received signal power by the mobile, the lower its transmitted power is set and vice versa. If closed-loop is used, mobile adjusts the transmitted signal power according to the commands from the base station based on the SINR measurements at the base station. Open-loop power control is only used to provide the coarse initial power setting at the beginning of a connection for the prime reason that the fast fading is essentially uncorrelated between uplink and downlink, due to the large frequency separation between uplink and downlink band of the wideband CDMA FDD mode.

Wideband CDMA systems employ fast closed-loop power control with 1500 Hz in both uplink and downlink, while IS-95 uses fast power control with 800 Hz only in uplink. Downlink power control is essential although no near-far problem occurs due to multipoint-to-point scenario because it is desirable to provide a marginal amount of additional power to mobile stations at the cell edge, as they suffer from increased other cell interference. Also on the downlink a method of enhancing weak signals caused by other error-correcting methods based on interleaving and error correcting codes do not yet work effectively. Therefore, downlink fast power control improves link performance and enhances downlink capacity. It requires new functionalities in the mobile , such as SIR estimation and outer loop power control, that are not needed in IS-95 mobiles.

2.2.3 Pilot Channel Structure

The purpose of applying pilot channel is for coherent RAKE combining, coherent code acquisition, channel tap weight estimation, power control and handoffs. Two types of pilot channels in wideband CDMA systems are common pilot channels and dedicated pilot channels according to whether the pilot symbol is shared by other users or not. According to the structure of pilot and data symbols, it is classified as time-multiplexed pilot channel and parallel pilot channel structure.

In parallel pilot channel structure, the pilot symbols are transmitted with the data symbols at the same time. The parallel transmission could be I/Q multiplexing, code multiplexing and frequency multiplexing. Parallel pilot channel shown in Figure 2.2 provides good tracking of channel status especially in fast fading environment. But the spectral efficiency is low and the pilot channel will cause interference to other users even when no data communications occur.

In time-multiplexed pilot channel structure shown in Figure 2.3, the known N_{pi} pilot symbols are periodically multiplexed into N_D transmitted data symbols. Therefore, it is not suitable for delay sensitive real-time traffic such as voice and video transmission in circuit-switched systems. To allow for high speed data transmission over packet switched wireless networks, time-multiplexed pilot structure is favorable and it is proposed in [22] [52].

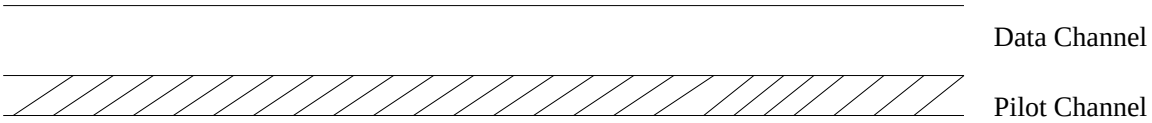

Figure 2.2: Parallel pilot channel structure

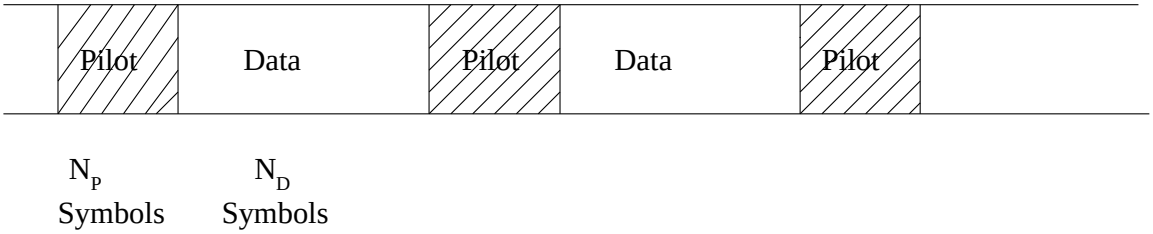

Figure 2.3: Time-multiplexed channel structure

2.3 Wideband CDMA Receiver Architecture

2.3.1 Basics of RAKE Receiver

In wideband CDMA systems, the transmitted radio signal bandwidth is typically larger than the coherent bandwidth of the channel. The higher chip rates in wideband CDMA communication systems give more multipath diversity than that in narrow band CDMA especially in small urban cells. Whereas conventional modulation schemes require an equalizer to undo the inter-symbol interference between adjacent symbols, CDMA spreading codes are designed to provide very low correlation between successive chips. If these multipath components are delayed in time by more than a chip duration, they appears like uncorrelated noise at a CDMA receiver and equalizer is not needed. These uncorrelated paths are called resolvable paths because they could be separated by the correlation of a specific shift of PN code [27].

The basic idea of a RAKE receiver was first proposed by Price and Green [43]. Since there is useful information in the multipath components, RAKE receiver attempts to collect the time-shifted replics of the original signal by providing separate correlation for each resolvable path and the output of each correlator is weighted to provide a better estimate of the transmitted signal than is provided by a single component. Demodulation and bit decision are then based on the weighted output of a bank of correlators.

The RAKE receiver is essentially a diversity receiver designed specially for CDMA where the diversity is provided by the fact that the multipath components are practically uncorrelated from one another when their relative propagation delays exceed a chip period [27]. Assume that L correlators are used in CDMA receiver to capture the L strongest multipath signal components, a weighting network is used to provide a linear combination of the correlator outputs for bit detection. Correlator 1 is synchronized to the strongest multipath l_1. Multipath component l_2 arrives τ_1 later than component l_1. The second correlator is synchronized to l_2. It correlates strongly with l_2 but has low correlation with l_1. Note that if only a single correlator is used in the receiver, once the output of the signal is corrupted by fading, the receiver cannot correct the value. Bit decisions based on only a single correlation may produce a large bit error rate. In a RAKE receiver, if the output from one correlator is corrupted by fading, the others may not be and the corrupted signal may be discounted through the weighting process. Decision based on the combination of the M separate decision statistics offered by the RAKE receiver provides a form of diversity which can

overcome fading and thereby improve CDMA reception. Assume that the outputs of L correlators are denoted as $r_1, r_2, \ldots, r_L$ and they are weighted by weighting coefficients $\omega_1, \omega_2, \ldots, \omega_L$, respectively. The weighting coefficients are decided based on different RAKE combining principles. The overall estimated signal $\tilde{s}$ is given by:

$$\tilde{s} = \sum_{i=1}^{L} r_i * w_i \tag{2.1}$$

To realize the high-speed implementation of RAKE receiver, correlators are replaced by code matched filters as explained in Section 4.1. Therefore, we address code matched filter implementaion later on.

2.3.2 RAKE Combining Techniques

In the literature, several approaches are proposed to combine the multipath components resolved by a bank of code matched filters. Selection combining is the simplest RAKE combining techniques, where the code matched filter output with the highest instantaneous SNR is used as final decision variable. The RAKE combining weight at the i^{th} code matched filter output is:

$$\omega_i = \begin{cases} 1 & \text{if } |r_i| = max\{|r_1|, |r_2|, \ldots, |r_n|\} \\ 0 & \text{otherwise} \end{cases} \tag{2.2}$$

where r_i is the despreaded signal amplitude at the output of i^{th} code matched filter output.

In order to exploit multipath signal components more efficiently, equal gain combining (EGC) is used. In such cases, the tap weights are all set to unity i.e. $\omega_1 = \omega_2 =$

$\ldots = \omega_L = 1$. Signal from each code matched filter is cophased and summed together to provide equal gain multipath diversity. The summation of the estimated multipath components makes it possible to produce an acceptable signal from a number of unacceptable transmitted signal versions and the performance is superior to selection diversity (SD) but is still poor since weaker multipath components are weighted just as much as the stronger ones.

In above two methods, the RAKE combining weights are independent of channel state information, therefore, channel estimation is not needed. It is easy to implement. As a performance trade-off, they are sub-optimal RAKE combining techniques. The optimal RAKE combining technique is maximal ratio combining (MRC), which achieves the highest SNR at the receiver all the time [27] [44]. In maximal ratio combining, the signals from a bank of code matched filters outputs are weighted according to their individual signal voltage to noise power ratio, cophased by the phase rotator and summed together. Maximal ratio combining produces an output SNR that is equal to the sum of the individual SNRs of each multipath component. Thus, the output SNR is maximized. This is an analytical technique that works only if we assume perfect knowledge of the channel [28], where the signal voltage of each multipath components at the transmitter could be perfectly estimated. It is impossible in practical RAKE receiver. An alternative method is to use the the known pilot symbols to provide an estimate of the momentary channel state. The channel sounding could be obtained by channel estimation filter. The weights are chosen such that $\omega_i = |r_i|$ according to the estimated channel information. In Figure 2.4, an example

is shown to illustrate how the MRC works in RAKE receiver [45].

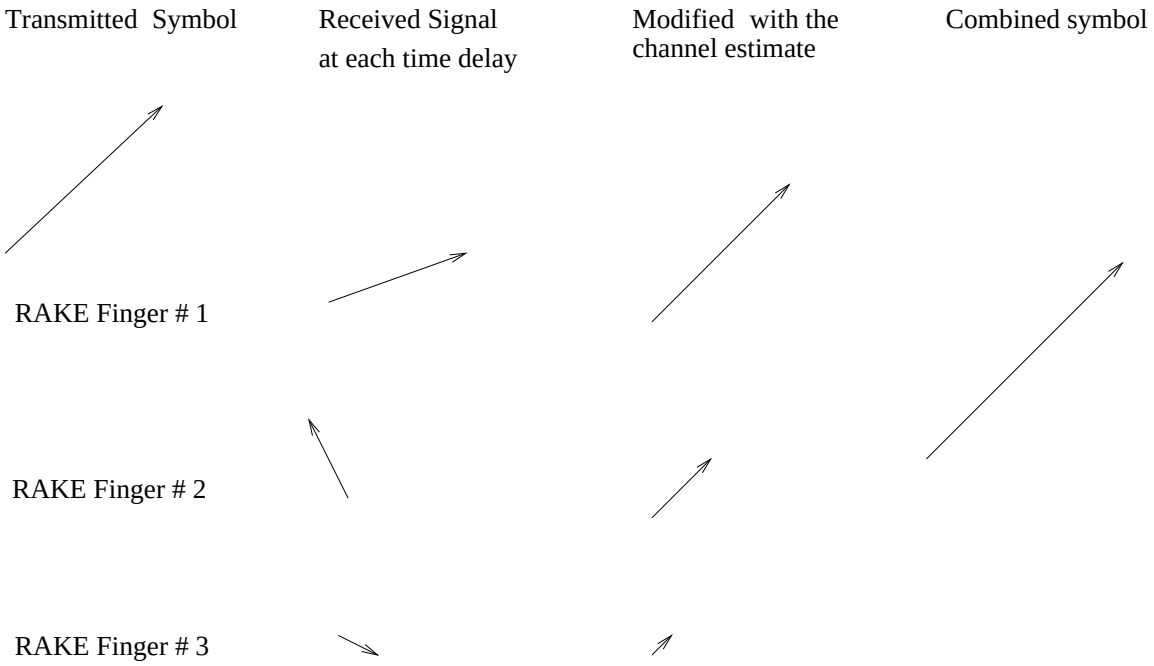

Figure 2.4: The principle of maximal ratio combining within the CDMA RAKE receiver

2.3.3 Channel Estimation

Channel estimation problem in wideband CDMA receivers could be divided to two categories: multipath delay estimation and multipath tap amplitude and phase estimation. In this thesis, the multipath delay estimation is accomplished by sequential PN code acquisition with tree search proposed in Chapter 4 and the channel tap weight estimation, needed for coherent RAKE reception is estimated by filtering the code matched filter outputs using a channel estimation filter after the effect of data symbols has been removed from them. In principle, the channel estimation filter can

be:

- a predictor: if it uses only the past samples to estimate the current channel coefficients
- a "filter": if it uses past and present samples for channel estimation
- a smoother: if it uses past, current and future samples

The removal of data modulation can be accomplished either in data-aided (DA), decision-directed (DD) or non data-aided (NDA) manner. In DA mode, the receiver knows some of the transmitted symbols which is called pilot symbols. Based on the received signal and known pilot symbols, the receiver can estimate the channel profile. The DD channel estimators utilize the decisions of the receiver to remove the effect of data modulation, where there is a decision feedback at the output of quantizer. The NDA channel estimators (also called blind channel estimators) estimates the channel without using data or decisions. Instead, the statistical properties of the transmitted signal are exploited.

Channel tap weights estimation can be based on linear interpolation, low-order Gaussian interpolation [46] [47] and Wiener filtering [48]. However, the Wiener filter requires the knowledge of fading channel statistical properties, i.e., fading covariance matrix, which is difficult to estimate, in practice, if it is not impossible. Furthermore, it should be noted that the reverse link requires fast transmit power control (TPC) [50] [51] discussed in Section 2.2.2. The wiener filter cannot be applied to the

power controlled reverse link because the fading channel's statistical properties are not preserved. It was recently pointed out [52] that the signal-to-noise ratio (SNR) of the channel estimate based on the linear interpolation is not the same over one slot and becomes maximum at the center position of each data slot and munimum at the beginning and the end position of each slot; thus the bit error rate (BER) differs at different positions in a slot. To avoid all of the above, in [21] Andoh proposed a weighted multislot averaging (WMSA) channel estimation filter that simply averages the pilot symbols belonging to more than two consecutive data slots.

2.3.3.1 Time-multiplexed Pilot Channel

In time-multiplexed pilot channel, there are N_p pilot symbols before N_D data symbols. Because fading remains almost constant over a period of N_p pilot symbols, the simple averaging of N_p consecutive pilot symbols improves the signal-to-noise (including MAI) power ratio (SNR). The resultant channel estimate is given by:

$$\hat{w}_l(n) = \frac{1}{N_p} \sum_{m=0}^{N_p-1} r_l(m,n) \tag{2.3}$$

which approximates the instantaneous channel gain at the time position $n * T_{slot} + (Np-1) * T/2$ in l^{th} slot of l^{th} path, where $r_l(m,n)$ is m^{th} received symbol at n^{th} data slot after RAKE combining. By averaging, the SNR of the channel estimate increases N_p times from the received SNR per symbol. In case of slow fading, since the channel gain remains static over a period of several slots, we can coherently add the several consecutive channel estimates by a linear filter with $2K$ taps to extend

the observation interval. However, in general, the channel gain varies slot-by-slot. Therefore, the instantaneous channel estimates need to be weighted and summed. The filter output is expressed as:

$$\tilde{w}_l(n) = \sum_{i=0}^{K-1} \beta_{n,i} \hat{w}_l(n-i) + \sum_{i=0}^{K} \beta_{n,i-1} \hat{w}_l(n+i) \tag{2.4}$$

where $\beta_{n,i}$ is the real-valued weighting factor and $2K$ is the observation interval represented by the number of slots. Using the weighting factors β's pre-stored in memory, the channel estimates $\hat{w}_l(n)$ are easily calculated from (2.3). In [21], the weighting factors optimized at the center of the slot are used for the reception of all the data symbols within the slot, that is $\beta_{n,i}$ is constant regardless of symbol position m.

$$\tilde{w}_l(m,n) = \tilde{w}_l(n), \quad m = N_{pi}, N_{pi}+1, \ldots, N_{pi}+N_D-1 \tag{2.5}$$

By selecting the appropriate weighting factor β_i, accurate channel estimation is possible, particularly in slowing fading environments, because a large number of pilot symbols belong to multiple slots can be used. If the fading is slow, the 2K-tap WMSA channel estimation filter increases the SNR of the channel estimate by a factor of $Np(\sum_{l=0}^{K-1} \beta_i)^2 / \sum_{l=0}^{K-1} {\beta_i}^2$. In the case of fast fading, the channel gain changes even within the slot. Consequently, we change the weight factors symbol-by-symbol within the slot to better track fast fading.

2.3.3.2 Parallel Pilot Channel

For parallel pilot channel, pilot symbols and data symbols are transmitted in the different channels at the same time. We also weight and sum the continuously received pilot symbols and the weight coefficients are updated symbol-by-symbol. The filter output is presented as

$$\tilde{w}_l(m,n) = \frac{1}{2Z} \sum_{h=-Z+1}^{Z} \alpha_h \hat{w}(mT + nT_{slot} + hT) \tag{2.6}$$

where α_h is the real-valued weighting factor and $2Z$ is the observation interval represented by the number of symbols.

In conclusion, the WMSA is a cascade of two filters: the first one is an integrator over a set of pilot symbols. It is followed by a linear filter with adaptive weights. Soft-decision statistics at the output of coherent RAKE combiner is represented at the m^{th} symbol of n^{th} slot associated with the l^{th} propagation path, $l = 0, 1, \ldots, L-1$, as

$$\tilde{d}(n,m) = \sum_{l=0}^{L-1} r_l(m,n) * \tilde{\omega}_l(n) \tag{2.7}$$

2.3.4 Receiver Architecture

In our work, we use a digital baseband block receiver at the base station to detect multipath signals of multiple users in the uplink of wideband CDMA communications systems. A generic description of digital baseband block receiver at the basestation is shown in Figure 2.5. The analog RF down-convertion, chip-matched filtering and

A/D convertion are assumed to be preprocessed so that we are focused on digital receiver design. A bank of RAKE receivers are matched to the PN code waveform of

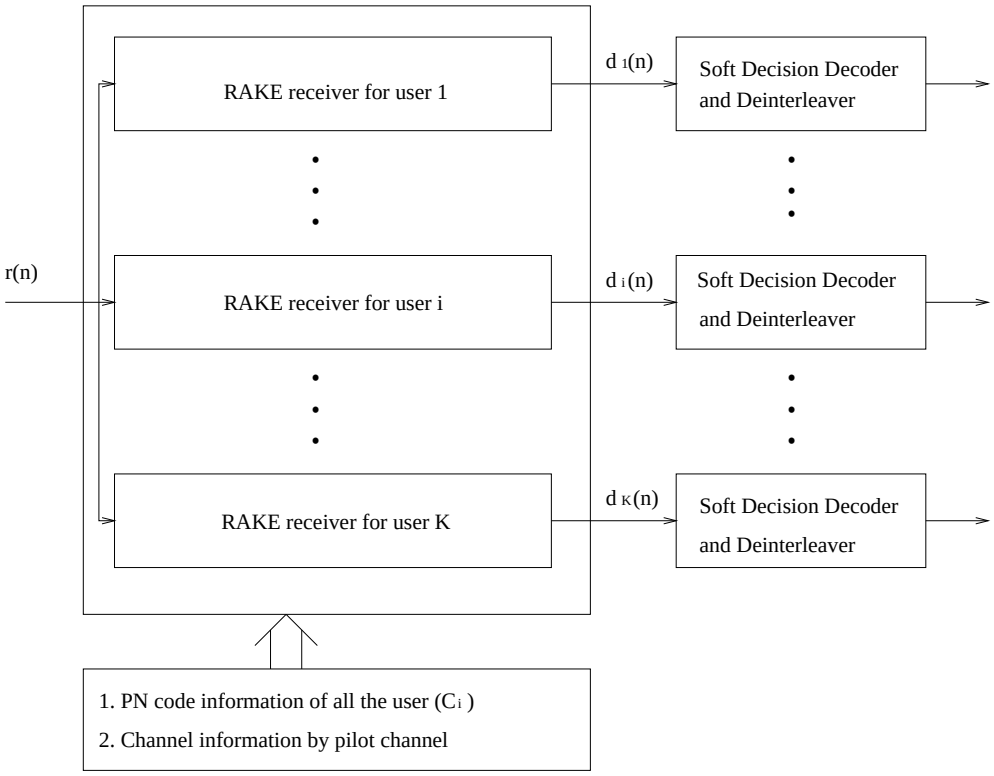

Figure 2.5: Basestation baseband wideband CDMA block receiver. A bank of RAKE receivers are matched to PN code waveforms of multiple users

each user and soft decision statistics at the output of the RAKE receiver is input to the soft-decision based decoder and deinterleaver to give an estimate of transmitted symbols.

In the RAKE receiver block diagram shown in Figure 2.6, the channel delay is estimated during code acquisition as is addressed in Chapter 4. The channel tap weights of the RAKE combiner is estimated by a channel estimation filter addressed in Section 2.3.3. A maximal ratio combining (MRC) type RAKE combiner with

estimated channel tap weights to combine the multipath components is shown in Figure 2.7.

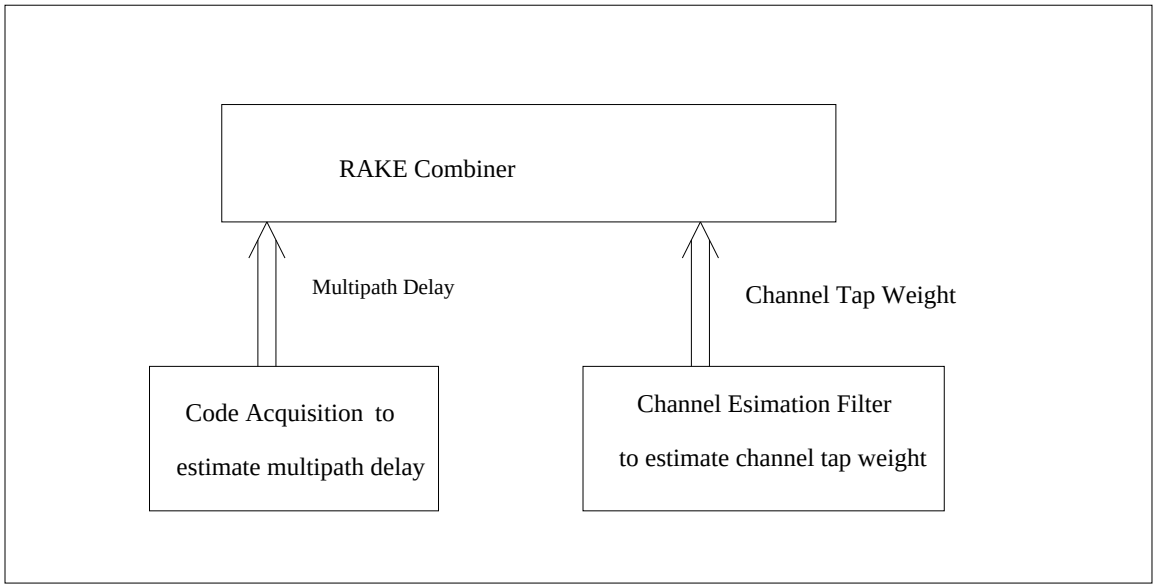

Figure 2.6: RAKE receiver architecture

2.4 Problem Formulation

Radio propagation in the land mobile channel is characterized by multiple reflection, diffraction and attenuation of the signal energy. These are caused by natural obstacles such as building, hills and so on, resulting in so-called multipath propagation. In the frequency-selective multipath channel, the signal energy is "smeared" into a certain multipath delay profile, where multiple versions of the transmitted signal are received with different amplitudes and times of arrival (TOA) [27] [45].

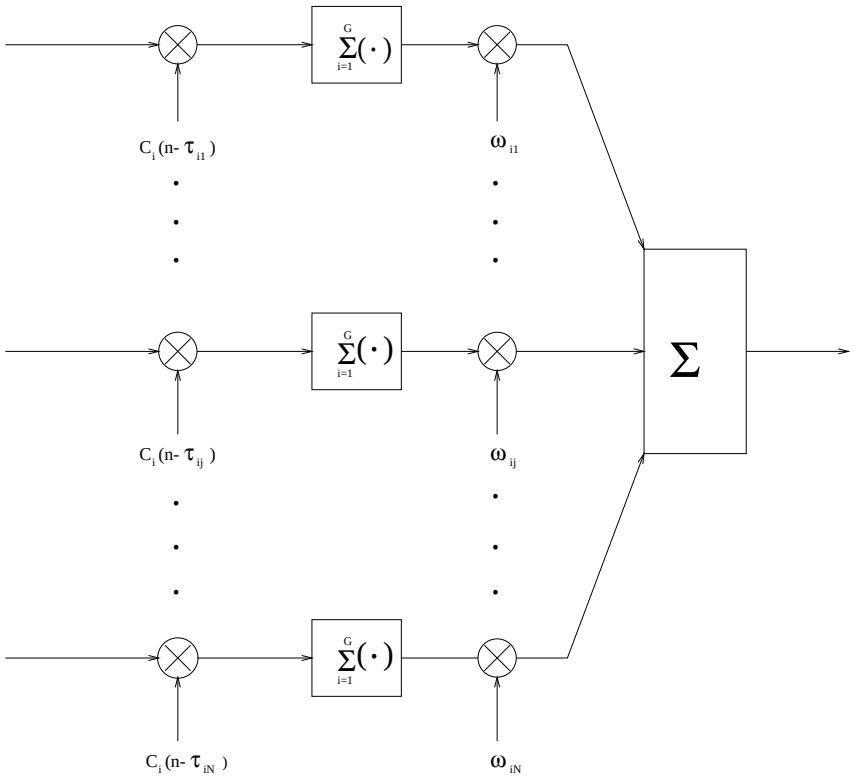

Figure 2.7: RAKE combiner based on maximal ratio combining. This RAKE receiver represents a specific branch of the receiver shown in Figure 2.5

In wideband CDMA systems, a wider bandwidth is allocated to support the multi-media services and higher chip rates are used to multiplex the data streams of different users. An increased chip rate, however, means a reduced chip duration and path delay spreads over a larger number of chip periods. Therefore, more resolvable multipath available at the receiver, where multipath components are spaced at least one chip period apart. For example, in our 7Mcps outdoor measurements from our wideband CDMA test-bed reported in [2], even when the transmitter and receiver are only 16m apart in an urban environment, delay spreads of 20 PN chips were recorded. Other researchers have observed wideband CDMA delay spreads as large as 50 PN chips in

larger cells [34]. Besides, multipath channel profile is dynamically time-varying which requires a RAKE receiver with a variable number of RAKE fingers adapting to the time-varying channel state information (CSI).

Here, we introduce an optimal RAKE receiver termed Full Search RAKE to describe the receiver with unlimited resources (taps or correlators) and instant adaptability, so that it can, in principle, combine all of the resolvable multipath components [41]. Nonetheless, optimal performance is practically difficult to achieve because of the prohibitive complexity and imperfect channel estimation. In the following chapters, we propose an alternative receiver design with the ultimate design goal of low complexity with a slight signal combining loss tradeoff.

2.5 System Model Used in Thesis

In this thesis, we consider a wideband CDMA communication systems, where K information channels are available. Each channel has the same data rate with L resolvable paths that are combined to provide multipath diversity. The receiver is designed for the basestation in the uplink with frequency division duplex (FDD). For simplicity of analysis, the following assumptions are made:

- Binary phase shift keying (BPSK) modulation is used at the transmitter with rectangular chip pulse shape.

- Extended Gold code family with length of 256 PN chips is used as the short scrambling codes.
- Coherent detection is used aided by a separate pilot channel.
- The multiple signal paths of each user are resolvable. An exponentially decaying multipath intensity profile (MIP) is used.
- Synchronous CDMA is achieved where the dominant path of each user are synchronized in terms of the symbol boundary.
- Fractional portion of PN chip offsets of multipath propagation are ignored
- Fast transmit power control of the dominant path is used to compensate the path loss, shadowing and fast fading so that the near-far problem is avoided.
- The number of resolvable multipaths is unknown at the receiver.
- A isolated cell is considered with one base station in the center and K active users, therefore, no inter-cell interference exists.
- The channel noise is modeled as additive white Gaussian noise (AWGN).

Chapter 3

Sequential Detection

3.1 Introduction

Most signal detection problems in wireless communications receiver design can be cast in the framework of M-ary hypothesis testing. There we wish to decide among M possible statistical situations describing the observations. Obviously, for any given detection problems, there are a number of possible decision strategies or rules that could be applied, however, we would like to choose a decision rule that is optimum in some sense. Among the three most common decision rules - Bayes, minimax and Neyman-Pearson, we would choose Neyman-Pearson criteria because the least prior knowledge is required, where a bound is placed on the false-alarm probability and the probability of detection is maximized within this constraint [1, 3]. In the following sections, fixed-sample size (FSS) hypothesis testing, sequential detection and multistage hypothesis testing (MHT) will be covered.

3.2 Fixed Sample Size Test

The basic physical observation model that we wish to consider is an observed waveform that consists of possible signal presence corrupted by additive noise and our objective is to decide whether the signal is present or not by processing a collection of samples with observation window size M taken from the observed waveform [3].

Suppose the signal has constant amplitude and the background noise is zero-mean Gaussian distribution, we want to test a positive shift in the mean. Let $\mathbf{y} \equiv y_1, y_2, \ldots$ be realizations of (i.i.d.) random variables $\mathbf{Y} \equiv Y_1, Y_2, \ldots$. We denote θ as the common mean of each of the Y_i's. Consider testing the hypothesis pair $\theta = 0$ versus $\theta = \theta_1$, where θ_1 is the nominal mean used for test design purposes:

$$\begin{aligned} H_0 &: Y_i \sim f(\mathbf{y} - \theta), \theta = 0 \\ H_1 &: Y_i \sim f(\mathbf{y} - \theta), \theta = \theta_1 > 0 \end{aligned} \tag{3.1}$$

for all i, where $f(y_i)$ is the zero-mean Gaussian probability density function of Y_i, with variance ν^2. The Neyman-Pearson fixed sample size (FSS) test for (3.1) is obtained by testing M samples and the log-likelihood function $L(\mathbf{y})$:

$$L(\mathbf{y}) = \sum_{\mathbf{i=1}}^{\mathbf{M}} \mathbf{z_i} \begin{cases} \geq \tau & \Rightarrow \text{choose} H_1 \\ < \tau & \Rightarrow \text{choose} H_0 \end{cases} \tag{3.2}$$

where z_i is the observed realization of the random variable

$$Z_i = \ln \left[\frac{f(y_i - \theta_1)}{f(y_i)} \right] = \theta_1 (Y_i - \theta_1/2)/\nu^2. \tag{3.3}$$

The first moment of the Z_i given θ is

$$\mu_\theta \equiv E(Z_i \mid \theta) = \theta_1(\theta - \theta_1/2)/\nu^2, \tag{3.4}$$

the second moment is

$$m_\theta \equiv E({Z_i}^2 \mid \theta) = \left(\frac{\theta_1}{\nu}\right)^2 + \left(\frac{\theta_1}{\nu}\right)^4 \left(\frac{\theta}{\theta_1} - \frac{1}{2}\right)^2, \tag{3.5}$$

and the conditional variance,

$${\sigma_\theta}^2 = m_\theta - {\mu_\theta}^2 = \left(\frac{\theta_1}{\nu}\right)^2 \equiv \sigma^2. \tag{3.6}$$

To reduce subscripts we define $\mu_1 \equiv \mu_{\theta 1}$. The sample size M and the threshold τ are prechosen so that the test has error probabilities $P(\text{choosing } H_1|H_0 \text{ true})$ and $P(\text{choosing } H_0|H_1 \text{ true})$ of α and $1-\beta$, respectively. For fixed sample-size tests, the error probabilities α and $1-\beta$ determine the threshold, τ,

$$\tau = M^{1/2}\left[\mu_1\Phi^{-1}(\alpha) + \mu_0\Phi^{-1}(1-\beta)\right](\sigma/(\mu_0 - \mu_1)) \tag{3.7}$$

and number of test samples,

$$M = \left[\Phi^{-1}(\alpha) + \Phi^{-1}(1-\beta)\right]^2 (\sigma/(\mu_1 - \mu_0))^2 \tag{3.8}$$

where Φ represents the standard (normalized) Gaussian distribution function. The inverse of Φ is denoted by Φ^{-1} [3].

3.3 Sequential Detection

An alternative approach to the above FSS test is to fix the desired performance and allow the number of samples to vary in order to achieve this performance. Namely,

for some realizations of the observation sequence we may be able to make a decision after only a few samples, whereas for some other realizations we may wish to continue sampling to make a better decision. A detection scheme that uses a random number of samples depending on the observation sequence is generally known as sequential detection. Wald's [54] sequential probability ratio test (SPRT) is obtained by testing, at the nth sample,

$$\sum_{i=1}^{n} z_i \begin{cases} < B & \Rightarrow H_0 \\ > A & \Rightarrow H_1 \\ \in (B, A) & \Rightarrow \text{ take another sample,} \end{cases}$$

where the boundaries A and B are chosen so that the error probabilities are α and $1-\beta$. The sample size $M = \min\{n : \sum_{i=1}^{n} z_i \notin (B, A)\}$ is now a random variable, and average sample number(ASN) depends on the actual distribution of Z_i, $i = 1, 2 \ldots$, which depends on the actual value of θ [53].

The main benefits of using the sequential probability ratio test (SPRT) lie in the following three facts:

1. Sequential detection achieves same probability of false alarm and detection as a fixed length test

2. The average test length for sequential detection is smaller than for a fixed length test

3. The reduced average test length can be exploited to reduce computation complexity

An obvious disadvantage of the SPRT is that occasional long tests may result if the observed data are ambiguous [1] [3]. As the Wald-Wolfowitz theorem implies the average test length of SPRT is much shorter than FSS [54]. However, these occasional long runs may not be practical for many applications. A practical compromise is a truncated SPRT where a finite-stage truncation exists. As a tradeoff, the optimality property in terms of minimizing ASN is lost by such a truncation. Nevertheless, the increase in ASN is usually slight [6]. In the truncation stage, $n = M^\star$, test

$$\sum_{i=1}^{M^\star} z_i \begin{cases} < t^\star & \Rightarrow \ H_0 \\ \geq t^\star & \Rightarrow \ H_1 \end{cases}$$

3.4 Multistage Hypothesis Test

In the previous section, the truncated SPRT was expressed in terms of the log likelihood function, which is impractical for realistic system design. In terms of the received samples, the truncated SPRT can be rewritten as:

$$\sum_{i=1}^{n} y_i \begin{cases} < B_n & \text{choose } H_0 \text{ and terminate} \\ > A_n & \text{choose } H_1 \text{ and terminate} \\ \text{else} & \text{continue to stage n+1} \end{cases}$$

in stage n, $1 \leq n < N_t$. At the N_tth stage, we test

$$\sum_{i=1}^{N_t} y_i \begin{cases} \geq A_{N_t} & \Rightarrow \text{choose} H_1 \\ \text{else} & \Rightarrow \text{choose} H_0 \end{cases} \tag{3.9}$$

where the A_n and B_n are thresholds at stage n. In the following, we give the transformation step by step.

$$\begin{aligned}
\sum_{i=1}^{n} z_i &= \sum_{i=1}^{n} \frac{\theta_1(y_i - \theta_1/2)}{\sigma^2} \quad \text{vs} \quad A \\
&\equiv \sum_{i=1}^{n} \frac{\theta_1 * y_i}{\sigma^2} \quad \text{vs} \quad A + \sum_{i=1}^{n} \frac{{\theta_1}^2}{2\sigma^2} \\
&\equiv \sum_{i=1}^{n} y_i \quad \text{vs} \quad \frac{A\sigma^2}{\theta_1} + \frac{n\theta_1}{2}
\end{aligned} \tag{3.10}$$

Here we redefine the upper threshold at stage n as:

$$A_n \equiv \frac{A\sigma^2}{\theta_1} + \frac{n\theta_1}{2} \tag{3.11}$$

Similarly, the lower threshold at stage n can be expressed as:

$$B_n \equiv \frac{B\sigma^2}{\theta_1} + \frac{n\theta_1}{2} \tag{3.12}$$

where $1 \leq n < N_t$ and the truncation threshold at stage N_t can be expressed as:

$$A_{N_t} = \frac{\tau\sigma^2}{\theta_1} + N_t\frac{\theta_1}{2} \tag{3.13}$$

From (3.11),(3.12) and (3.13), the $2N_t - 1$ parameters for an N_t-stage test are reduced to four parameters: A, B , truncation point τ and truncation stage N_t. The truncated SPRT can be viewed as a mixture of the SPRT and FSS tests. If c_0 and c_1 are mixing constants each on [0,1], using Wald's inequalities [54], we set

$$A = \ln\left[\frac{1-(1-c_1)P_M}{(1-c_0)P_F}\right] \tag{3.14}$$

$$B = \ln\left[\frac{(1-c_1)P_M}{1-(1-c_0)P_F}\right] \tag{3.15}$$

$$N_t = \left[\Phi^{-1}(c_0P_F) + \Phi^{-1}(c_1P_M)\right]^2\left(\frac{\sigma}{\theta_1}\right)^2 \tag{3.16}$$

and

$$\tau = \sqrt{N_t}[\theta_1 \Phi^{-1}(c_0 P_F)] \left(\frac{\sigma}{-\theta_1}\right) \tag{3.17}$$

The design may be optimized by varying c_0 and c_1: values of c_0 and c_1 near 0 yield a test similar to the SPRT. Alternatively, values of c_0 and c_1 near 1 result in similarity to an FSS test [3]. In the test design, σ, μ_0, and μ_1 are known, P_F and P_M are nominally chosen design values of the error probabilities. Once c_0 and c_1 are chosen, test is completely specified by $\hat{A}$, $\hat{B}$, N_t and τ. The design guarantees that for independent and identically distributed samples, the actual probability of false alarm and missed detection will be lower than nominal values [3, 6].

3.5 Performance Analysis

In the following, we derive exact expressions for probability that MHT reaches a certain stage and the probability of accepting H_0 and H_1 given θ. For the Gaussian case, let

$$f(x) = \frac{1}{\sqrt{2\pi}\sigma} \exp[-\frac{1}{2}(\frac{x-\theta}{\sigma})^2] \tag{3.18}$$

and $F(x) = \int_{-\infty}^{x} f(t)dt$. For $1 \leq i \leq N_t$, define

$$r_i(\theta) \equiv \Pr(\text{MHT reaches ith stage} \mid X_i \sim f(x)), \tag{3.19}$$

$$\begin{aligned} \gamma_i(\theta) \equiv \Pr(&\text{accept } H_1 \text{ at ith stage} \mid X_i \sim f(x) \\ &\text{and test reaches ith stage}). \end{aligned} \tag{3.20}$$

$$\xi_i(\theta) \equiv \Pr(\text{choose } H_0 \text{ at ith stage} \mid X_i \sim f(x)$$

and test reaches ith stage). (3.21)

Since the probability density function(pdf) of the decision variable is a truncated Gaussian distribution, it can only be calculated by recursion [5]. The initial state for recursion is:

$$\begin{aligned} f_1 &= f \\ r_1(\theta) &= 1 \\ r_2(\theta) &= \int_{B_1}^{A_1} f(x)dx \\ \gamma_1(\theta) &= F(-A_1) \\ \xi_1(\theta) &= 1 - F(B_1) \end{aligned}$$

Then, for $i = 1, 2, 3, \ldots$ and $B_{i+1} < w < A_{i+1}$, the recursive convolution is performed:

$$f_{i+1}(w) = \int_{B_i}^{A_i} \int_{B_{i-1}}^{A_{i-1}} \cdots \int_{B_1}^{A_1} f(x_1) * f(x_2) * \cdots * f(x_i) \, dx_1 \cdots dx_{i-1} dx_i \quad (3.22)$$

where $*$ denotes the convolution operation.

After each iteration, the probability of the test continuing after stage $i+1$, i.e., reaching stage $i+2$, is given by the total area under f_{i+1}:

$$r_{i+2}(\theta) = \int_{B_{i+1}}^{A_{i+1}} f_{i+1}(x)dx \quad (3.23)$$

Given that the test reaches stage $i+1$, the probability of accepting hypothesis H_1 can be calculated as:

$$\Pr(\text{ MHT accept } H_1 \mid \text{MHT reaches stage } i+1)$$

$$= \quad 1 - \Pr(\text{ MHT reject } H_1 \mid \text{MHT reaches stage } i+1)$$

$$= \qquad 1 - \frac{\Pr(\text{MHT reject } H_1 \mid \text{ MHT reaches stage } i+1)}{\Pr(\text{ MHT reaches stage } i+1)}$$

Therefore,

$$\gamma_{i+1}(\theta) = 1 - \frac{\int_{B_i}^{A_i} F(A_{i+1} - x) f_i(x) dx}{r_{i+1}(\theta)} \tag{3.24}$$

where $F(A_{i+1} - x)$ is calculated by evaluating the following equation at $y = A_{i+1}$

$$F(y - x) = \int_{-\infty}^{y} f(\omega - x) d\omega \tag{3.25}$$

Similarly, given that the test reaches stage $i + 1$, the probability of accepting hypothesis H_0 can be calculated by evaluating (3.25) at $y = B_{i+1}$ and normalizing, which yields

$$\xi_{i+1}(\theta) = \frac{\int_{B_i}^{A_i} F(B_{i+1} - x) f_i(x) dx}{r_{i+1}(\theta)} \tag{3.26}$$

Since the test must terminate at exactly one of the N_t stages, the power function consists of N_t mutually exclusive events. Thus the probabilities of detection can be summed yielding

$$\Pr(\text{accept } \ H_1 \text{ at any stage} \mid X_i \sim f(x)) = \sum_{i=1}^{N_t} \gamma_i(\theta) r_i(\theta). \tag{3.27}$$

and the probability of missing can be summed yielding

$$\Pr(\text{accept } \ H_0 \text{ at any stage} \mid X_i \sim f(x)) = \sum_{i=1}^{N_t} \xi_i(\theta) r_i(\theta). \tag{3.28}$$

Chapter 4

Code Acquisition of Uplink CDMA Signals Using Sequential Detection

4.1 Introduction

In DS-CDMA systems, code synchronization is important because reception of CDMA signals is possible only after the receiver is able to synchronize the local PN code with the PN code in the transmission intended for it [40]. Besides, other channel parameters can be estimated given a reliable delay estimate. Code synchronization is usually done in two steps, code acquisition and tracking. Code acquisition is the process by which the receiver attempts to align its local Pseudo-noise (PN) code's phase to the incoming signal within half of a chip duration. Since the autocorrelation peak is much greater than the sidelobes, a correlation between the local PN code and the received signal yields an estimate of whether the sequences are aligned.

While many types of PN code acquisition architecture exist, the most commonly used architecture are the active synchronous correlator and passive matched filter implementation [19] [20]. For synchronous correlator implementation, each new offset value must be computed with integration over the symbol period T_s, which results in longer acquisition time. For passive matched filter implementation, a code filter matched to the PN code is used. Since the despread signal components appear sequentially at the matched-filter output, the passive matched filter can compute the code correlations for different offsets much faster than the serial correlator even though output values are mathematically equivalent [19] [23]. The disadvantage of matched filters is high complexity.

According to the types of searching strategies, PN code acquisition methods could be divided into serial, parallel and hybrid. In serial search, each possible code phase is tested once at a time. In spite of the low complexity of serial search schemes, the acquisition time is very long. In parallel schemes, all the possible code phases are tested simultaneously, where the short acquisition time is achieved at the expense of high complexity. To provide a tradeoff between the low complexity of serial schemes and the high speed of parallel schemes, in [13], a hybrid acquisition scheme is proposed in which all the possible code shifts are divided into groups and each group is tested simultaneously.

4.2 Previous Work

Extensive research on PN code acquisition has been carried out during the past two decades[17] [18] and typically use the traditional additive white Gaussian noise (AWGN) channel model.

In serial search method, Deng [19] proposes a burst mode PN acquisition processor for noncoherent detection. This matched filter-based PN code acquisition processor achieved a mean acquisition time of less than 10 bits over a range of chip-to-noise ratio (CNR) from -7 dB to 8 dB. Chang, Park and Lee [30] propose a two-dwell code acquisition system with a serial search that operates simultaneously with verification in long code CDMA. For the search block, a matched filter is used for fast acquisition. For the verification block, an active correlator is used to reduce the complexity. The performance enhancement of this scheme mainly lies in reducing the false alarm probability by adding the verification stage while maintaining short acquisition time.

In the case of parallel schemes, Rick and Milstein [32] present a parallel PN code acquisition scheme for the reverse link of a cellular CDMA system. The model of a terrestrial mobile communication channel incorporates the effect of multiple access interference, shadowing, power control error, vehicle speed, voice activity and sectorization. The result shows that the system user capacity based on acquisition performance criteria is less than the capacity based on BER criteria for certain ranges of system parameters. The effects of data modulation on the performance of parallel code acquisition scheme are reported in [31].

In [12] a hybrid acquisition scheme in non-coherent DS-CDMA system is investigated. The performance is analyzed in a AWGN channel. The analysis is also extended to systems containing multiple access interference in [13]. The simulation results show that the sequential scheme significantly outperforms the non-sequential scheme.

Tree-search detector has been studied as a low complexity approach in various research areas of wireless communication sytems. In [75], a simple reduced tree-search detection of the breadth-first type is applied to suboptimal joint multiuser detection in bit-synchronous code division multiple access (CDMA) systems over both Gaussian and two-path Rayleigh fading channel by Wei and Rasmussen. Xie and Rushforth combined suboptimum tree-search algorithm with a recursive least-squares estimator of complex signal amplitude for joint Maximum Likelihood (ML) sequence detection and paramter estmation [76]. In [74], tree strcutured signal detection in V-BLAST system is proposed. It is found in [74] [75] [76], that tree-search detector achieves near-optimum performance at a very low complexity. However, tree-search scheme in conjuction with sequential PN code acquisition to reduce prohibitive complexity of parallel PN code acquision have not yet been suggested.

The effective utilization of multipaths becomes more important in next generation CDMA communication systems, where wide bandwidths are allocated to support high data rate and multimedia service, resulting in an increase in the number of resolvable paths. The result in [32] shows that the acquisition performance for frequency selective fading channels is better than that for flat fading due to the diversity gain

achieved with more than one resolvable paths. However, PN code acquisition in multipath channels is least studied because of the difficulty of performance analysis. In [73], a joint triple-cell code acquisition in frequency-selective Rayleigh fading channel is proposed. Unfortunately, the number of multipaths that can be acquired is fixed, which may be a problem in realistic time-varying wideband CDMA multipath channels, where the number of multipath components are variable.

In the following chapters, we propose a novel matched-filter-type parallel code acquisition scheme. A tree-structured parallel adaptive network of RAKE fingers are created for all possible delay shifts and users. Employing sequential detection scheme in Section 3.4, only viable RAKE fingers are used to generate the output decision statistics. Our acquisition scheme is designed for wideband CDMA communication systems described in Section 2.5.

4.3 Uplink Signal and Channel Model

In this section, we consider the multipath uplink channel, including fading and shadowing effects. It is also assumed that perfect power control is used for the generic CDMA environment, such that the average power for the dominant path is constant. For simplicity, binary phase shifted keying (BPSK) modulation and square pulse shape are assumed. The following wideband CDMA system uses baseband discrete-time signal and system model.

4.3.1 Wideband CDMA Transmitter

The transmitter uses direct sequence spread spectrum (DSSS) modulation. The information data symbols are spread by user-specified short spreading PN code with symbol length and binary phase shifted keying (BPSK) modulated. Finally, it is transmitted on a radio carrier. The transmitted digtial spread-spectrum signal from user i in one symbol interval can be represented by:

$$s_i(n) = c_i(n)d_i \tag{4.1}$$

where the chip time index $n = 1, \ldots, G$ and G is the number of chips per symbol or processing gain. $c_i(n)$ is the chip value of PN code of user i at time index n, $c_i(n) \in \{-1, 1\}$. d_i is the transmitted symbol value at this symbol interval. The transmitted signal will be dispersive by the channel and it is subject to interference and additive white Gaussian noise (AWGN).

4.3.2 The Multipath Channel Model

Frequency selective Rayleigh fading is used to model the reverse channel from the mobile terminal to the basestation. The multipath radio channel for i^{th} mobile may then be described as a wide band tapped delay line (WTDL) model with statistically independent time-variant tap weight $\beta_{i,j}$:

$$h_i(n) = \sum_{j=1}^{L} \beta_{ij}\delta(n - \tau_{ij}) \tag{4.2}$$

where L is the total number of multipaths, which is dynamic because of the time-varying characteristic of wideband wireless channels. The index j represents one of L multipaths experienced by the i^{th} user and $\tau_{i,j}$ is the relative integer chip time delay with respect to the first arriving component for j^{th} path of i^{th} user.

4.3.3 Wideband CDMA Receiver

In multipoint-to-point uplink CDMA channels, the received wideband CDMA signal is the superposition of K channel outputs from K active users, corrupted by channel noise,

$$r(n) = \sum_{i=1}^{K} s_i(n) * h_i(n) + z(n) \tag{4.3}$$

where symbol * indicates convolution and z(n) is addtive white Gaussian noise (AWGN) with a double sided power spectral density of $\frac{N_0}{2}$. K is the total number of users. Therefore, after RF analog downconversion, chip pulse shaping filtering and chip-rate sampling, the equivalent received baseband discrete-time signal in one symbol period is obtained by inserting (4.2) into (4.3), yielding:

$$r(n) = \sum_{i=1}^{K} \sum_{j=1}^{L} \beta_{i,j} d_i c_i(n - \tau_{ij}) + z(n) \tag{4.4}$$

where $c_i(n-\tau_{ij})$ is the PN code of user i after a τ_{ij} circular shift. Since code acquisition is aided by pilot symbols, which are not data modulated, $d_i = 1$.

4.4 Code Acquisition of Multipath Signals

Code acquisition is the process of determining the time delay of each path of each user. Strictly speaking, determining the exact sampling time is an estimation problem. However, to reduce the problem to one of finite dimensionality, the delay is assumed to be a multiple of T_c. In other words, chip-synchronous environment is assumed.

4.4.1 Conventional Matched Filter Approach

In a conventional matched filter CDMA receiver, the received signal is filtered by a predetermined code matched filter, where each possible delay of the PN sequence of the desired user is encoded as a separate set of coefficients. The hardware diagram corresponding to one of the matched filers is shown in Figure 4.1 and the corresponding decision circuit is given in Figure 4.2. To simplify notation, we define $C_i(n - \tau_{ij})$ as $C_{ij}(n)$ in the following figures.

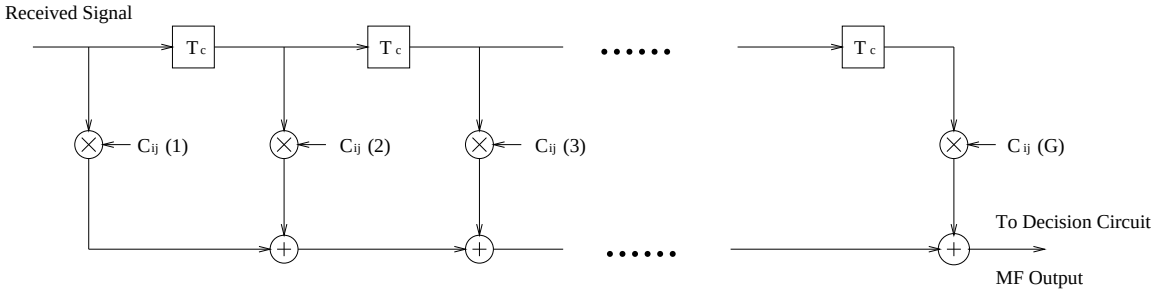

Figure 4.1: Shown is one of the $K * L_d$ matched filters, K is the number of users and L_d is the multipath spread

The received signal is matched filtered by the PN sequence for the i^{th} user with

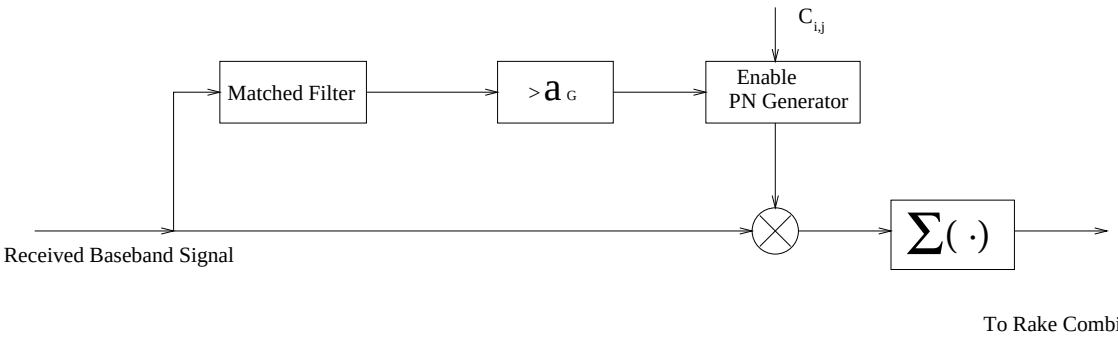

Figure 4.2: Decision circuit for one of the parallel method filters

integer time delay τ_{ij} of the j^{th} path and is denoted by $Z_{i,j}$,

$$\begin{aligned} Z_{i,j} &= \sum_{n=1}^{G} r(n)c_i(n-\tau_{ij}) \\ &= \beta_{ij}G + \sum_{n=1}^{G}\sum_{k=1}^{N}\sum_{\substack{l=1 \\ k,l\neq i,j}}^{L} \left(\beta_{kl}d_k c_k(n-\tau_{kl}) + z(n)\right) c_i(n-\tau_{ij}) \\ &= \beta_{ij}G + IN_{ij} \end{aligned} \tag{4.5}$$

where (4.4) is used and where,

$$IN_{ij} = \sum_{n=1}^{G}\sum_{k=1}^{N}\sum_{\substack{l=1 \\ k,l\neq i,j}}^{L} \left(\beta_{kl}d_k c_k(n-\tau_{kl}) + z(n)\right) c_i(n-\tau_{ij}) \tag{4.6}$$

The signal from the i^{th} mobile with shift τ_j will have a processing gain of G chips per bit, and interference from other users can be modeled as additive white Gaussian interference [26]. The correlation statistic $Z_{i,j}$ can be used to test for the presence of the signal delayed by jT_c seconds from the i^{th} mobile. Define H_{ij} as the hypotheses that there exists a strong path at the j^{th} delay for the i^{th} mobile. The test statistic $Z_{i,j}$ can belong to one of two mutually exclusive subsets, Γ_0 and Γ_1 of the observation space. Let

$$Z_{i,j} \in \Gamma_0 \qquad \text{if no signal is present} \tag{4.7}$$

$$Z_{i,j} \in \Gamma_1 \qquad \text{if } H_{i,j} \text{ is true} \tag{4.8}$$

Modeling the effects from interfering users using a Gaussian approximation [27], we can test for the presence of a signal using $Z_{i,j}$ using a fixed sample size test. The following is the decision rule:

$$Z_{i,j} \begin{cases} < a_G & \text{no signal present} \\ \\ \geq a_G & \text{signal present} \end{cases} \tag{4.9}$$

where the threshold a_G will depend on the design criterion and the probability distribution of the interference and noise.

If the hypotheses H_{ij} is true, then the correlation statistic $Z_{i,j}$ is directly related to the signal strength from the j^{th} path of the i^{th} mobile. Otherwise, we assume that there is zero signal strength arriving from the j^{th} multipath. In effect, a cut-off is chosen such that only a multipath component with the correlation statistic above threshold a_G is to be included in the RAKE receiver.

4.4.2 Truncated Sequential Detection of Multipath Signals

A search for a large number of hypotheses where the vast majority contain no signal consumes significant resources if a full search were employed. By quickly rejecting paths that are deemed to contain noise-only components and detecting signal paths deemed to contain energy, sequential detector is shown to greatly decrease the nubmer of calculations needed by the RAKE receiver as compared to a "brute-force" full search [7]. In this section we will apply sequential detection to code acquisition using

additive noise to model multiuser interference.

Instead of deciding after G samples whether $Z_{i,j}$ contains a signal or not, a sequential test with a maximum number of stages, N_t, can be used. Define the individual multiplicative term in the correlation metric at stage n of the test for signal presence in $Z_{i,j}$ as $\chi_{i,j}(n)$:

$$\chi_{i,j}(n) = r(n)c_i(n - \tau_{i,j}) \tag{4.10}$$

where $r(n)$ is the received signal. Using a Gaussian approximation,

$$\chi_{i,j}(k) \sim \begin{cases} \mathcal{N}(0, \sigma_{i,j}^2) & \text{if a signal path does not exist} \\ \mathcal{N}(\beta_{ij}, \sigma_{i,j}^2) & \text{if a signal path exists} \end{cases} \tag{4.11}$$

where $\sigma_{i,j}^2$ contains both interference and additive thermal noise experienced by the j^{th} path of the i^{th} user. Since the thermal noise and interference are uncorrelated, we have that

$$\sigma_{i,j}^2 = Var\{IN_{i,j}\} + \sigma_t^2 \tag{4.12}$$

where σ_t^2 is the additive thermal noise variance.

The decision at stage n $(1 \leq n < N_t)$ of the test can be written as:

$$\sum_{k=1}^{n} \chi_{i,j}(k) \begin{cases} > A_n & \Rightarrow \text{choose } H_1 \text{ and terminate test} \\ \leq B_n & \Rightarrow \text{choose } H_0 \text{ and terminate test} \\ \text{otherwise} & \Rightarrow \text{continue to stage n+1} \end{cases}$$

At the stage N_t, the test is terminated, i.e. a final decision is reached,

$$\sum_{k=1}^{N_t} \chi_{i,j}(k) \begin{cases} > A_{N_t} & \Rightarrow \text{choose } H_1 \text{ and terminate test} \\ \leq A_{N_t} & \Rightarrow \text{choose } H_0 \text{ and terminate test} \end{cases}$$

The above threshold parameter to detect multipath signal, namely A_n, B_n A_{N_t} and N_t are designed according to multistage hypothesis testing framework presented in Section 3.4. As a remark, the above sequential detection can allow the implementation of a RAKE receiver with a variable number of RAKE fingers, which is very suitable for wideband CDMA system, where the multipath is dynamically time-varying.

4.5 Tree Structured Temporal Search of Multipath Signals

4.5.1 Short Spreading Code Design

Since the interference is the same in every symbol in a short code DS-CDMA system as is explained in Section 2.2.1, it is possible to limit the interference between any two users to a small value by selecting sequence sets with known good correlation properties, thus increase the system capacity. If the number of users are less than the length of the spreading sequence, it is possible to eliminate interference altogether by using orthogonal sequences [39]. In our wideband CDMA systems, the orthogonal Gold code family with length 256 is used as short spreading codes. Orthogonal Gold codes are produced by adding a "zero" at the end of the Gold codes [4]. It is well known that a family of Gold codes is generated from the preferred pairs of m-sequences and there are a total of $G+1$ codes in any family of Gold codes. Here G is the length of the short code or spreading factor [16] [24] [25]. The preferred pairs of m-sequences

could be chosen by Gold-drived algorithm in [25]. We define a family of orthogonal Gold codes as follows.

$$\{m_1, m_2, g_0, g_1, \cdots, g_{N-2}\}$$

where m_1 and m_2 are modified m-sequences and they are the members of orthogonal Gold code family. The modified m-sequence is constructed by adding zero at the end of an m-sequence. Three desirable properties of orthogonal Gold codes are:

1) Even if m_1 and m_2 are modified m-sequences, low autocorrelation properties are preserved [17] [65].

2) With the exception of m_2, the above extended Gold code family forms an orthogonal set.

3) The cross correlations between codes are low.

4.5.2 Code Tree Construction

Instead of testing all possible circular shifts of all users' PN codes independently by a bank of code matched filters, we propose to test them jointly and utilize common testing statistics. Due to the fact that some shifts of PN codes have initial chips in common, simultaneous hypothesis testing is possible by organizing all the users' PN codes into a code tree. We achieve this by first enumerating all possible shifts of PN codes of all users in a code book, where each codeword denotes a shift of some user's PN code. Then we proceed through the codebook, codeword by codeword. Each codeword is processed chip by chip: each chip value is encoded in a code tree node.

In wideband CDMA systems, there are K users transmitting the data symbols simultaneously in the same channel. We assume that the multipath spreads over L_d chips in time. Let code book C denote a matrix with $K * L_d$ rows. Each row corresponds to a shift of a PN code of a user in the system with length G chips. For the convenience of algorithm description, we identify each node at a particular depth level of the tree search by the following labeling rule:

Tree Node Labeling Rule

Node (i,j) denotes the j^{th} tree node at tree depth level i
Node (i,j)'s left child is labeled as node (i+1,2j-1).
and the right child is labeled as (i+1,2j).
$i = 1, \ldots, G, 1 \leq j \leq 2^i$, where G is the length of the code

The procedure of constructing the code tree works recursively. The chip values of codebook C are labeled row by row according to the labeling rule. For row i, chip j:

If $C[i][j] = -1$,

then generate a left child

If $C[i][j] = 1$,

then generate a right child

The last column of the code book consists of $K * L_d$ leaf nodes of the tree, i.e., no children are generated at the end of each row. The depth of the tree is, therefore, G levels.

To illustrate the tree construction procedure, a simple example is provided. Here, we consider a CDMA system with 2 users and code spreading factor G is equal to 4.

Let the PN code of user 1 be : $\{1, -1, -1, 1\}$

The possible shifts of the PN code of user 1 are:

$$\begin{array}{l} \{\quad 1,\ -1,\ -1,\quad 1\ \} \\ \{\ -1,\ -1,\quad 1,\quad 1\ \} \\ \{\ -1,\quad 1,\quad 1,\ -1\ \} \\ \{\quad 1,\quad 1,\ -1,\ -1\ \} \end{array} \tag{4.13}$$

Let the PN code of user 2 be: $\{1, -1, 1, -1\}$

The possible shifts of PN code of user 2 are:

$$\begin{array}{l} \{\quad 1,\ -1,\ -1,\ -1\ \} \\ \{\ -1,\quad 1,\ -1,\quad 1\ \} \end{array} \tag{4.14}$$

The codebook C is given as:

$$\text{Code book } C \begin{bmatrix} 1 & -1 & -1 & 1 \\ -1 & -1 & 1 & 1 \\ -1 & 1 & 1 & -1 \\ 1 & 1 & -1 & -1 \\ 1 & -1 & 1 & -1 \\ -1 & 1 & -1 & 1 \end{bmatrix} \tag{4.15}$$

Since the number of tree nodes in the initial depth levels of the tree is much less than the number of all possible shifts of PN codes, tree-structuring the PN code search

reduces the number of operations in terms of multiplications and additions (MADs). The code tree diagram of this example is shown in Figure 4.3. In this example, the number of code shifts of all users are 6. The complexity of tree structured FSS test compared to non-tree structured FSS test are listed in Table 4.1 stage by stage in terms of MADs. By comparison, we observe significant complexity reduction even in such a small code tree. Larger complexity reduction occurs when a larger code tree is used as in practical wideband CDMA systems.

stage	1	2	3	4
non-tree structured	6	6	6	6
tree structured	2	4	6	6

Table 4.1: Stage-by-stage complexity comparison in each stage between the tree structured FSS and non-tree structured FSS in terms of MADs. Stage 4 is the truncation stage.

4.5.3 Data Structure and Algorithm Description of Tree Search

In our search procedure, we use multistage hypothesis testing described in Section 4.4.2 to prune the tree. Because multiple hypotheses are tested jointly, some paths that are deemed to contain noise-only components will be eliminated simultaneously

while other paths that are deemed to contain signal energy are detected simultaneously. The lower truncated SPRT thresholds B_i and upper thresholds A_i are also designed using (3.11), (3.12), (3.13) by setting the following parameters:

$$\theta = E\{\beta_{ij}\} \tag{4.16}$$

$$\sigma^2 = \sigma_{i,j}^2 \tag{4.17}$$

where β_{ij} is the signal strength of each multipath and $\sigma_{i,j}^2$ is the interference plus noise given by (4.12). Because we expect to finish code acquisition in one symbol period, the maximum number of stages in the multistage hypothesis test is less than the number of chips per symbol G, therefore, we rewrite:

$$N_t = \min(\tilde{N}_t, G) \tag{4.18}$$

where $\tilde{N}_t$ is calculated by (3.16). The designed thresholds are stored in the receiver firmware. The following information is stored within each tree node:

1. The current test stage i, i.e, the tree depth level of node j.
2. PN code value of tree node j.
3. The test statistic of its father node,$ZF_{i,j}$, where i is tree depth level and j is the tree node identifier.
4. A linked list that contains all paths that intersect this node.

The CDMA receiver code acquisition is a combination of tree search, code correlation and sequential detection. We denote, $Z_{i,j}$ as the truncated SPRT test statistic

of tree node (i,j), $r(i)$ as the i^{th} signal chip sample to be processed and $ZF_{i,j}$ is the input test statistic of the father node of tree node (i,j). The array df with size of $K * L_d$ is used to record the detected paths in the code acquisition procedure. The algorithm is executed as follows:

1. Initialize test statistic value at the tree root node (tree depth level 0) as: $Z_{0,1} = 0$ and input this value to tree nodes (1,1), (1,2), i.e., $ZF_{1,1} = ZF_{1,2} = 0$

2. Recursively execute the test in depth level i by breadth-first tree search. All the tree nodes at tree depth level i are tested. The test statistic value at tree node (i,j) is computed by:

$$Z_{i,j} = C_{i,j} * r(i) + ZF_{i,j} \tag{4.19}$$

   If $Z_{i,j} \leq B_i$, the subtree from this tree node is discarded from further processing.

   If $Z_{i,j} \geq A_i$, record the detected paths intersecting with this tree node.

   If $A_i < Z_{i,j} < B_i$, output $Z_{i,j}$ to its child nodes at stage $i+1$ and proceed to the next tree depth level, i.e., set $i = i + 1$ and repeat.

3. If the final stage is reached, i.e., $i = N_t$, and if all the tree nodes in this stage are tested, then terminate the test.

Continuing with the previous example, we assume that the input signal, sampled at the chip rate is $r(n) = [\ 0.7\ \ -0.4\ 0.6\ \ -0.1\ ]$ and the thresholds for multistage hypothesis testing are listed in Table 4.2. The truncation stage $N_t = 4$ and threshold

at the truncation stage 4, $\hat{\tau} = 1.3$. The possible RAKE fingers intersecting with corresponding tree nodes are listed in Table 4.3.

stage	1	2	3	4
lower threshold	-1.0	-0.5	0	1.3
upper threshold	0.5	1.0	1.5	1.3

Table 4.2: The upper threshold and lower thresholds of the example test where stage 4 is the truncation stage.

The algorithm works as follows: initially, $Z_{0,1} = 0$ and its value is saved in tree node (1,1) and (1,2), i.e, $ZF_{1,1} = ZF_{1,2} = 0$. The test starts from the tree node (1,1), tree node (1,2) in parallel in tree depth level 1. The test statistic with tree node (1,1) is computed as:

$$\begin{aligned} Z_{1,1} &= r(1) * C_{1,1} + Z_{0,1} \\ &= 0.7 * (-1) + 0 \\ &= -0.7 \end{aligned}$$

Since $-1.0 < Z_{1,1} < 0.5$, test will go to its subtree in tree depth level 2 and the statistic value is saved as $ZF_{2,1}$, $ZF_{2,2}$ in tree node (2,1) and (2,2). Test statistic $Z_{1,2}$ of tree node (1,2) is evaluated as:

$$Z_{1,2} = r(1) * C_{1,2} + Z_{1,0} = 0.7$$

Since $Z_{1,2} > 0.5$, all the paths through this node are detected signal paths . The entries in the flag array corresponding to these signal paths are set to 1. ie. $df(4) =$

$df(5) = df(6) = 1$.

As the test goes to tree depth level 2, Node (2,1) in tree depth level 2 is first tested and test statistic $Z_{2,1}$ is computed as:

$$Z_{2,1} = r(2) * C_{2,1} + Z_{1,1} = -0.3$$

Since $-0.5 < Z_{2,1} < 1.0$, test will continue to its subtree in stage 3 and the test statistic $Z_{2,1}$ will be input to its child nodes as $ZF_{3,1}$ and $ZF_{3,2}$. Hypothesis testing in tree node (2,2) is performed in parallel with tree node (2,1) by computing the test statistic as:

$$Z_{2,2} = r(2) * C_{2,2} + Z_{1,1} = -1.1$$

Because $Z_{2,2} < -0.5$, the subtree starting from node (2,2) is discarded. Path 2, path 3 intersecting with this tree node are eliminated. Therefore, we have made a decision that these two signal paths are not present in the input signal. The elements of flag array $df[2], df[3]$ are set to 0.

Test continues to stage 3. Tree node (3,2) is first tested because tree node (3,1) has been pruned. Test statistic value of tree node (3,2) is computed as:

$$Z_{3,2} = r(3) * C_{3,2} + Z_{2,1} = 0.3$$

Since $0 < Z_{3,2} < 1.5$, test will continue to tree depth level 4 and the statistic value is saved in tree nodes in level 4. Because tree node (4,4) is the only child of node (3,2), it is tested first and the test statistic value $Z_{4,4}$ is computed as:

$$Z_{4,4} = r(4) * C_{4,4} + Z_{3,2} = 0.2$$

Since this node is in the truncation stage 4, a hard decision needs to be made as to whether the signal path is present or not. Because $Z_{4,4} < 1.3$, RAKE finger 1 is not detected. Until now, the test within all the nodes in the final test stage has been completed. Multistage hypothesis test termination is declared. As a multipath detection result, the detected RAKE fingers are:

path 4: {1,-1,-1,1}

path 5: {1,-1,1,-1}

path 6: {1,1,-1,-1}

The detected RAKE fingers provide multipath delay information in RAKE combining stage. The final test statistics corresponds to matched filter output amplitude. We could extract a subtree from the hypothesis tree corresponding to all the detected paths and form a matched filter tree, on which the data demodulation is based.

4.6 Test Modification for Code Cross-Correlation

In a large code tree found in practical CDMA systems, a large number of code paths shared the same node in early stages. The first few samples of practical PN codes have high cross-correlation which results in a large number of paths detected and eliminated simultaneously at an early stage. As an undesirable result, it causes higher probability of false alarm or missed detection. As is demonstrated in the above example, all the paths passing through right node in tree depth level 1 are detected while all the paths

going through tree node (2,2) in tree depth level 2 are eliminated. Due to the tree structure, three paths are eliminated and two paths are detected simultaneously at stages 1 and 2 respectively, which will increase the probability of missed detection and false alarm.

This problem is more obvious in a practical wideband CDMA system where the number of users and resolvable paths are large. For illustration, in a system with 10 users and spreading factor 256. There are a total of 2560 paths. In stage 1, 1280 paths share the same tree node, and in stage 2, 640 paths share 4 nodes at tree depth level 2. To alleviate the above problem, we modify the test to be a decision delayed version of a multistage hypothesis test. This is achieved by setting the upper and lower test thresholds to $+\infty$ and $-\infty$, respectively, for the fist a few stages. The number of stages that multistage hypothesis test is delayed is an important parameter in the test design procedure and will have impact on the system performance.

4.7 Performance Analysis

Before we define performance measures, we first present two types of RAKE receivers assuming the knowledge of channel impulse response (CIR). Practical RAKE receivers requiring channel estimation based on the received data samples will be discussed in Section 5.4.1.

In Full-Search-MRC RAKE Receiver, full search is used to acquire multipath components so that all the multipath components will be detected and the probability

of missed detection of each multipath components is zero. Furthermore, the receiver requires the knowledge of channel so that all the multipath components could be optimally combined by maximal ratio combining (MRC).

In MHT-MRC RAKE receiver, tree structured MHT is used to acquire the multipath delays and uses maximal ratio combining (MRC) to combine all the detected multipath components after information despreading. Because of the thresholding in MHT, strong multipath components above the upper threshold will be detected while weak multipath components below the lower threshold will be eliminated. Therefore, some multipath energy will be lost. The performance of the proposed MHT-MRC RAKE receiver is quantified by steady-state computational complexity and signal combining loss.

4.7.1 Steady-state Computational Complexity Savings

Steady-state complexity savings, η_1, is measured in terms of the number of multiplications and additions (MADs) of the Full-Search-MRC RAKE receiver, C_{FS-MRC}, compared to that of the MHT-MRC RAKE receiver, $C_{MHT-MRC}$, and is given by:

$$\eta_1 = 1 - \frac{C_{MHT-MRC}}{C_{FS-MRC}} \tag{4.20}$$

In the acquisition procedure, at most chip delays, there are no multipath components present in the uplink channel. Therefore, the steady-state computational complexity of MHT-MRC RAKE receiver can be lower bounded by the case that

noise-only is present at the receiver input.

$$C_{MHT-MRC} = \sum_{i=1}^{N_t} r_0(i,0)\rho(i) \tag{4.21}$$

where $r_0(i,0)$ is the probability that the truncated sequential test reaches stage i assuming no signal present, and is numerically calculated in (3.19) and $\rho(i)$ is the number of tree nodes at stage i as constructed in Section 4.5.2. The generalization of the complexity saving analysis to multipath channels will be given in Section 5.2.

To calculate the complexity of the Full-Search-MRC RAKE receiver, we need to consider the computation required for testing each shift of each PN code with length G by full code matched filtering, which introduces G multiplications and addisions (MADs) over one bit interval, resulting in $K * L_d$ possible PN code shifts. Therefore, the overall complexity of Full-Search-MRC RAKE receiver can be calculated by:

$$C_{FS-MHT} = K * L_d * G \tag{4.22}$$

where G is the processing gain of the short-code DS-CDMA system and K is the number of active users in the system, L_d is the mutlipath spread.

4.7.2 Signal Combining Loss

The signal combining loss, $\Gamma_{MHT-MRC}$, is measured by the received signal-to-noise ratio after maximal ration combining (MRC) of MHT-MRC RAKE receiver, compared to that of the Full-Search-MRC RAKE receiver.

$$\Gamma_{MHT-MRC} = SNR_{FS-MRC} - SNR_{MHT-MRC} \tag{4.23}$$

where SNR_{FS-MRC} is the signal-to-noise ratio(SNR) at the output of the Full-Search-MRC RAKE receiver after averaging over all the active users in the system. Similarly, $SNR_{MHT-MRC}$ is SNR at the output of the MHT-MRC RAKE receiver after averaging.

$$SNR_{FS-MRC} = \frac{\sum_{i=1}^{K} SNR_{FS-MRC,i}}{K} \tag{4.24}$$

$$SNR_{MHT-MRC} = \frac{\sum_{i=1}^{K} SNR_{MHT-MRC,i}}{K} \tag{4.25}$$

In Full-Search-MRC RAKE receiver, the combined SNR is the summation of SNR of all multipath components and no signal combining loss occurs. This is the optimal RAKE receiver that the other types of receivers described in the remainder of the thesis will be compared against. The signal-to-noise (SNR) after RAKE combining of user i in Full-Search-MRC RAKE receiver is evaluated by

$$SNR_{FS-MRC,i} = \sum_{j=1}^{L} SNR_{ij} \tag{4.26}$$

where SNR_{ij} is the SNR of path j of user i.

In the MHT-MRC RAKE receiver, the combined SNR is the summation of each multipath component weighted by the corresponding probability of detection. The signal combining loss stems from missed detection of multipath components. Assuming channel knowledge, the SNR after RAKE combining of user i is given by

$$SNR_{MHT-MRC,i} = \sum_{j=1}^{L} SNR_{ij} * P_{d_{ij}} \tag{4.27}$$

where $P_{d_{ij}}$ is the probability of detection of path j of user i. The paths have known SNR and $P_{d_{ij}}$ and it is calculated by analysis of truncated sequential detection in

Section 3.5 via (3.27). By inserting (4.27) into (4.25), yielding,

$$SNR_{MHT-MRC} = \frac{\sum_{i=1}^{K} \sum_{j=1}^{L} SNR_{ij} * P_{d_{ij}}}{K} \tag{4.28}$$

In addition to signal combining loss from missed detection, false alarm paths will appear because of the additive white Gaussian noise (AWGN), multiple access interference (MAI) and interpath interference (IPI). This creates additional computation and lowers SNR.

4.8 Software Experiments

4.8.1 Experimental Setup

In our software experiment, we compare the proposed MHT-MRC RAKE receiver with the optimal Full-Search-MRC RAKE receiver in single-path channels by Monte Carlo simulation. The wideband wireless channel model is obtained by field data of wideband CDMA measurement system in 1.9 GHz radio frequency band [2]. The simulated performance is verified by the theoretical analysis through numerical calculations.

In our simulated system, 10 active users are transmitting data or voice in the same wideband CDMA channel in the uplink. Each user's bit stream is spread by a unique PN sequence, which is one of the orthogonal Gold codes with a spreading factor of 256. The tested Gold sequences of length 255 are constructed from the preferred pairs of m-sequence generated by the generating polynomial given in Table 4.4.

In Table 4.4 for example, $\{1, 2, 3, 8\}$ represents a generating polynomial $1 + z^1 + z^2 + z^3 + z^8$, which generates the sequence by adding the input bits to the outputs of the first, second, third and eighth shift registers in a modulo-2 mode. r is the length of the linear feedback shift registers (LFSR). We assume that perfect power control of dominant path is achieved to offset the near-far effect so that SNR of the dominant path of all users are in the same level. For the simplicity and without loss of generality, we use the same multipath intensity profile (MIP) for all the users. Multistage hypothesis testing decisions are delayed to 9^{th} stage so that the maximum number of paths to be detected or eliminated simultaneously is less than 10 (See Section 4.6).

In this chapter, single path propagation is considered corresponding to narrowband CDMA systems such as IS-95, which assumes that multiple access interference (MAI) is removed by using orthogonal PN codes. Therefore the channel for each user and each path is AWGN. The performance of single path case serves as an experimental verification of the performance analysis in the previous section. This analysis will also be applied to a simulated multipath environment in Chapter 5.

4.8.2 Receiver Design Tradeoffs

To illustrate the tradeoff between complexity savings and signal combining loss in the receiver designs, we design three receivers based on different nominal error probabilities in the multistage hypothesis test. To assess the mismatch performance since the

actual path strengths are unknown, six tests of each set are designed to optimally detect the strongest path at six different SNR environments, where SNR ranges from -10 dB to 15 dB in step size of 5 dB. For each receiver, the mixing constants $c_1 = c_2 = 0.5$. The noise floor $\sigma_{i,j}$ in Section 4.4.2 is varied to achieve the SNRs $(-10, -5, 0, 5, 10, 15)$ dB

The lowest complexity receiver (#1) is designed to achieve the goal of the highest complexity saving η by designing thresholds with the highest probability of missed detection among these three receiver designs. Referring to Section 3.4, MHT design parameter P_M has a value of 0.01 corresponding to a probability of detection of 0.99 and P_F has a value of 0.0001 corresponding to a probability of rejecting noise-only components of 0.9999. The design thresholds are calculated by (3.11), (3.12).

A moderate complexity and performance receiver (#2) is designed to decrease the signal combining loss at the expense of increasing the receiver complexity. The choice of $P_M = 0.001$ will result in a probability of detection of 0.999 while maintaining the $P_F = 0.0001$. The design thresholds are given by (3.11),(3.12).

The highest performance receiver (#3) is designed to achieve the lowest signal combining loss by dropping down the threshold. As a result, more false alarm RAKE fingers are detected. MHT design parameter P_M has a value of 0.0001 corresponding to a probability of detection of 0.9999 while maintaining the $P_F = 0.0001$. Given the above parameters, the design thresholds are evaluated by (3.11), (3.12).

4.8.3 Simulation and Numerical Calculation

The complexity savings is obtained both by Monte Carlo simulation and numerical calculation via (4.20). Monte Carlo simulation of the complexity of proposed receiver could be obtained by counting the number of tested tree nodes when no user signal is present at the receiver input. In this case, the received chip-rate sampled baseband discrete time signal is:

$$r(k) = n(k) \tag{4.29}$$

where $k = 1, \ldots, G$ and $n(k)$ is the k^{th} white guassian noise sample at the chip matched filter output.

Using Monte Carlo simulation to generate the uplink cell environment, the signal combining loss is obtained by (4.23) where signal amplitudes are assumed to be known at the receiver and $P_{d_{i,j}}$ is the experimentally obtained probability of detection of path j of user i. $P_{d_{i,j}}$ is obtained by counting the times that the j^{th} path of all the users is detected in the receiver when R Monte Carlo trials are executed. For user i, $n_{i,j}$ counts the times that the j^{th} path is detected. Here we assume that perfect power control is used to offset the near-far problem. The amplitude $A_{i,j}$ of path j of user i is set to μ_j, where μ_j denotes the amplitude of the j^{th} path. To count $n_{i,j}$, the chip-rate sampled signal at the receiver is generated as:

$$r(k) = A_{i,j} * C_{i,j}(k) + n(k) \tag{4.30}$$

where $C_{i,j}(k)$ is the k^{th} chip sample of PN code of j^{th} path of user i and $n(k)$ is

the k^{th} white Guassian noise sample at the chip matched filter output. The multi-stage hypothesis test is designed to detect the strongest path of each user. When the wideband CDMA signal is input to the proposed tree structured MHT-MRC RAKE receiver, the probability of detection is measured. To smooth the effect of PN code choice on system performance, signal combining loss is calculated by averaging the probability of detection over all active users in the system. The experimentally obtained probability of detection of path j of user i is given by:

$$P_{i,j} = \frac{n_{i,j}}{R} \tag{4.31}$$

To achieve a confidence interval of less than 10 percent over the range of nominal probabilities of missed detection as low as 10^{-4}, we use 10,000-100,000 Monte Carlo trials to obtain the simulation results [11].

In our theoretical analysis, the complexity savings is calculated numerically through (4.20) where $r_0(i,0)$ is obtained through (3.19) by setting $\theta = 0$. The signal combining loss is obtained by (4.23) where the probability of detecting path j of user i is calculated by (3.27), where θ is set to be the amplitude of path j of user i, i.e, $\theta = \mu_j$. And the upper threshold A_i and lower thresholds B_i are designed to optimally detect the strongest path with amplitude μ_1 (i.e., $\theta_1 = \mu_1$). Numerical integration is carried out using Simpson's rule with 2048 samples of accuracy.

4.8.4 Experimental Results for No Multipath

In this section, we present the Monte Carlo simulation and numerical calculation results of the performance of proposed MHT-MRC RAKE receiver assuming that no multipath exists. The case of multipath will be discussed in Chapter 5. For receiver design #1, the complexity savings vs. SNR curve is plotted in Figure 4.4 and signal combining loss vs. SNR curve is plotted in Figure 4.5. From these figures, we observe that in a low SNR environment, the test will be more likely to survive to a later stage which causes high complexity and therefore small complexity savings are achieved. Here, the signal is severely distorted at the receiver input which causes a large number of existing paths to be eliminated and the probability of detection of paths are lower in comparison to a high SNR scenario. With an increase of SNR, the receiver becomes more computationally efficient. For instance, in SNR= 5 dB, more than 97% complexity savings is achieved for only 1.1 dB signal combining loss.

The performance trade-offs for different test designs are investigated next. The effect of test design parameter P_M on complexity savings could be seen from Figures 4.4, 4.6, 4.8. When the nominal probability of missed detection decreases, the complexity of the receiver increases. Setting smaller P_M ensures that more paths are detected. On the other hand, the corresponding signal combining loss is also reduced as shown in Figures 4.5, 4.7 and 4.9 because a larger probability of detection of each path is achieved. Therefore, there is a trade off between receiver complexity and signal combining loss performance as illustrated from these three sets of receiver

designs.

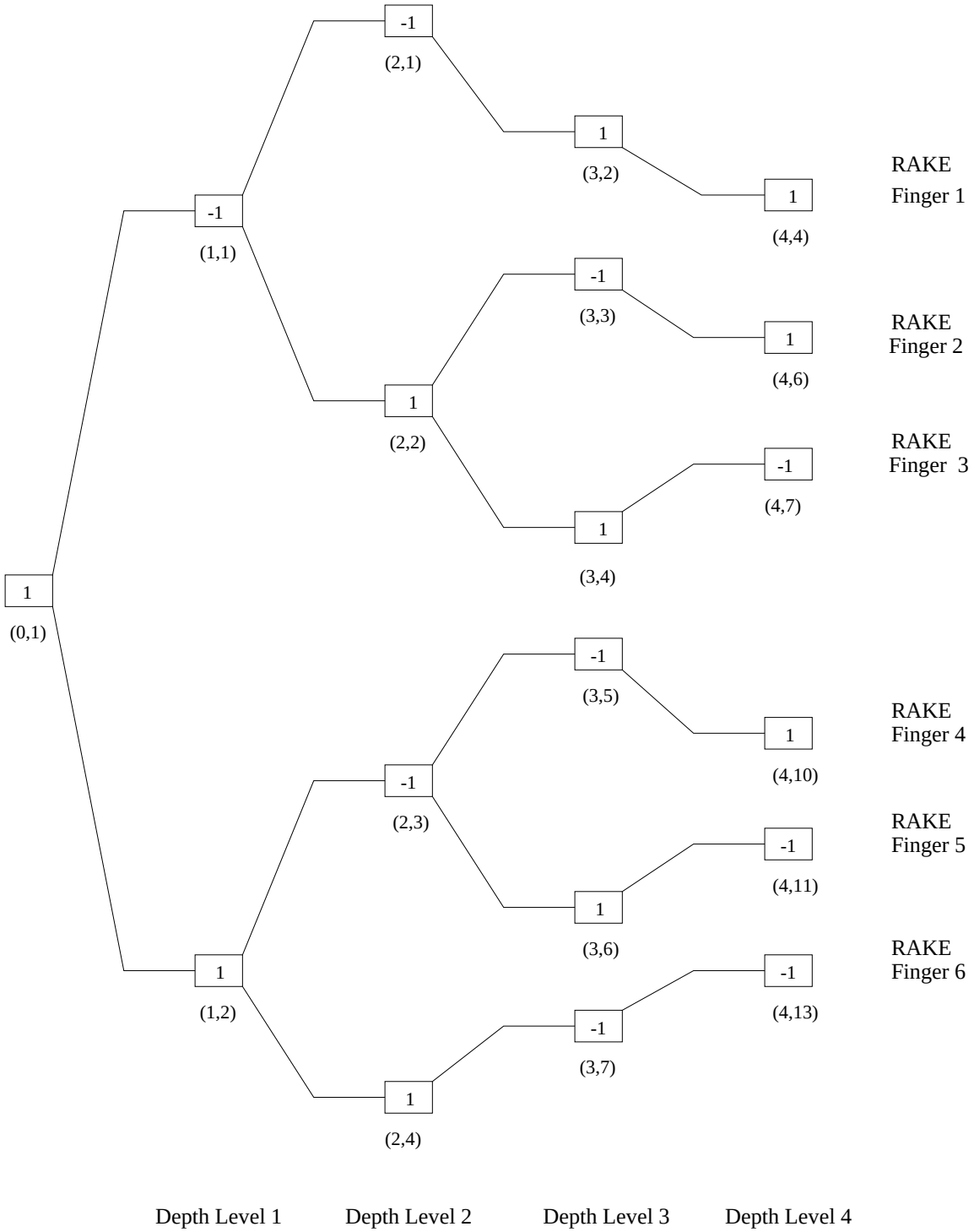

Figure 4.3: Constructed code tree T_0

Tree Node	Corresponding RAKE Finger
Node (1,1)	finger 1, finger 2, finger 3
Node (2,1)	finger 1
Node (2,2)	finger 2, finger 3
Node (3,2)	finger 1
Node (3,3)	finger 2
Node (3,4)	finger 3
Node (4,4)	finger 1
Node (4,6)	finger 2
Node (4,7)	finger 3
Node (1,2)	finger 4, finger 5, finger 6
Node (2,3)	finger 4, finger 5
Node (2,4)	finger 6
Node (3,5)	finger 4
Node (3,6)	finger 5
Node (3,7)	finger 6
Node (4,10)	finger 4
Node (4,11)	finger 5
Node (4,13)	finger 6

Table 4.3: Tree node and its associated possible RAKE fingers

r	8
Generating polynomial	{1,2,3,4,7,8}, {1,2,3,8}
initial loaded value	{1,2,3,4,5,6,7,8}, {2,4,6,8}

Table 4.4: Generating polynomial and initial loaded value for generating orthogonal Gold code

4.9 Chapter Summary

In this chapter we have proposed a novel parallel matched-filter-type PN code acquisition to detect uplink short-code CDMA signals. Assuming knowledge of users' spreading sequences, we formulate code acquisition in terms of multiple hypothesis testing for all the possible shifts of all PN codes. The complexity is further reduced by organizing all the possible shifts of all PN codes into a code tree. Tree is pruned by sequential detection. The tree search was designed by finding thresholds that would satisfy a designer-specified probability of detection using sequential detection. Only viable RAKE fingers are used to generate the output decision statistics.

Monte Carlo computer simulation and numerical calculation have been carried out to study the performance of the algorithm in single-path and multipath channels corrupted with co-channel interference (CCI) and additive white Gaussian noise (AWGN). Both the simulation and numerical calculation results demonstrate that the proposed algorithm can, at the expense of slight signal combining loss, significantly reduce the computation complexity and latency of the receiver. For example, in a system with 10 users and 4 paths per user with 5 dB SNR, a computation savings of more than 97% can be achieved at a cost of only 1.1 dB signal combining loss. When the design parameter P_M increases, lower complexity and latency is obtained while only a small increase in signal combining loss as performance tradeoff.

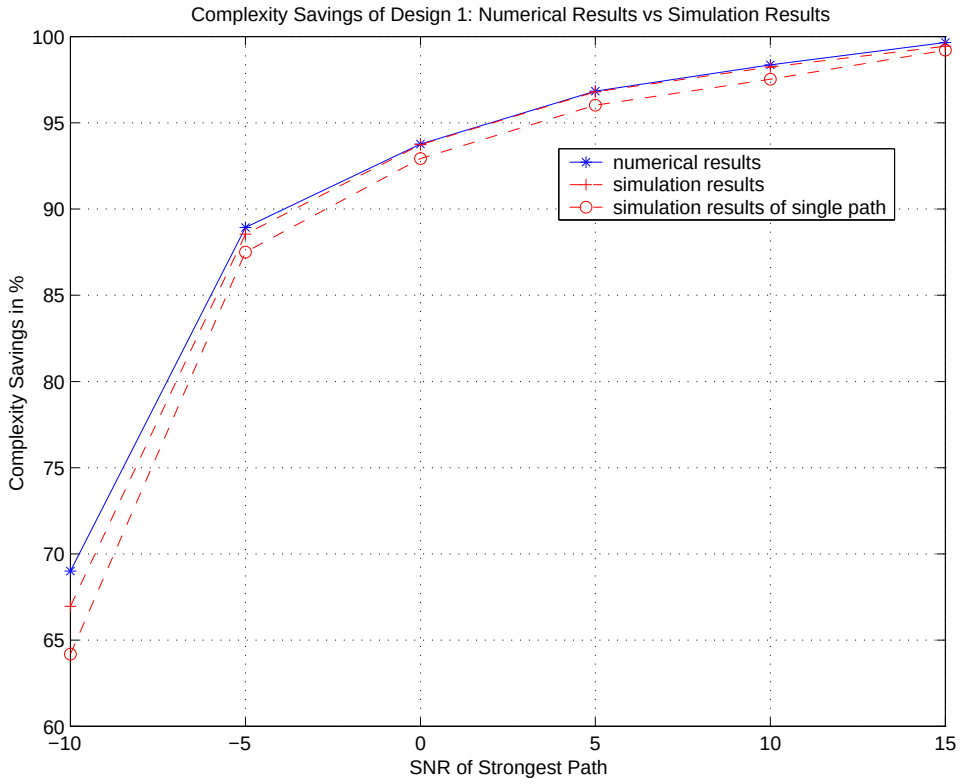

Figure 4.4: Steady-state complexity savings for test design 1 in Section 4.8.2 as predicted by (4.20). $K = 10$ users, $P_M = 0.01$, $P_F = 0.0001$

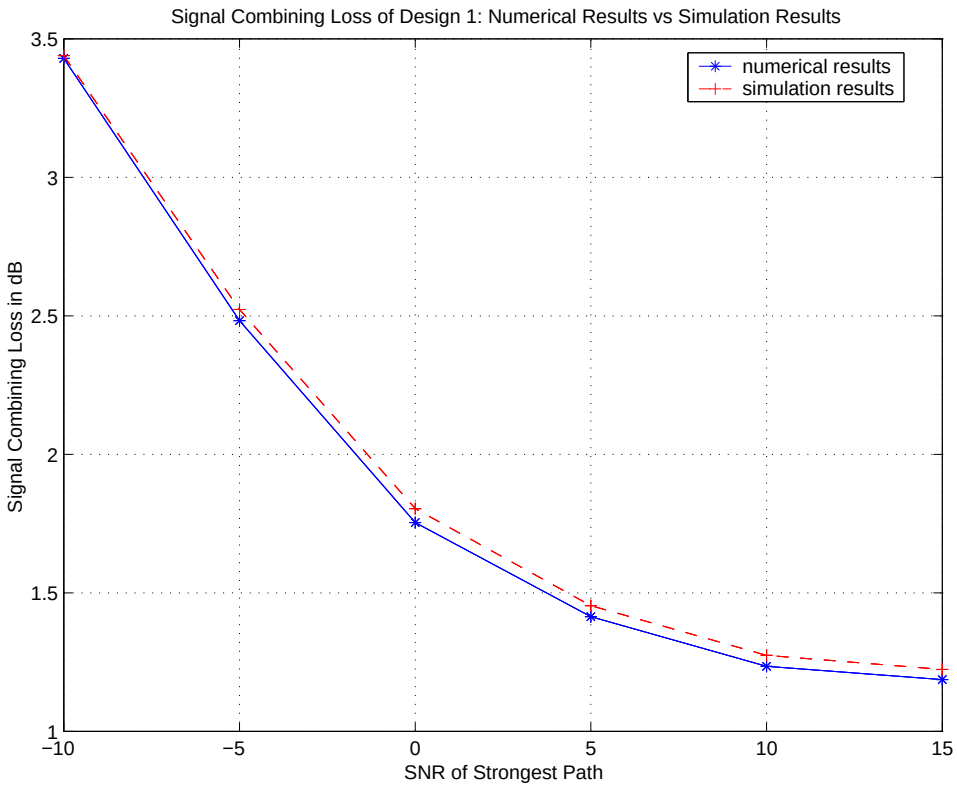

Figure 4.5: Signal combining loss for test design 1 in Section 4.8.2 as predicted by (4.23). $K = 10$ users, $P_M = 0.01$, $P_F = 0.0001$

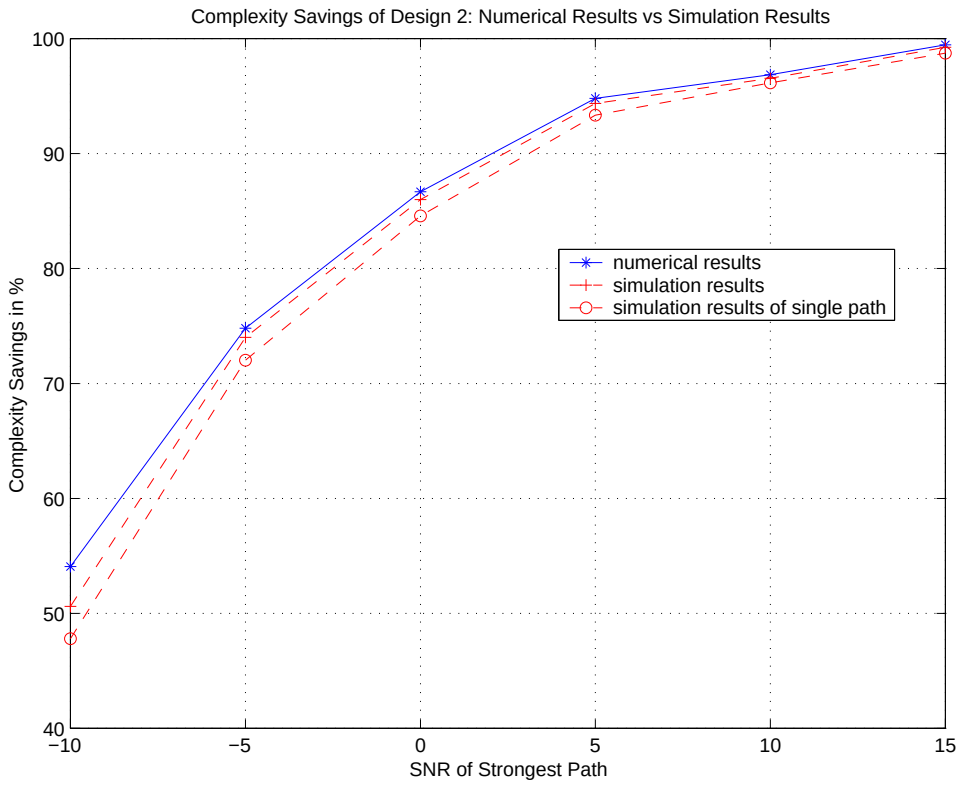

Figure 4.6: Steady-state complexity savings for test design 2 in Section 4.8.2 as predicted by (4.20). $K = 10$ users, $P_M = 0.001$, $P_F = 0.0001$

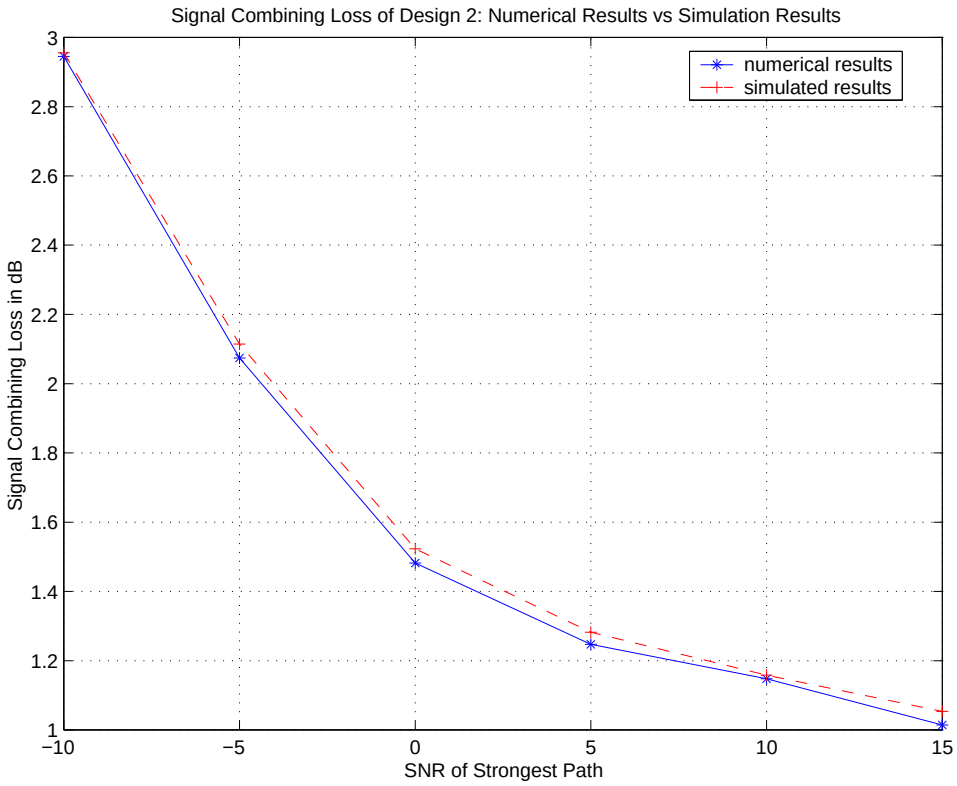

Figure 4.7: Signal combining loss for test design 2 in Section 4.8.2 as predicted by (4.23). $K = 10$ users, $P_M = 0.001$, $P_F = 0.0001$

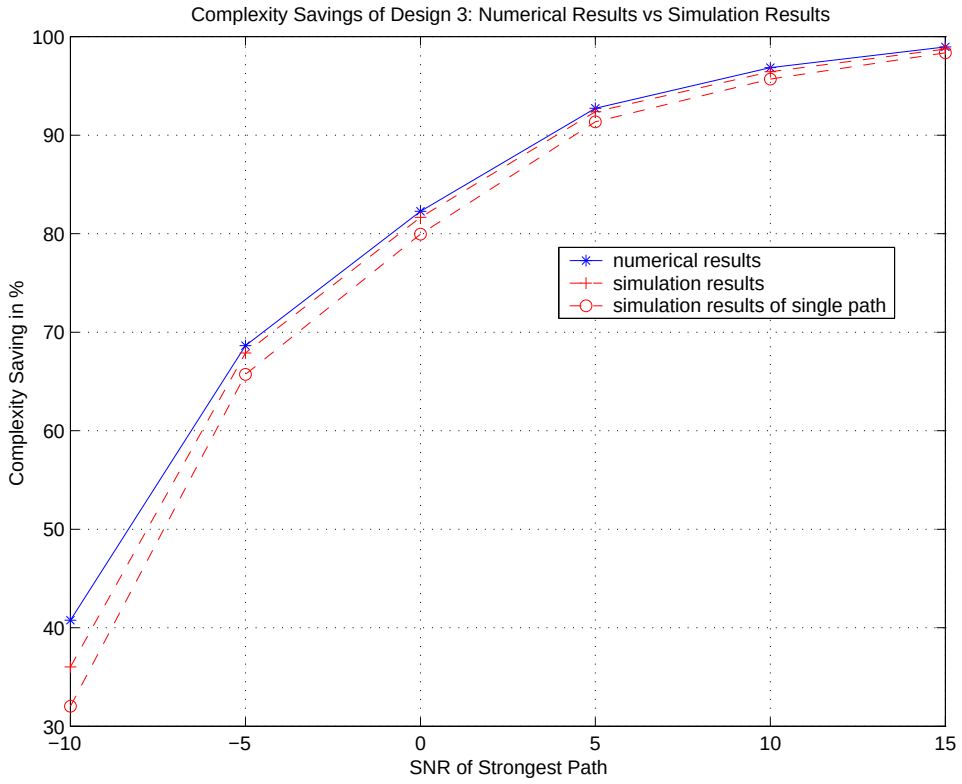

Figure 4.8: Steady-state complexity savings for test design 3 in Section 4.8.2 as predicted by (4.20). $K = 10$ users, $P_M = 0.0001$, $P_F = 0.0001$

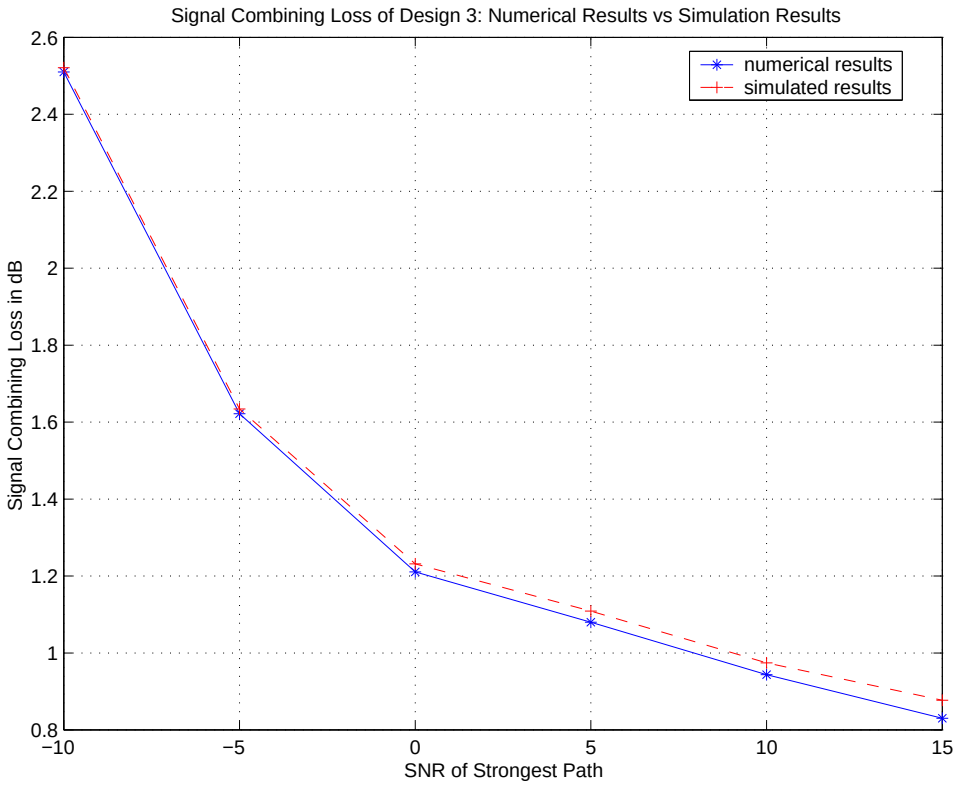

Figure 4.9: Signal combining loss for test design 3 in Section 4.8.2 as predicted by (4.23). $K = 10$ users, $P_M = 0.0001$, $P_F = 0.0001$

Chapter 5

Performance of Code Acquisition in Wideband CDMA Multipath Channels

5.1 Characterization of Wideband CDMA Multipath Channel

The performance of wideband systems is determined by the channel over which the transmission takes place. It is thus indispensable to have a good knowledge of wideband (time-dispersive) mobile radio channels. Research in wideband systems has been going on for some 25 years [2], [66], [67], [68],[69], [70] and has concentrated mainly on: (i) Collection of results from extensive measurement campaigns. Since wideband measurements are much more complicated than simple field strength (i.e. narrowband) measurements, the number of measurement campaigns is considerably smaller than for the narrowband case. (ii) from these measurements, channel models

are derived. These models should fulfill the following two criteria:

- They must be simple enough to allow an analytical computation of basic system performance.
- They must be close to the physical reality; in other words, the performance computed by these models must be close to the performance measured in actually existing radio channels.

These requirements are contradictory, so models of various complexity and accuracy have been developed for different systems. In order to characterize a wideband CDMA multipath channel, Noel Tin [2] designed and constructed a low-cost modular wideband CDMA smart antenna measurement system operating in 1.9 GHz band with an over sampling rate of 5 samples per chip at the chip rate of 7Mcps. To our knowledge, it is among the first experiments where data from both multiple transmitters and receivers are collected. In a wideband CDMA channel, a multipath intensity profile (MIP) quantifies the relationship of temporal delay and attenuation amplitude of each multipath component in received multipath signals. According to the wideband CDMA channel sounding results in typical urban area in [2], the multipath intensity profile has an exponentially decaying power distribution as a function of temporal delay given by:

$$E[\beta_{ij}^2] = \begin{cases} \exp(-\frac{\tau_{ij}^2}{\sigma_\tau^2}) & \tau_{ij} \geq 0 \\ 0 & \tau_{ij} < 0 \end{cases} \tag{5.1}$$

where σ_τ is the root mean square (RMS) delay spread. The RMS delay spread is calculated by:

$$\sigma_\tau = \sqrt{\bar{\tau^2} - \bar{\tau}^2} \tag{5.2}$$

where the first moment of delay $\bar{\tau} = E\{\tau\}$ and the second moment of delay $\bar{\tau^2} = E\{\tau^2\}$. The specific parameter values used will be discussed in Section 5.5.1.

5.2 Numerical Analysis of Complexity Saving in Multipath Channel

In a wideband CDMA system, there are K users communicating simultaneously in the same wireless channel and each user's signal propagates through L paths. We assume that the channel delay spreads over a maximum L_d chip periods for each of the L paths with a processing gain of G. The computational complexity of the proposed tree-structured MHT-MRC RAKE receiver is generalized to a multiuser multipath wideband CDMA communication systems. This is accomplished by labelling the constructed code tree T_0 as described in Section 4.5.2 with hypotheses H_0 and H_1, followed by the classification of each hypotheses labelled path in terms of the stage at which hypotheses H_1 transits to hypotheses H_0. Therefore, the overall complexity is the summation of the complexity of each path type.

As in Section 4.5.2, we also consider each shift of each PN code as a separate codeword. These shifts correspond to multipath signals present at the receiver input.

We represent all L paths of all K users in the system as a code book C_1 which has $K*L$ rows. Each row had length G, corresponding to the depth of the tree to be searched. After constructing the code tree T_0 for all the possible delay shifts of PN codes of all the users as described in Section 4.5.2, we traverse the code tree T_0 and label all the branches that codewords pass through as H_1. We refer to this newly labelled code tree as $\tilde{T}$. Since all the paths initially have a certain number of H_1 labels until a signal-absent label H_0 is reached, we can label all the paths as a concatenation of H_1 labels followed by H_0 labels. Figure 5.1 illustrates hypotheses along one possible path type l, where $v(l)$ denotes the stage (i.e. tree depth level) at which the first H_0 label is present.

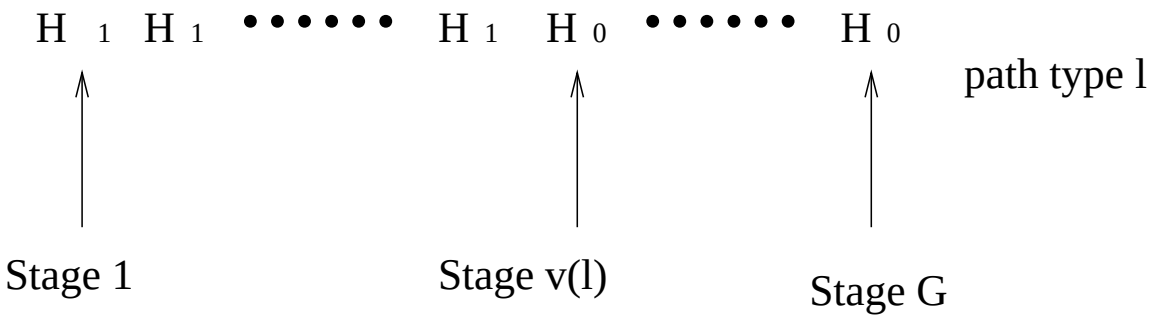

Figure 5.1: Hypotheses corresponding to all paths of type l

After the tree labelling, we need to determine $v(l)$ for each path and form its subtree of code tree $\tilde{T}$. The l^{th} subtree contains all nodes of $\tilde{T}$ corresponding to all type l paths. There are at most G subtrees. Based on the topology of l^{th} subtree, we record the number of tree nodes at stage m of subtree l in a matrix ρ as $\rho[l][m]$. ρ is $P * G$, where P is the total number of path types.

Let us apply the above path classification approach to the example introduced in Section 4.5.2. We assume that ther received signal is composed of zero chip shifted PN code of user 1, one chip shifted PN code of user 1 and zero chip shifted PN code of user 2. The code book C_1 is generated as:

$$\text{Code book } C_1: \quad \begin{bmatrix} 1 & -1 & -1 & 1 \\ -1 & 1 & -1 & 1 \\ 1 & -1 & 1 & -1 \end{bmatrix}$$

Next, we produce the code tree $\tilde{T}$ by adding labels H_1 from code book C_1. According to first row in code book C_1, i.e, [-1 1 -1 1], corresponding tree nodes (1,1) (2,2) (3,3) (4,6) in Figure 4.3 are labelled as H_1. The second row [-1 1 -1 1] labels tree nodes (1,1), (2,2), (3,3), (4,6) as H_1. The last row in code book C_1, [1 -1 -1 1] labels tree nodes (1,2) (2,3) (3,5) (4,10) as H_1. The labelled code tree $\tilde{T}$ is shown in Fig 5.2.

We can classify all the paths in the labelled code tree $\tilde{T}$ according to different concatenations of H_1 and H_0 labels. The path classification is shown in Table 5.1.

The topologies of subtrees T_1, T_2 and T_3 are obtained from hypotheses labelled code tree $\tilde{T}$ by collecting different paths of the same type. The number of subtree nodes after path classification is recorded in matrix ρ:

$$\rho = \begin{bmatrix} 2 & 2 & 2 & 2 \\ 1 & 1 & 1 & 1 \\ 2 & 3 & 3 & 3 \end{bmatrix} \tag{5.3}$$

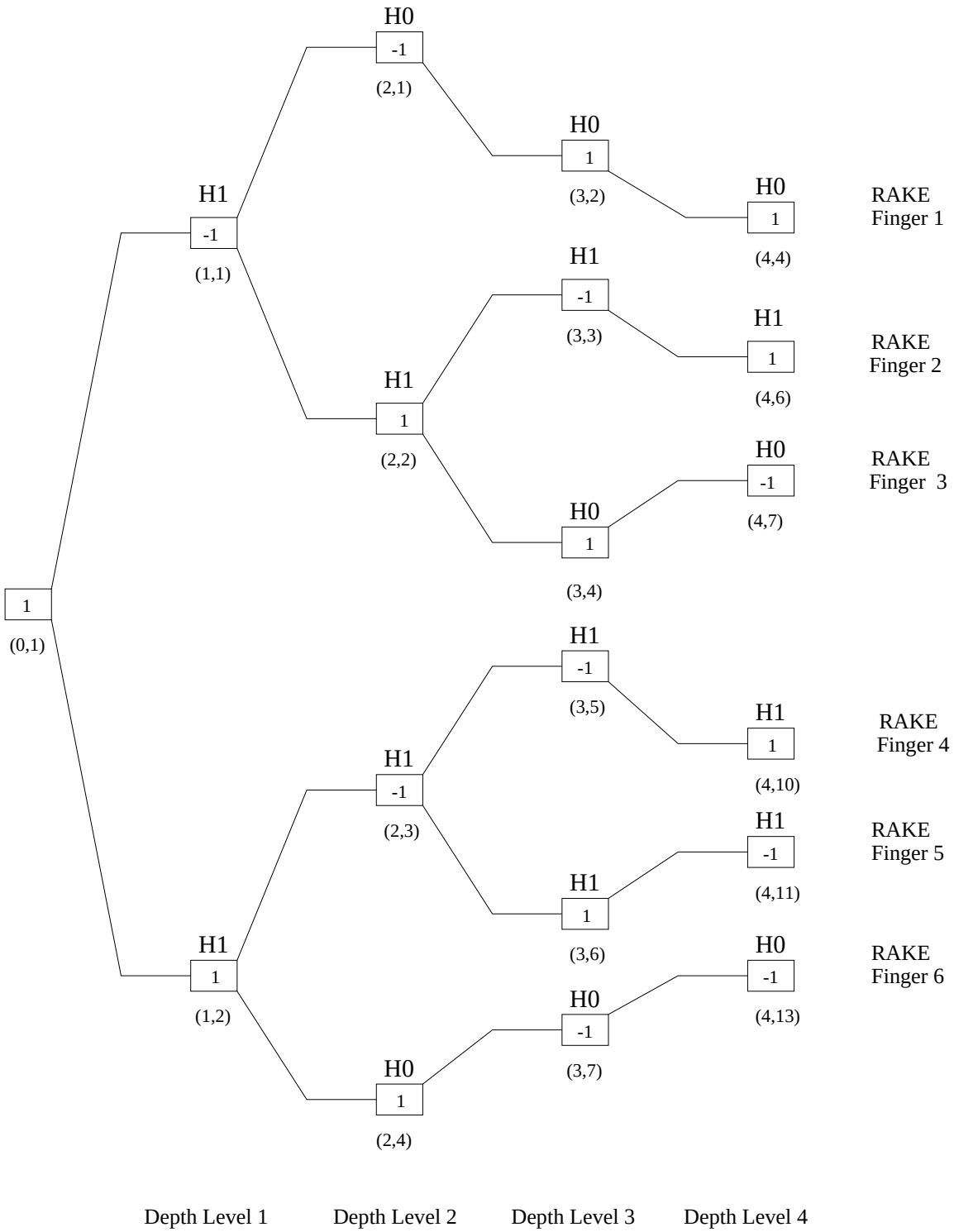

Figure 5.2: Hypotheses labelled code tree $\tilde{T}$ corresponding to the example tree T_0 of Figure 4.3 and code book C_1.

Path type k	1	2	3
Transition stage v(k)	2	3	5
Hypothesis combination	H1 H0 H0 H0	H1 H1 H0 H0	H1 H1 H1 H1
Signal path	path 1, path 6	path 3	path 2, path 4, path 5

Table 5.1: Path type classification of example tree $\tilde{T}$, where the number of path type $P = 3$

After path type determination and tree node counting, we need to determine the probability that MHT continues at a certain stage at each path type. For path type l, we use numerical integration to calculate the probability of continuing at stage m, $r(l,m)$. Since path type l is characterized by H_1 labels at the first $v(l)-1$ stages followed by $N_t - v(l)$ H_0 labels, the signal samples in the first stages have mean $\mu = \theta$ and switch to $\mu = 0$ in the later stages. Thus the probability density function of signal samples along path type l (conditioned on the signal amplitude and variance) could be expressed as:

$$f(x,l) = \begin{cases} \frac{1}{\sqrt{2\pi}\sigma} \exp[-\frac{1}{2}(\frac{x-\mu}{\sigma})^2] & \text{for } \ 1 \leq i < v(l) \\ \frac{1}{\sqrt{2\pi}\sigma} \exp[-\frac{1}{2}(\frac{x}{\sigma})^2] & \text{for } \ v(l) \leq i \leq N_t \end{cases} \tag{5.4}$$

The steady-state computational complexity of the proposed MHT-MRC RAKE receiver in multipath channels, $C_{multipath}$, is given by:

$$C_{multipath} = \sum_{l=1}^{P} \sum_{m=(v(l) mod G)}^{T} r(l,m)\rho_(l,m) \tag{5.5}$$

where $v(l)$ is the stage where the first H_0 label appears in path type l, $r(l,m)$ is the probability of continuing of path type l at stage m and $\rho(l,m)$ is the number of tree

nodes at stage m in subtree T_l. Note that $r(l,m)$ is calculated by (3.23) in truncated sequential analysis in Section 3.5 using the above probability density function in (5.4).

As a comment, we discuss two special cases of the above framework. On one extreme, we consider the situation where all nodes of the tree are identically labelled by H_1, corresponding to multipath components present for all the users. In that special case, $v(l) = G + 1$. On the other extreme, the path type with all H_0 labels corresponding to no multipath signal at the receiver input as is discussed in Section 4.7.1. By setting $v(l) = 1$ and $P = 1$, the complexity savings in wideband CDMA multipath channels given by (5.5) degenerates to (4.21) the complexity savings assuming that no signal is present.

5.3 Numerical Analysis of Signal Combining Loss in Multipath Channel

5.3.1 Analysis of Signal Combining Loss

For the convenience of explanation, the problem of detecting L paths of K users can be perceived as one of detecting any of KL paths. Average signal-to-noise ratio (SNR) after maximal ratio combining (MRC) at the RAKE combiner output could be calculated by enumerating the combination of all the test results of KL hypothesis tests, where K is the number of users and L is the number of paths per user. The

observed discrete-time waveform is:

$$X_n = N_n + S_{n,j} \tag{5.6}$$

where the chip time index $n = 1, \ldots, G$ and path index $j = 1, \ldots, KL$. The hypothesis test is generated for each path j, $1 \leq j \leq KL$, as

$$T_j : \ H_1 \ \text{ vs } \ H_0$$

where hypotheses H_1 and H_0 are:

$$H_1 : \quad S_{1,j} = S_{2,j} = \cdots = S_{G,j} = 0, \quad \text{path } \ j \text{ is detected}$$

$$H_0 : \quad S_{1,j} = S_{2,j} = \cdots = S_{G,j} = \mu_j, \quad \text{path } \ j \text{ is not detected}$$

If the j^{th} signal path is despreaded with a correct shift of PN code, then the despreaded signal has the constant amplitude μ_j. Therefore, we use the constant amplitude in hypotheses. We note that a path is G PN-chips in duration, where G is the processing gain. Let I denote a binary-valued $2^{KL} * KL$ matrix. Each row of I denotes a distinct subset of KL paths where H_1 is true. There are a total of 2^{KL} such subsets of the KL paths. The element $I_{i,j}$ is the decision indicator that path j is detected within the i^{th} combinations of path events. Let $P_i \geq 0$ denote the joint probability corresponding to the event denoted by the i^{th} row of I , $\sum_{i=1}^{2^{KL}} P_i = 1$. Finally, we allow for the possibility that each path may have a different constant signal amplitude under H_1. We denote this amplitude by μ_j, $1 \leq j \leq KL$.

The average SNR at the MRC RAKE combiner output is obtained by calculating all SNR values of the possible detection results. The SNR of i^{th} possible multipath

detection result is given by:

$$\hat{SNR}_i = \sum_{j=1}^{KL} I_{i,j} * SNR_j \tag{5.7}$$

where SNR_j is the signal-to-noise ratio of the path j given by

$$SNR_j = \frac{{\mu_j}^2}{\sigma^2} \tag{5.8}$$

The overall SNR is found by weighting each SNR_j by the corresponding probability P_j, calculated by

$$SNR_{m,MHT-MRC} = \frac{\sum_{i=1}^{2^{KL}} \hat{SNR}_i * P_i}{K} \tag{5.9}$$

The signal combining loss of MHT-MRC RAKE receiver in multipath channel is finally determined by:

$$\Gamma_{m,MHT-MRC} = SNR_{FS-MRC} - SNR_{MHT-MRC} \tag{5.10}$$

where the subscript m denotes the number of signal paths in multipath channels, and $m = KL$. By setting $m = 1$, SNR at the output of MHT-MRC RAKE receiver in wideband CDMA multipath channels given by (5.9) generates to (4.28) the signal combining loss in single-path case. The multipath diversity gain is quantified by comparing the SNR at RAKE combiner output to the RAKE receiver employing selection diversity (SD), where only the strongest path is selected.

$$\Upsilon = SNR_{m.MHT-MRC} - SNR_s \tag{5.11}$$

where

$$SNR_s = \frac{\sum_{i=1}^{K} SNR_1 * P_{i,1}}{K} \tag{5.12}$$

The following example will be used to clarify the SNR calculation at the output of the MHT-MRC RAKE receiver in multipath channels. Assuming a CDMA system with processing gain $G = 4$ and two signal paths that exist for one user with amplitude μ_1 and μ_2 respectively. Here, constant path amplitude is assumed, i.e.,

$$S_{1,1} = S_{2,1} = S_{3,1} = S_{4,1} = \mu_1$$

$$S_{1,2} = S_{2,2} = S_{3,2} = S_{4,2} = \mu_2$$

The received discrete-time signal in one symbol period for path j is expressed as:

$$X_n = S_j + N_n \tag{5.13}$$

where chip sample index $i = 1, 2, 3, 4$ and path $j = 1, 2$, the j^{th} hypothesis test T_j is formulated as H_1 vs H_0, where H_1 and H_0 are:

$$H_0 : S_{1,j} = S_{2,j} = \cdots = S_{4,j} = 0, \text{ path j is present}$$

$$H_1 : S_{1,j} = S_{2,j} = \cdots = S_{4,j} = \mu_j, \text{ path j is present}$$

All the multipath detection results are enumerated in indicator matrix I:

$$I = \begin{bmatrix} 0 & 0 \\ 0 & 1 \\ 1 & 0 \\ 1 & 1 \end{bmatrix} \tag{5.14}$$

The probability of each multiuser multipath detection result is defined as:

$$P_0 \equiv \Pr(T_1 \text{ chooses } H_0 \text{ and } T_2 \text{ chooses } H_0)$$

$$\equiv \Pr(\text{signal path 1 is not detected and signal path 2 is not detected})$$

$$P_1 \equiv \Pr(T_1 \text{ chooses } H_1 \text{ and } T_2 \text{ chooses } H_0)$$

$$\equiv \Pr(\text{signal path 1 is detected and signal path 2 is not detected})$$

$$P_2 \equiv \Pr(T_1 \text{ chooses } H_0 \text{ and } T_2 \text{ chooses } H_1)$$

$$\equiv \Pr(\text{signal path 1 is not detected and signal path 2 is detected})$$

$$P_3 \equiv \Pr(T_1 \text{ chooses } H_1 \text{ and } T_2 \text{ chooses } H_1)$$

$$\equiv \Pr(\text{signal path 1 is detected and signal path 2 is detected})$$

The signal-to-noise ratio of path 1 is calculated by:

$$SNR_1 = \frac{{\mu_1}^2}{\sigma^2} \tag{5.15}$$

The signal-to-noise ratio of path 2 is calculated by:

$$SNR_2 = \frac{{\mu_2}^2}{\sigma^2} \tag{5.16}$$

The formulation of the average SNR at the output of MHT-MRC RAKE receiver is obtained by

$$SNR_{multipath} = \frac{\sum_{i=0}^{3}(\sum_{j=0}^{1}(I_{i,j} * SNR_j) * P_i)}{1} \tag{5.17}$$

As (5.9) implies, it may be possible to obtain the explicit expressions of the signal combining loss. Unfortunately, for our system with K users and L paths per user, there are a total of 2^{KL} composite events. In addition, each composite event is an intersection of a family of KL subevents, which further complicates the situation. Due to the exponentially increasing complexity of analysis in terms of the number of

users and number of paths per user, an accurate calculation of the signal combining loss in a multiuser multipath wideband CDMA channel is difficult to calculate.

5.3.2 Lower Bound of Signal Combining Loss

In the following, we use some approximations to bound the signal combining loss. To simplify the analysis of the probability that the composite events occurs, the De-Morgan's Law is applied to transform intersection into union [71].

Lemma 1 (De-Morgan's Law) Let $A_1, A_2 \ldots A_N$ be any finite family of events in a probability space (Ω,P).

$$P(A_1 \bigcap A_2 \cdots \bigcap A_n) = 1 - P(\overline{A_1} \bigcup \cdots \bigcup \overline{A_n}) \tag{5.18}$$

where $\overline{A_i}$ is the complement event of A_i

In [72] a lower union bound known as De Caen's bound is established in terms of only the probability of individual events $P(A_i)'s$ and the probabilities of pairwise events $P(A_i \bigcap A_j)'s$

Lemma 2 (De Caen [72]) Let $A_1, A_2 \ldots A_N$ be any finite family of events in a probabilities space (Ω,P).

$$P(\bigcup_{i=1}^{N} A_i) \geq \sum_{i=1}^{N} \frac{P(A_i)^2}{\sum_{j=1}^{N} P(A_i \bigcap A_j)} \tag{5.19}$$

The above two lemmas can be applied to our analysis since multipath detection result is symmetric. If subevent $A_{i,j}$ exists in composite event A_i, then there must

exist another event containing subevent $\overline{A_{i,j}}$. By calculating the probability of individual and pairwise events, 2^{KL} probability calculations of composite events can be reduced to $O((KL)^2)$ pairwise event probability calculations and $O(KL)$ individual event probability calculations.

The method of calculating the probability that an individual event occurs is similar to the single path case presented in Section 4.8.3. A generic two path model is present in Figure 5.3. We observe the following:

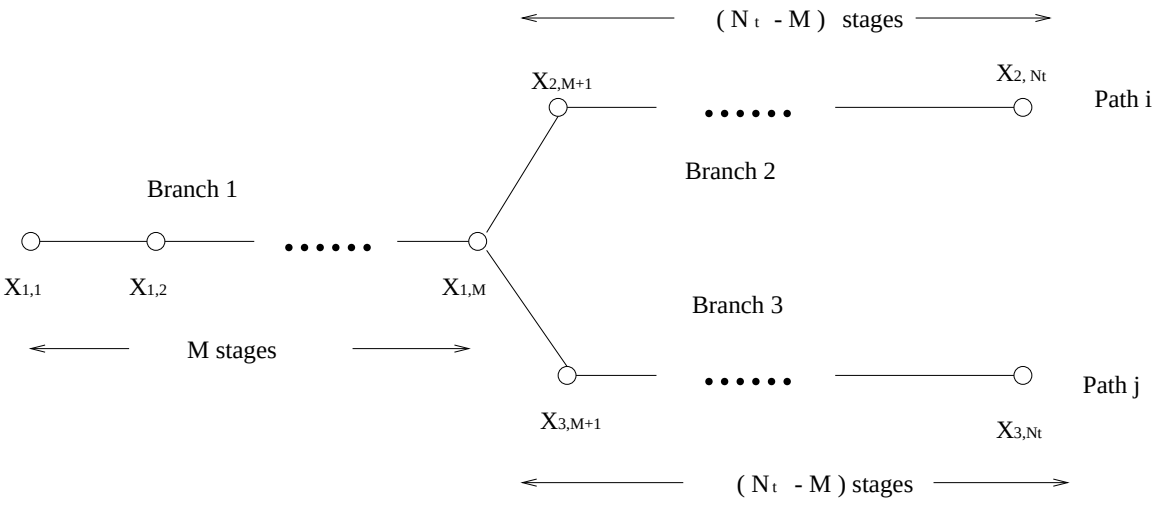

Figure 5.3: A generic two path model used to calculate the probability of pairwise events. M is the number of stages that a path branches into two paths

1. The single path case is a special case of the above generic model, where $M = N_t$.

2. The case of two independent paths is also a special case of the above generic model, where $M = 0$.

For the case of two independent paths, the probability of a pairwise event could

be simplified to the product of the probabilities of two single path events:

$$P(A_i \bigcap A_j) = P(A_i) * P(A_j) \tag{5.20}$$

For the case of two dependent paths, i.e., those that have PN chips in common, the received signal samples are multiplied by the code value encoded in the code tree node, which is either 1 or -1, therefore the signal samples in brance 2 and 3 satisfy:

$$X_{3,i} = C_i * X_{2,i} \quad \text{for } i = M+1, \ldots, N_t \tag{5.21}$$

where C_i is a constant, $C_i \in (-1, 1)$. The pairwise events of path i and path j are mathematically expressed as follows:

Case 1: path i and path j are both detected

$$\begin{aligned} P_{i1,j1} &\equiv P(\text{ case 1 }) \\ &= P(\text{ choose } H_1 \text{ in branch 1}) \\ &\quad + P(\text{ choose } H_1 \text{ in branch 2 and choose } H_1 \text{ in branch 3 }) \\ &= P([\bigcup_{k=1}^{M}(\sum_{i=1}^{K} X_{1,i} > A_k)] \bigcup \\ &\quad ([\bigcup_{k=M+1}^{N_t}(\sum_{i=1}^{k} X_{2,i} > A_k)] \bigcap [\bigcup_{k=M+1}^{N_t}(\sum_{i=1}^{k} C_i X_{2,i} > A_k)])) \end{aligned} \tag{5.22}$$

The Case 2: path i is detected while path j is not detected

$$\begin{aligned} P_{i1,j0} &\equiv P(\text{ case 2 }) \\ &= P(\text{ choose } H_1 \text{ in branch 2 and choose } H_0 \text{ in branch 3 }) \\ &= P([\bigcup_{k=M+1}^{N_t}(\sum_{i=1}^{k} X_{2,i} > A_k)] \bigcap [\bigcup_{k=M+1}^{N_t}(\sum_{i=1}^{k} C_i X_{2,i} < B_k)]) \end{aligned} \tag{5.23}$$

Case 3: path i is not detected while path j is detected

$$\begin{aligned} P_{i0,j1} &\equiv P(\text{ case 3 }) \\ &= P(\text{ choose } H_0 \text{ in branch 2 and choose } H_1 \text{ in branch 3 }) \\ &= P([\bigcup_{k=M+1}^{N_t}(\sum_{i=1}^{k} X_{2,i} < B_k)] \bigcap [\bigcup_{k=M+1}^{N_t}(\sum_{i=1}^{k} C_i X_{2,i} > A_k)]) \end{aligned} \tag{5.24}$$

Case 4: neither path i nor path j is detected

$$\begin{aligned} P_{i0,j0} &\equiv P(\text{ case 4 }) \\ &= P(\text{ choose } H_0 \text{ in branch 1}) \\ &\quad + P(\text{choose } H_0 \text{ in branch 2 and choose } H_0 \text{ in branch 3 }) \\ &= P([\bigcup_{k=1}^{M}(\sum_{i=1}^{K} X_{1,i} < B_k)] \bigcup \\ &\quad ([\bigcup_{k=M+1}^{N_t}(\sum_{i=1}^{k} X_{2,i} < B_k)] \bigcap [\bigcup_{k=M+1}^{N_t}(\sum_{i=1}^{k} C_i X_{2,i} < B_k)])) \end{aligned} \tag{5.25}$$

The calculation of the above pairwise events involves the N_t dimension integration of N_t dimension joint probability density function over an N_t dimensional probability space. Furthermore, although the joint pdf of random sample sequence could be decomposed to the multiplication of pdf of each random sample since the independent property holds, it can hardly be decomposed to multiple one dimensional pdf region because The pdf space of interest is constrained by complicated union, intersection and variable length summation operations of received samples. Therefore, lower and upper limiters of each integral is difficult to determine. In addition, the probability changes as constants value C_i vary for distinct path pairs. For instance,

$$P(case1) = \int \cdots \int_{(\bigcup_{k=1}^{M}(\sum_{i=1}^{k} X_{1,i} > A_k)) \bigcup [\bigcup_{k=M+1}^{N_t}(\sum_{i=1}^{k} X_{2,i} > A_k)] \bigcap [\bigcup_{k=M+1}^{N_t}(\sum_{i=1}^{k} C_i X_{2,i} < B_k)])}$$

$$f(X_{1,1},\ldots X_{1,M},X_{2,M+1},\ldots,X_{2,N_t})dX_{1,1}\ldots dX_{1,M}dX_{2,M+1},\ldots,dX_{2,N_t}$$

$$= \int\ldots\int_{(\bigcup_{k=1}^{M}(\sum_{i=1}^{k}X_{1,i}>A_k))\bigcup[\bigcup_{k=M+1}^{N_t}(\sum_{i=1}^{k}X_{2,i}>A_k)]\bigcap[\bigcup_{k=M+1}^{N_t}(\sum_{i=1}^{k}C_iX_{2,i}<B_k)])} f(X_{1,1})\ldots f(X_{1,M})f(X_{2,M+1}),\ldots,f(X_{2,N_t})dX_{1,1}\ldots dX_{1,M}dX_{2,M+1},\ldots,dX_{2,N_t} \tag{5.26}$$

Alternatively, we use the Monte Carlo approach to obtain the above probabilities. By inserting all the pairwise and individual probabilities into (5.19) and (5.18), and inserting (5.7), (5.19) into (5.9), we obtained the upper bound of SNR at RAKE combining output and the corresponding lower bound of signal combining loss via (5.10).

5.4 Performance Analysis of RAKE Receiver with Channel Estimation

5.4.1 Single Pilot Symbol Case

In this section we extended the performance evaluation to practical RAKE receiver assuming the multipath channel knowledge is not available at the receiver. The extention is based on two types of RAKE receivers described in Section 4.7, i.e, Full-Search MRC RAKE receiver and MHT-MRC RAKE receiver. The practical RAKE receivers employ channel estimation.

In practical Full-Search-MRC RAKE receivers, all the multipath components are

detected by exhaustive search. Because the channel state information is not available at the receiver, channel estimation is a prerequisite before RAKE combining. The channel tap weights could be estimated by the instantaneous soft-decision amplitude statistics of the received signal at the matched filter output.

$$\tilde{\beta_{ij}} = \frac{1}{G}\sum_{n=1}^{G} r(n) * C_i(n - \tau_{ij}) \tag{5.27}$$

where $r(n)$ is received signals sampled at $n * T_c$ and $C_i(n - \tau_{ij})$ is the chip value of PN code of user i after τ_{ij} chips circular shifts. The average SNR at the output of practical Full-Search MRC RAKE receiver is calculated as:

$$SNR_{P-FS-MRC} = \frac{1}{K}\sum_{i=1}^{K}\sum_{j=1}^{L} \tilde{SNR}_{i,j} \tag{5.28}$$

where signal-to-noise ratio of path j of user i is estimated by:

$$\tilde{SNR}_{i,j} = \frac{E(\tilde{\beta_{ij}}^2)}{\sigma^2} \tag{5.29}$$

The channel estimation error is quantified by the signal combining loss of the practical Full-Search (P-FS-MRC) RAKE receiver when compared to the Full-Search-MRC (FS-MRC) RAKE receiver.

$$\Gamma_{P-FS-MRC} = SNR_{FS-MRC} - SNR_{P-FS-MRC} \tag{5.30}$$

Similarly, in the practical MHT-MRC RAKE receiver, the estimated signal-to-noise ratio and probability of detection of path j of user i are used to calculate the average SNR after maximal ratio combining (MRC) at the RAKE receiver output.

$$SNR_{P-MHT-MRC} = \frac{1}{K}\sum_{i=1}^{K}\sum_{j=1}^{L} \tilde{SNR}_{i,j} * P_{d_{i,j}} \tag{5.31}$$

The signal combining loss of P-MHT-MRC RAKE receiver, $\Gamma_{P-MHT-MRC}$, could be obtained by:

$$\Gamma_{P-MHT-MRC} = SNR_{FS-MRC} - SNR_{P-MHT-MRC} \tag{5.32}$$

5.4.2 Extension to Multiple Pilot Symbols Scenario

Instead of detecting the multipath signals in one pilot symbol duration, we can also extend the observation window to multiple pilot symbol periods. The maximum number of stages of the tree-structured sequential hypotheses test will be extended to $N_w * G$ stages, where N_w is the number of pilot symbols or observation window size. Therefore, the truncation stage is also extended as:

$$N_t = \min(\tilde{N}_t, G * N_w) \tag{5.33}$$

where $\tilde{N}_t$ is calculated by (3.16).

As an illustration, the system mentioned in Section 4.5.2 is used. The observation window is extended to 2 symbols interval and each codeword has the length of 2 periods of PN code. The code book C in Section 4.5.2 is extended over two PN code

periods as:

$$\text{code book } C \begin{bmatrix} 1 & -1 & -1 & 1 & 1 & -1 & -1 & 1 \\ -1 & -1 & 1 & 1 & -1 & -1 & 1 & 1 \\ -1 & 1 & 1 & -1 & -1 & 1 & 1 & -1 \\ 1 & 1 & -1 & -1 & 1 & 1 & -1 & -1 \\ 1 & -1 & 1 & -1 & 1 & -1 & 1 & -1 \\ -1 & 1 & -1 & 1 & -1 & 1 & -1 & 1 \end{bmatrix} \tag{5.34}$$

The received baseband signal in uplink wideband CDMA channel in Section 4.3 is modified in multiple bits scenario, where the short spreading codes repeat several time in the observation window. The chip-rate sampled baseband discrete-time signal at the receiver input is:

$$r(q * G + n) = \sum_{k=1}^{K} \sum_{l=1}^{L} \beta_{kl} d_q c_k (n - \tau_{kl}) + z(q * G + n) \tag{5.35}$$

where $q = 1, \ldots, N_w$

The channel tap weights could be estimated by simplified WMSA channel estimation filter with the parameters $N_p > 1, K = 1$ and $\beta_0 = 1$:

$$\hat{\beta}_{ij} = \frac{1}{N_w} \sum_{q=1}^{N_w} \frac{1}{G} \sum_{n=1}^{G} r(q * G + n) C_i (n - \tau_{ij}) \tag{5.36}$$

where $\hat{\beta}_{ij}$ is the estimated channel tap weight of path j of user i.

Assume that the multiple access interference (MAI) and interpath interference (IPI) are much smaller than the AWGN, the noise floor could be reduce to $\frac{\sigma^2}{N_w}$ by averaging the bit decision statistics after signal despreading. The SNR of user i at

the output of P-MHT-MRC RAKE receiver by multiple bits is obtained by applying channel tap weights estimates in (5.36) to (5.29) (5.31).

In a practical MHT-MRC RAKE receiver, the complexity is composed of two parts. One part is introduced by code acquisition while another part is introduced by channel estimation. In the system described in Section 4.8, there exists four resolvable multipaths per user and multipaths spreads over 256 chips. Code acquisition introduced 256 code matched filterings while the complexity introduced by channel estimation is 4 code matched filterings, which is less than 2 % of complexity consumed by code acquisition. Therefore, the complexity introduced by channel estimation is negligible. Here, we would expect that the complexity savings of the practical MHT-MRC RAKE receiver in multipath channels is almost the same as that of MHT-MRC RAKE receiver predicted in Section 5.2.

5.5 Experimental Results (Multipath Case)

5.5.1 Experimental Setup

In the following experiments, the same wideband CDMA communications system in Section 4.8.1 and multipath channel model in Section 5.1 are used. We consider a chip-synchronous multipath channel, where the chip boundary is assumed to be known at the receiver. Moreover, the delay of each multipath component is uniformly distributed over $[0, 256]$ chips. Therefore, the root mean square (RMS) value of

random delay could be calculated by (5.2). As a result, $\sigma_\tau = 73.6$ chips. In [2], outdoor measurements of a wideband CDMA channel demonstrates that as many as three resolvable multipath components besides the strongest multipath component exist and the signal powers of the second, third and fourth strongest paths are on average $-5dB$, $-6dB$ and $-7dB$ below the strongest mutipath component. The exponentially decaying multipath intensity profile (MIP) given by (5.1) is applied to calculated the corresponding mean of random temporal delay of each path according to its relative average signal-to-noise ratio. The calculated result is listed in Table 5.2. For the simplicity of evaluating receiver performance, we use the deterministic

Path	Amplitude	Delay spread in chips
1 st	0.0 dB	0
2 nd	-5.0 dB	79
3rd	-6.0 dB	87
4th	-7.0 dB	94

Table 5.2: Multipath delay profile obtained from wideband CDMA measurements [2]

multipath intensity profile.

Here, we concentrated on receiver thresholds design #2 in Section 4.8.2, i.e, moderate complexity and performance where the nominal probability of missed detection $P_M = 0.001$. In actual wideband CDMA systems, receiver has no knowledge of the SNR of each transmitted signal. Therefore, the hypothesis testing thresholds can not be designed to optimally detect all the user signals in the system. Here we consider

two receiver designs: low SNR receiver design and high SNR receiver design. In low SNR receiver design, the decision thresholds are designed to optimally detect a signal with -5 dB SNR while in high SNR receiver design, the decision thresolds are designed to optimally detect a higher SNR signal of 5 dB. SNR environments ranging from -10 dB to 15 dB with the step size of 5 dB are evaluated.

5.5.2 Complexity Savings

The steady-state computation complexity savings of the proposed code acquisition algorithm in wideband CDMA multipath channels is determined both by Monte Carlo simulation and numerical calculation. Monte Carlo simulation is performed by counting the number of tested tree nodes when multi-user multipath signals are present at the receiver input. Therefore, the generated discrete-time CDMA signal input to the receiver in one symbol interval is:

$$r(k) = \sum_{i=1}^{10} \sum_{j=1}^{4} A_{i,j} * C_i(k - \tau_{i,j}) + n(k) \tag{5.37}$$

where $A_{i,j}$ is the amplitude of user i and path j, and $C_i(k - \tau_{i,j})$ is the PN code chip value of user i after a $\tau_{i,j}$ circular shifts at time index k.

To verify the Monte Carlo simulation results, the numerical analysis described in Section 5.2 is performed. Code tree T_0 is first constructed according to code book C_0 with size of $2560 * 256$, where 256 possible shifts of PN codes of 10 users are stored. Multipath components of 10 users with 4 paths per user are stored in code book C_1 with size of $40 * 256$. Code tree T_0 is labelled according to C_1 followed by

path classification. After determining the transition stage $v(l)$ and assigning the path identifier l in increasing order of $v(l)$, we list the path classification result in Table 5.3. The overall complexity of the receiver is the summation of the complexities of each path type. Here, we also give a detailed summary of the analysis procedure:

Path type l	transition stage v(l)	number of paths
1	4	313
2	5	311
3	6	715
4	7	505
5	8	296
6	9	186
7	10	104
8	11	46
9	12	31
10	13	8
11	14	3
12	15	2

Table 5.3: Path classification result of the simulated wideband CDMA systems with 10 users and 4 paths per user

1. Initialization: organize the code tree T_0 according to code book C_0, initialize hypothesis type value and path type value within each tree node to 0, which

corresponds to H_0 hypotheses label and the path type with all H_0 labels, respectively. Generate code book C_1 which corresponds to the multipath signal at the receiver input

2. Traverse tree T_0 according to code book C_1 and relabel each tree node that signal path goes through with the label H_1

3. Traverse code tree T_0 according to codebook C_0. Determine the stage where the first H_0 label appears, $v(l)$. For paths with all H_1 labels, $v(l) = G + 1$

4. Classify all the paths according to increasing order of transition stage $v(l)$ and assign path identifier l for each path

5. Traverse the hypotheses labelled code tree $\tilde{T}$ and add path type information l to all H_0 labelled tree nodes

6. Traverse the tree and form the subtree T_l of code tree $\tilde{T}$ for path type l. Count the tree node of subtree T_l in tree depth level m and record it in matrix $\rho[l][m]$

7. Calculate the probability of continuing at stage m of path type l and record it in $r[l][m]$

8. Calculate steady-state computation complexity in multipath channels by (5.5)

5.5.3 Signal Combining Loss

Monte Carlo simulation of signal combining loss in multipath channels is performed on the received signal (5.37) by measuring the probability of detection for every

signal paths of each user. To verify the simulation results, analysis is necessary. As explained earlier, because complexity of the analysis is exponential in the number of users and resolvable multipaths per user, we consider a fewer users and paths for analysis purposes.

Here, we apply our analysis method to a CDMA system with 3 users and 4 paths per user. The multipath channel profile is the same as that described in Section 5.5.1. Since $K = 3, L = 4$, there are altogether $2^{3*4} = 2^{12} = 4096$ joint events. A brief description of the analysis procedure is given as follows:

1. Generate code book C_1 which corresponds to the multiple user multipath signal at the receiver input

2. Count the number of stages before each possible pair of paths diverge and record in a matrix $cn[K * L][K * L]$

3. Calculate the probability of detection and missed detection of each path assuming that no other paths are present by numerical integration similar to the single path case and record in $P_1[2 * K * L]$

4. Calculate the probabilities of pairwise events according to the case of two independent path and two dependent paths. For the case of independent paths, $P_2[i][j] = P_1[i] * P_1[j]$. For dependent case of path i and path j, we use the numerical (Monte-Carlo) approach described in Section 5.3.2. The probabilities of pairwise events are obtained by 1000,000 to 10,000,000 Monte Carlo trial

to achieve the confidence interval of less than 10 % over the range of actual probabilities of pairwise events.

5. Enumerate all multipath results in indicator matrix $I[2^{KL}][KL]$ and calculate the upper bound probability of each multipath detection result according to De-Caen's lower union bound (5.19) and De-Morgan's Law in (5.18) and record in $P_{event}[2^{KL}]$

6. Calculate the SNR at the MRC output by (5.9) and calculate the corresponding signal combining loss compared to Full-Search-MRC RAKE receiver and multipath diversity gain compared to RAKE receiver employing selection diversity.

5.5.4 Experiment Results (Multipath Case)

First, we consider that the test thresholds are varied to optimally detect signals of SNRs (-10,-5,0,5,10,15) dB as in Section 4.8. The complexity savings and signal combining loss performance in multipath channels are compared to signal path channels in Figures 5.4, 5.5. Both Monte Carlo simulation and numerical calculation results show that the complexity is less than that predicted for the single path case while the signal combining loss is a little larger . The multiple user multipath signals present at the receiver input create the false alarm paths, resulting in additional acquisition complexity. In addition, multiple access interference (MAI) and interpath interference (IPI) decrease the probability of detection of multipath components, which lowers SNR.

Referring to Figures 5.6, 5.7, we examine the impacts of test design mismatch on system performance. In Figure 5.6, the result of complexity savings of low SNR receiver (nominal -5 dB) and high SNR (nominal $+5$ dB) receiver are plotted, obtained through both numerical calculations as discussed in Section 5.2 as well as Monte Carlo simulation. The corresponding signal combining loss through Monte Carlo simulation is plotted in Figure 5.7. Referring to Figures 5.6 and 5.7, the following observations are made:

1. As expected, the computation complexity of the low SNR receiver is higher than that of high SNR receiver while the signal combining loss is smaller. For instance, fixing the SNR of the strongest path to 0 dB and referring to the complexity savings and signal combining loss curves of the low and high SNR receivers, we observe that 74% vs 93 % complexity savings and 1.9 dB vs 3.3 dB signal combining loss . This demonstrates a trade-off between receiver complexity and signal detection performance.

2. The complexity savings curves reach a minimum where no test design mismatch occurs. Specifically, the complexity savings of the low SNR receiver reaches a minimum where the SNR of the strongest path is -5 dB while complexity savings of the high SNR receiver reaches a minimum where SNR of strongest path is 5 dB. This result is expected because if the SNR level of the signal is exactly the same as the nominal SNR that the hypothesis is designed to optimally detect, the test will reach a later stage in comparison to signals with

other SNRs, resulting in larger receiver complexity.

3. Finally, the numerical analysis results agrees strongly with the Monte Carlo simulation results.

5.5.5 Analysis Results of Signal Combining Loss (Multipath)

In the previous experiment with the system of 10 users and 4 paths per user, we didn't obtain the numerical analysis result of signal combining loss because in such a large system the number of joint events is $2^{10*4} = 10^{12}$. According to the previous numerical calculation experience, it will take several years to calculate by computer programs even using the most efficient C/C++ language. Therefore, we will use a smaller system with 3 users and 4 paths per user.

Referring to Figures 5.8, 5.9, we compare the numerically calculated signal combining loss lower bound to signal combining loss by Monte Carlo simulation in low SNR (nominal -5 dB) and high SNR (nominal $+5$ dB) receivers, respectively. From observations, we can conclude that our signal combining loss lower bound is very close to actual signal combining loss. More precisely, the gap between actual signal combining loss and signal combining loss lower bound is consistently less than 1 dB.

Figures 5.10, 5.11 illustrate the multipath diversity gain and corresponding numerical upper bound. We observe that as the SNR of the strongest path increases, the

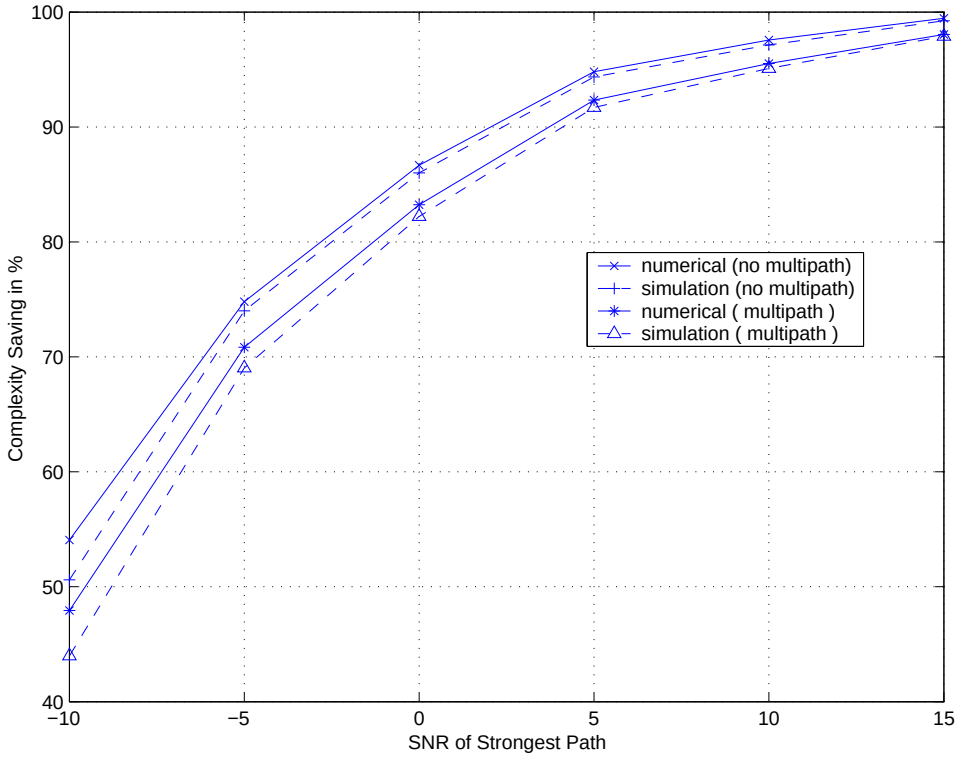

Figure 5.4: Complexity (multipath): K = 10 users, $L = 4$ paths per user and nominal false alarm probability $P_F = 0.0001$ and nominal missed detection probability $P_M = 0.001$

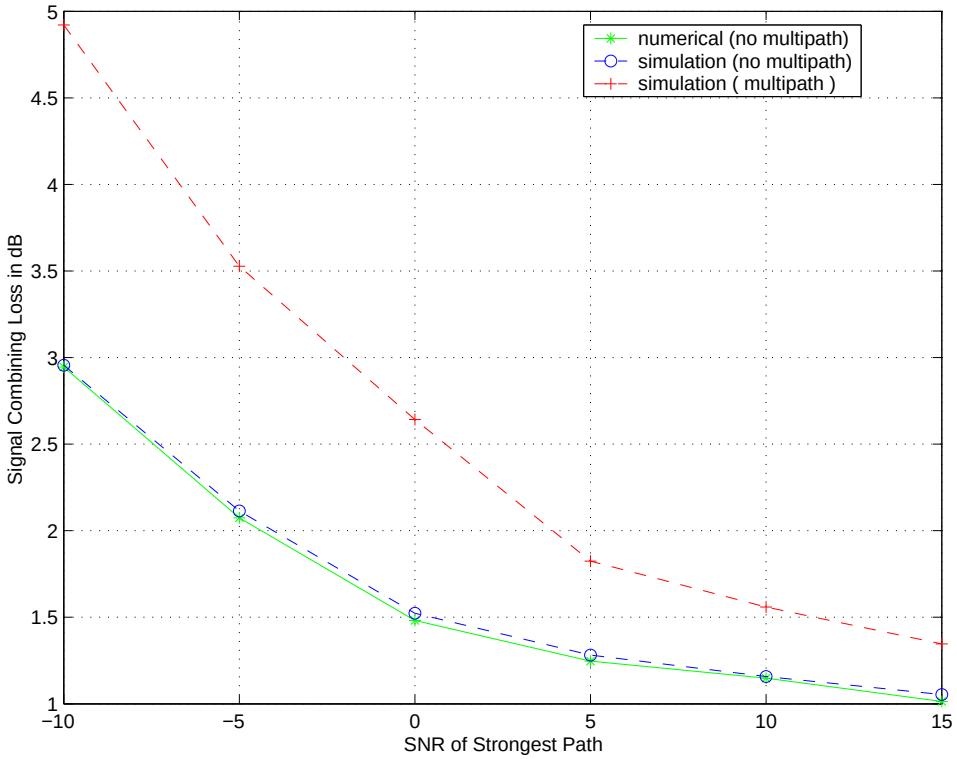

Figure 5.5: Signal combining loss (multipath): K= 10 users, $L = 4$ paths per user and nominal false alarm probability $P_F = 0.0001$ and nominal missed detection probability $P_M = 0.001$

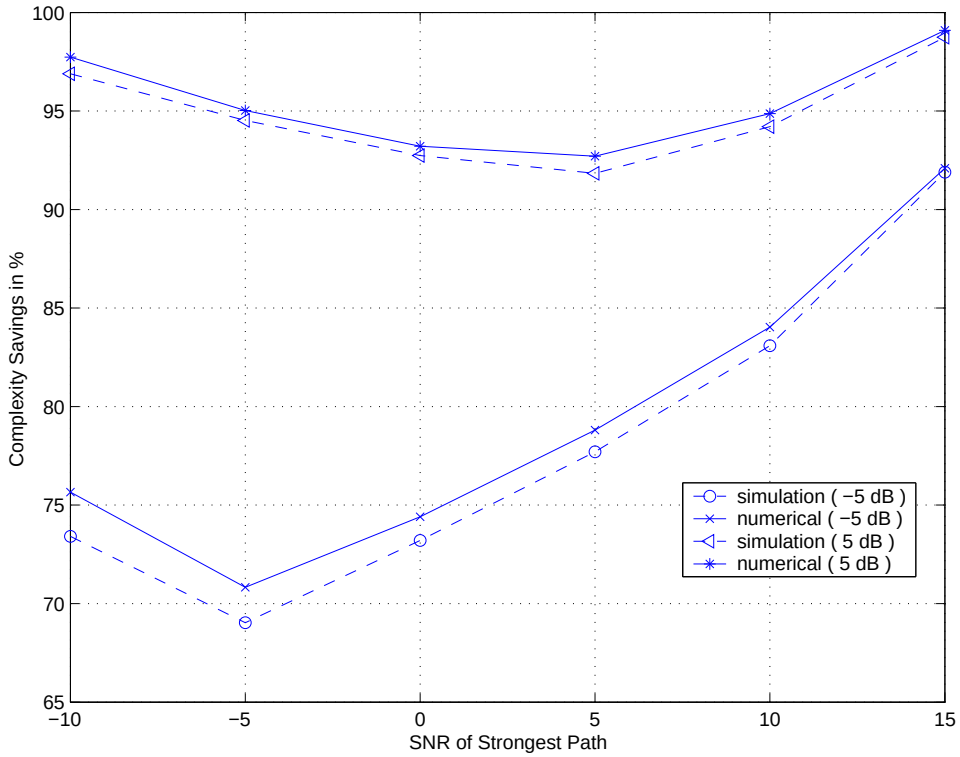

Figure 5.6: Complexity savings with test design mismatch (multipath): K= 10 users, $L = 4$ paths per user and nominal false alarm probability $P_F = 0.0001$ and nominal missed detection probability $P_M = 0.001$

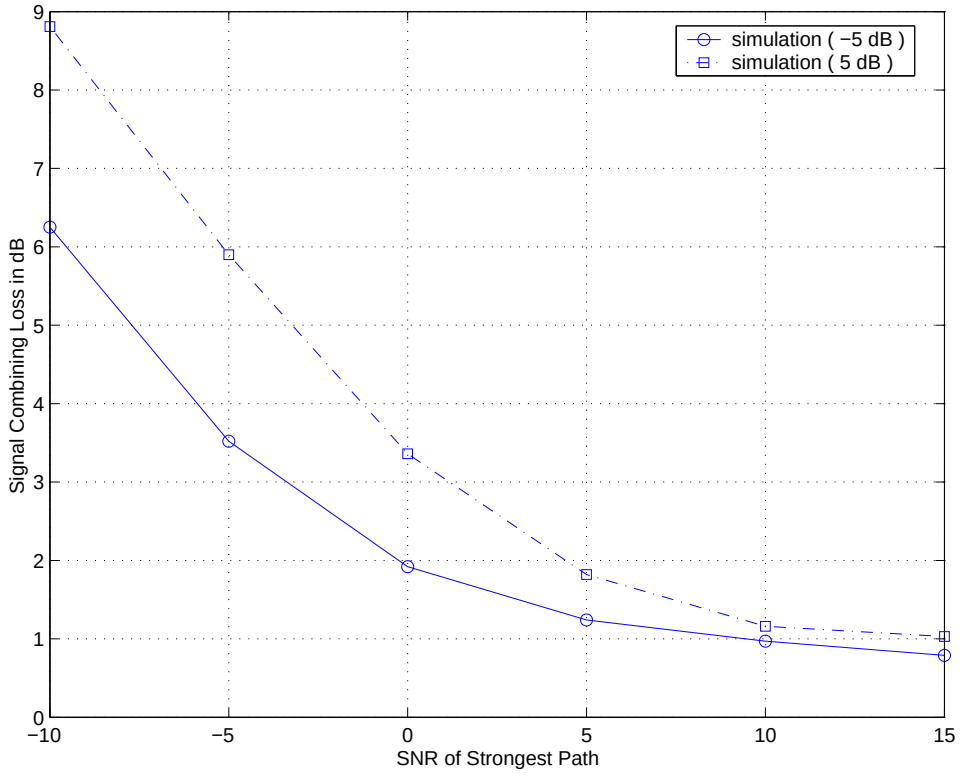

Figure 5.7: Signal combining loss with test design mismatch (multipath): K= 10 users, $L = 4$ paths per user and nominal false alarm probability $P_F = 0.0001$ and nominal missed detection probability $P_M = 0.001$

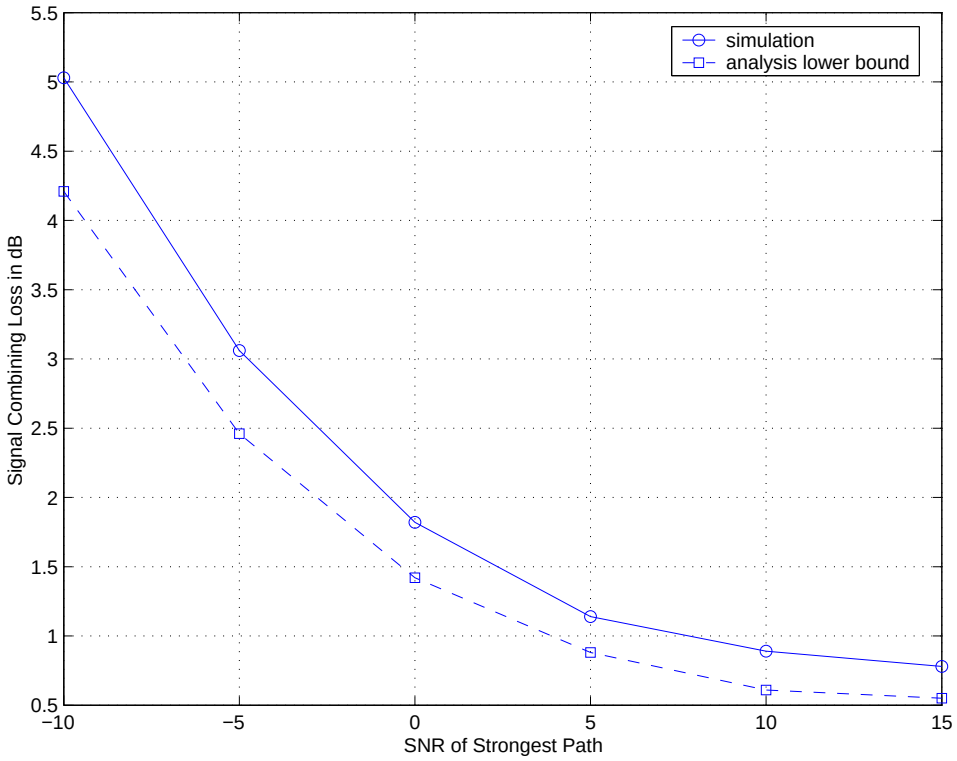

Figure 5.8: Signal combining loss (multipath): K = 3 users and L = 4 paths, nominal probability of detection $P_F = 0.0001$ and nominal missed detection probability $P_M = 0.001$, nominal SNR = -5 dB

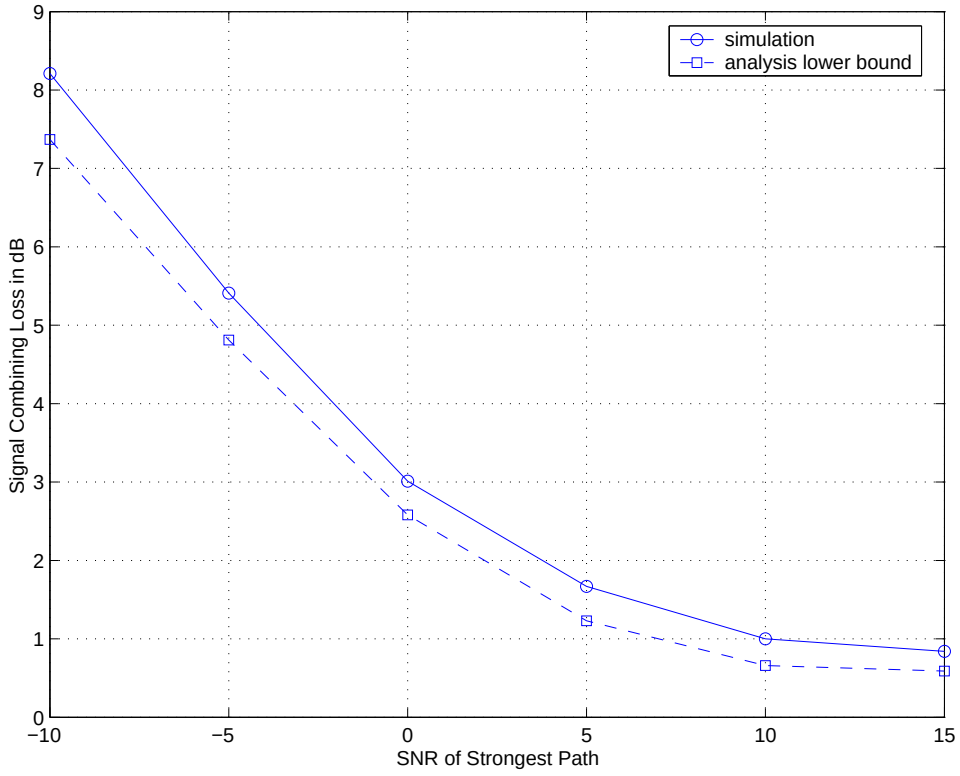

Figure 5.9: Signal combining loss (multipath): K= 3 users and L = 4 paths and nominal false alarm probability $P_F = 0.0001$ and nominal missed detection probability $P_M = 0.001$, nominal SNR = 5 dB

multipath diversity gain increases. This trend suggests that in higher SNR evniron-ment, more multipath will be available for fixed hypothesis testing thresholds, thereby, more multipath diversity gain is achieved.

5.5.6 Experiment Results of Practical RAKE Receiver

In this section, Monte Carlo simulation is performed to investigate the signal detection performance of practical RAKE receiver. The same CDMA system and receiver design in Section 5.5.4 are used. Signal combining loss of practical RAKE receivers with channel estimation is compared to the corresponding receivers with perfect channel knowledge. Since only one pilot symbol is used to estimate the instantaneous channel state information (CSI). Matched filter outputs give channel tap weights estimates. It is a special case of WMSA channel estimator by setting $N_p = 1, K = 1$ and $\beta_0 = 1$.

In Figure 5.12, 5.13, we compare the signal combining loss performance of P-MHT-MRC RAKE receiver to MHT-MRC RAKE receiver in low SNR receiver (nominal -5 dB SNR) and high SNR receiver (nominal 5 dB SNR), respectively. The signal combining loss of P-FS-MRC RAKE receiver is also plotted to give insight into channel estimation error. From these figures, we can observe that the signal combining loss of P-MHT-MRC RAKE receiver descreases as the SNR of strongest path increase and it is slightly higher than MHT-MRC RAKE receiver and the difference comes from the channel estimation error. From the triangular-labelled curve, we can see that the signal combining loss of P-FS-MRC RAKE receiver increases smoothly as SNR of

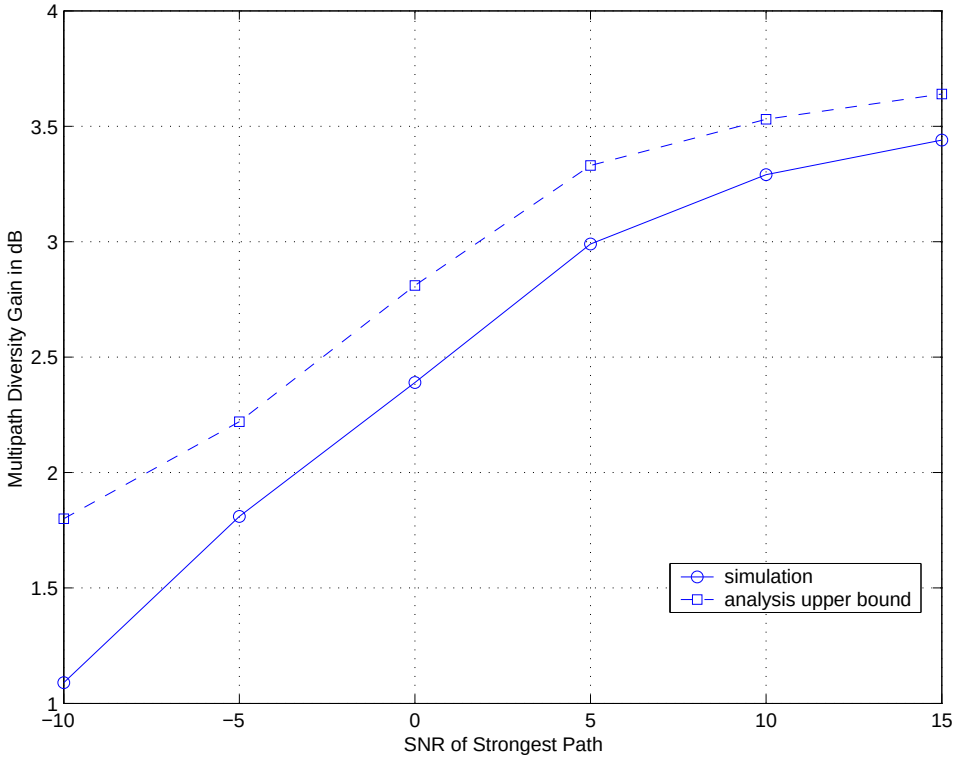

Figure 5.10: Multipath diversity gain: K = 3 users and L = 4 paths, nominal probability of detection $P_F = 0.0001$ and nominal missed detection probability $P_M = 0.001$, nominal SNR = -5 dB

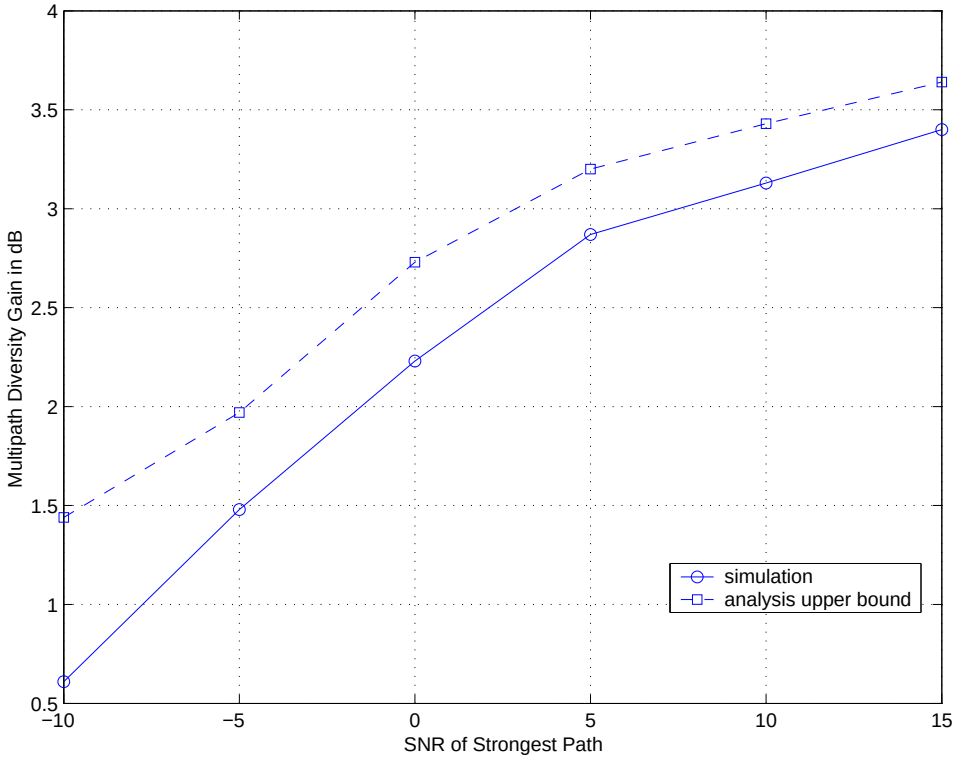

Figure 5.11: Multipath diversity gain: K= 3 users and L = 4 paths and nominal false alarm probability $P_F = 0.0001$ and nominal missed detection probability $P_M = 0.001$, nominal SNR = 5 dB

strongest path increases. It is explained by the fact that in high SNR environment, SNR estimation is less accurate, resulting in less accurate channel estimation. As a result, more performance loss is observed compared to the receiver with perfect channel knowledge.

Next, we examine the impact of observation window size for channel estimation on performance of practical MHT-MRC RAKE receiver. From Figures 5.14, 5.15, we observe that channel estimation is improved when the number of pilot symbol increases from 1 to 3 to 10 and the signal combining loss vs SNR of strongest path curves becomes more and more closer to that of MHT-MRC RAKE receiver with channel state information. This agrees with the general consensus that as the number of samples increases, the Crame-Rao lower bound of channel estimation error will decrease and asympototically goes to zero.

5.6 Chapter Summary

In this chapter, we have presented a detailed analysis of the performance of the proposed code acquisition algorithm in wideband CDMA multipath channels.

First, the exponential delaying multipath delay profile (MIP) provides a model for the wideband CDMA multipath channels. This model agrees strongly with the outdoor wideband CDMA channel sounding results in [2].

Secondly, the steady-state computation complexity saving and signal combining loss of the proposed tree-structured MHT-MRC RAKE receiver in multipath channel

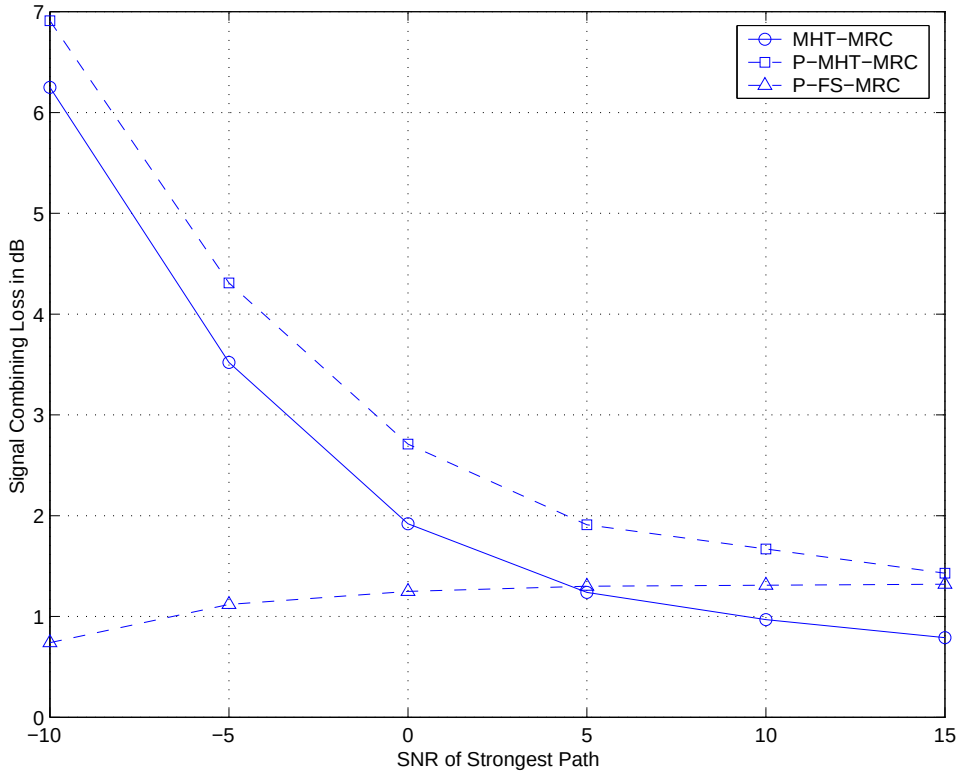

Figure 5.12: Signal combining loss in practical RAKE receiver: K= 10 users, $L = 4$ paths per user and nominal false alarm probability $P_F = 0.0001$ and nominal missed detection probability $P_M = 0.001$, test is designed to detect signal with $SNR = -5dB$

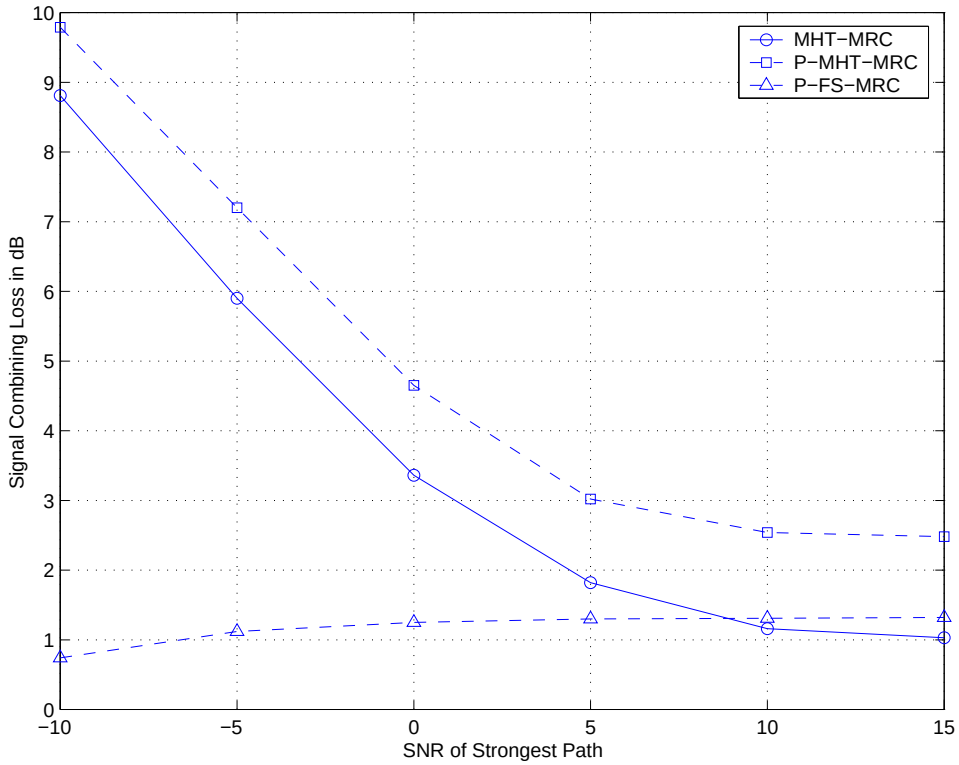

Figure 5.13: Signal combining loss in practical RAKE receiver: K= 10 users, $L = 4$ paths per user and nominal false alarm probability $P_F = 0.0001$ and nominal missed detection probability $P_M = 0.001$, test is designed to detect signal with $SNR = 5dB$

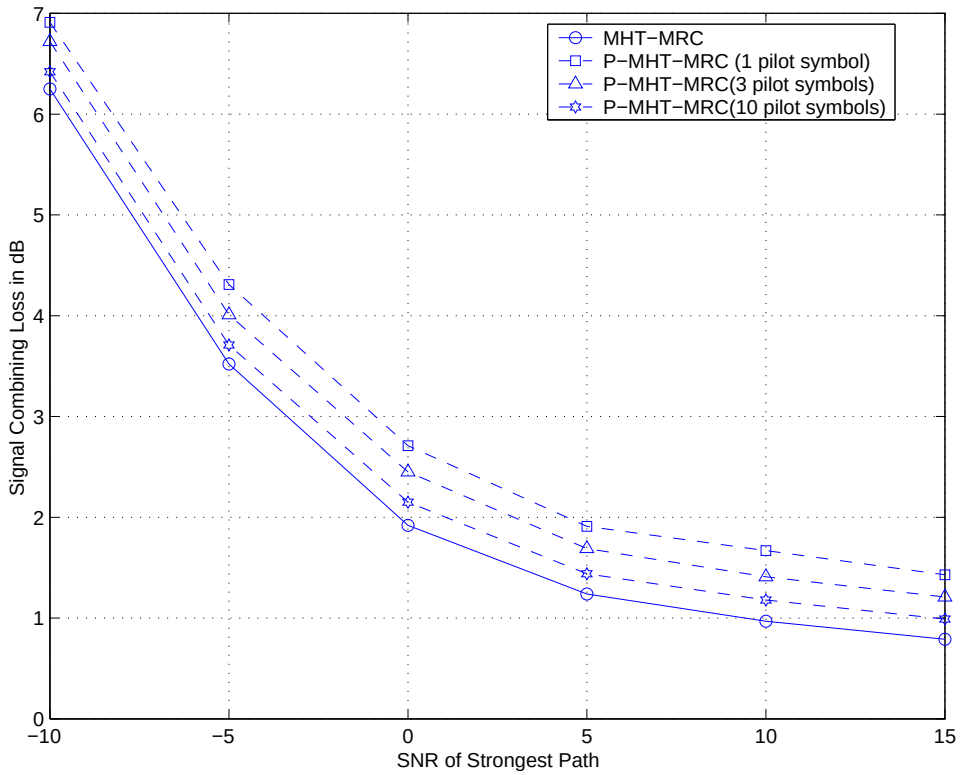

Figure 5.14: Signal combining loss in practical RAKE receiver: K= 10 users, $L = 4$ paths per user and nominal false alarm probability $P_F = 0.0001$ and nominal missed detection probability $P_M = 0.001$, test is designed to detect signal with $SNR = -5dB$. Observation window size $N_w = 1, 3, 10$ are compared.

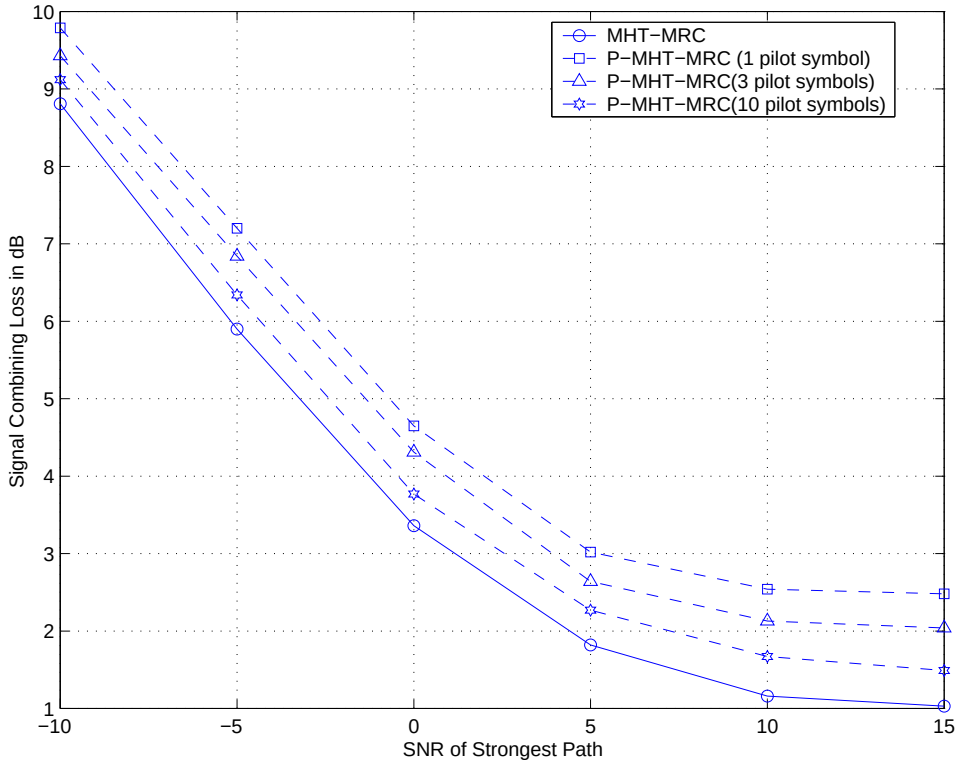

Figure 5.15: Signal combining loss in practical RAKE receiver: K= 10 users, $L = 4$ paths per user, nominal probability of false alarm $P_F = 0.0001$ and nominal missed detection probability $P_M = 0.001$, test is designed to detect signal with $SNR = 5dB$. Observation window size $N_w = 1, 3, 10$ are compared.

is analytically determined. The analysis is based on the assumption that channel state information is available at the receiver. The complexity savings in multipath channels is analyzed by the method of labelling the code tree with H_1 and H_0 hypotheses according to the multipath components at the receiver input. The signal combining loss is analyzed by enumerating the signal power of all the possible multipath detection results weighted by the corresponding probability of detection. The upper bound of the probability that each detection result occurs is given by applying De-Caen's union bound to reduce analysis complexity .

Thirdly, the experimental results obtained both by Monte Carlo simulation and by numerical analysis shows that the proposed algorithm can, at the expense of small signal combining loss, significantly reduce the complexity. In comparison to single-path case, a little increase in complexity and signal combining is observed. Moreover, the impact of test design mismatch on system performance is also investigated. The experimental results have shown that the complexity savings reach minimum at a specific SNR where no test design mismatch occurs.

Finally, we evaluate the performance of the proposed MHT-MRC RAKE receiver without perfect channel knowledge. We apply pilot-symbol-aided weighted multi-slot averaging (PSA-WMSA) technique to estimate channel tap weights of proposed MHT-MRC RAKE receiver. The effect of channel estimation on the signal detection performance is examined. The Monte Carlo simulation results show that the performance loss due to channel estimation error is small while significant complexity savings are still maintained. As the number of pilot symbols increases, the channel

estimation performance becomes better.

Chapter 6

Conclusions and Future Work

This chapter synmmarizes the major contributions in this thesis and presents possible future directions which could be extensions of the research work in this thesis.

6.1 Summary

This thesis has investigated low-complexity wideband CDMA receiver designs in multipath channels, where the code acquisition, RAKE combining and channel estimation are combined. We consider the synchronous CDMA uplink with time varying multipaths. The objective of this work is to propose a new receiver architecture to significantly reduce the receiver complexity with slight signal detection performance trade-off in comparison to the optimal full-search receiver.

We first developed a code acquisition algorithm for signal-path channels and analyzed the steady-state computation complexity and signal combining loss in Chapter

4. Assuming knowledge of users' spreading sequences, we formulate code acquisition in terms of multiple hypothesis testing for all the possible shfits of all PN codes in Section 4.4. The receiver employs truncated sequential decision-making in Section 3.4 as well as tree structured joint hypothesis testing in Section 4.5.2.

To extend the results we obtained in single-path systems to the case of multipath system, we generalize the analysis approach. In Section 5.2, the complexity savings in multipath channels is analyzed by the method of labeling the code tree by H_1 and H_0 hypotheses. By setting particular parameters, the method of analysis in multipath channels degenerates to that in single-path. By enumerating the signal power of all the possible multipath detection results weighted by the corresponding probability of detection, an explicit form of signal combining loss in provided. To reduce the complexity of analysis, De-Caen's union bound is used to approximate the signal detection performance.

To relax the assumption that channel state information is available at the receiver in the above analysis, we also combine the channel estimation with the proposed receiver. The matched filter outputs of survivor RAKE fingers are averaged over the observation windows to generate the estimated channel tap weights.

6.2 Future Work

Although this thesis has investigated the problem of joint code acquisition and channel estimation by using tree search, there are several issues that remain to be explored.

In this section, we discuss several important areas which require further study.

We use the chip synchronous multipath channel model in our study. This assumption assures that the delay estimation could be casted in multiple hypothesis testing framework. To give an more accurate performance analysis in realistic systems, it is necessary to extend our research results to chip-asynchronous environment where the practional portion of PN chip offsets of multipath propagation are considered. In [33] [80], it is shown that asynchronous environment can be expressed as a linear combination of two adjacent shifted version of user spreading codes. And in [11], an asynchronous CDMA discrete-time signal and system model is provided for the study of multiuser detection and array processing. It could also be utilized in the design and performance analysis of our proposed receiver structure in chip-asynchronous systems, which needs incisive investigations.

In our receiver design and performance analysis. we use the widely accepted Guassian approximation to model the statistic of the interference. The experimental results in Section 5.5.4 show that the performance in multipath channels is inferior to that in single-path channels. Multiple access interference (MAI) and interpath interference (IPI) deteriorate the performance. Therefore, more accurate modelling of interference is needed. If it is combined with joint multiuser detection and interference cancel techniques, the performance will be improved, which could be a furture research topic.

In our thesis work, we address code acquisition in pilot channels, where the tranmitted spread spectrum signal is not data modulated. It has low spectum efficiency since pilot symbols didn't transfer data information while they still occupy frequence bandwidth or time slot. Therefore, it will be benificial to extend our proposed code acquisition algorithm to data channels, where data modulation occurs.

6.3 Conclusion

The proposed sequential PN code acquisition algorithm in conjunction with tree-search detector significantly reduces receiver complexity. Both numerical analysis and Monte Carlo simulation results in single-path channels have shown that a large complexity reduction is achieved with only a moderate degradation in output SNR. Specifically, more than 97% complexity savings is obtained with only less than 1.3 dB signal combining loss in SNR of more than 5 dB or higher. When the design parameter P_M increases, lower complexity and latency is obtained while only a small increase in signal combining loss as performance tradeoff.

Analytic approach of performance analysis in single-path channels is also generalized to that in multipath channels. It has been demonstrated that a slight increase in complexity and signal combining loss occurs in comparison to those in single-path channels. The result of test design mismatch has shown that the complexity savings reaches minimum where no test design mismatch occurs.

As an extension, the performance of the code acquisition in conjunction with

channel estimation is also investigated through simulation. Additional Signal combining loss of less than 1.0 dB is observed in comparison to the receiver with perfect channel knowledge. When the observation window size increases, the signal detection performance converges to the receiver with perfect channel knowledge.

Bibliography

[1] Poor.H.Vincent, *An Introduction to signal detection and estimation*, Spring-Verlag, New York, 1994

[2] Noel.T.Tin,*An experimental systems for characterizing wideband CDMA wector channels and smart Antennas*, M.Sc. Thesis, Queen's University Dec. 2000

[3] Blostein.S.D. and Huang.T.S, "Detection small moving Oobjects in image sequences using sequential hypothesis testing", *IEEE Transactions on Signal Processing*, SP-39(7):1611–1629, 1991.

[4] Kim.I.G, Kim.K. and Lim.B.W, "A fast cell search algorithm for inter-cell asynchronous W-CDMA system using code hopping method", *In 1998 Global Telecommunication Conference*, Page 1373–1377, 1998.

[5] L. Aroian and D. Robison, "Direct methods for exact truncated sequential tests of the mean of a normal distribution", *Technometrics*, 11(4):661–675, 1969.

[6] S.Tantaratana and H.V.Poor, "Asympototic efficiencies of truncated sequential tests", *IEEE Transactions on Information Theory*, vol. IT-28, no. 6, pp. 911-923, 1982.

[7] Li Pan, *Base Station Baseband Digital Processing for Next Generation CDMA Systems*, M.SC. Thesis Queen's University, Nov.,1999.

[8] S.T.Stanley Chia and William C.Y.LEE, "A synchronized radio system without stable clock sources", *IEEE Personal Communication Magazine*, Apr.,2001 45-50

[9] F.Adachi, M. Sawahashi, and H. Suda, "Wideband DS-CDMA for next-generation mobile communications systems" *IEEE Communications Magazine*, Sept. 1998 pp56-69

[10] E.Dahlman, B.Gudmundson, M.Nilsson and J.Skold, "UMTS/IMT-2000 based on wideband CDMA", *IEEE Communications Magazine*, Sept. 1998, pp 70-80

[11] R. Wang, *Spatial-Temporal Signal Processing for Multiuser CDMA Communication Systems*, PhD Dissertation, Queen's University July. 1999

[12] G.S.Hosangadi, C.W.Baum, "Hybrid sequential acquisition schemes for noncoherent chip-asynchronous DS/SS systems", *In 1998 Vehicular Technology Conference*, May 1998, CDROM

[13] G.S.Hosangadi, C.W.Baum, "Hybrid sequential acquisition schemes for noncoherent chip-asynchronous DS/SS systems", *In 1999 Vehicular Technology Conference*, May. 1999, VTC CD-ROM

[14] Y.H.Lee, S.Tataratana, "Sequential acquisition of PN sequences for DS/SS communications: design and performance", *IEEE Journal on Selected Areas in Communications*, vol.10, No 4, May 1992

[15] S.Tataratana, A.W.Lam, P.J.Vincent, "Noncoherent sequential acquisition of PN sequences for DS/SS communications with/without channel fading", *IEEE Transactions on Communications*, vol.43, No 2/3/4, February/March/April 1995

[16] K.Y.Wong, *Multi-user interference cancellation in DS-CDMA with forward error correction*, Queen's University, Sep 2000

[17] R.L.Peterson, R.R.Ziemer and D.E.Borth, *Introduction to Spread Spectrum Communications*, Prentice Hall 1995

[18] M.K.Simon, J.K.Omura, R.A.Scholtz, B.K.Levit, *Spread Spectrum Communications, Volumn III* Computer Science Press 1984

[19] C.H.Deng, *A Burst Mode PN Acquisition Processor for Direct Sequence Spread-Spectrum*, M.Sc. thesis, University of California at Los Angeles, 1998

[20] J.W.Chung, I.Jang, J.Lee, Y.Jeong, "Effect of code acquisition design parameters in the IMT-2000 system", *In 2000 Vehicular Technology Conference*

[21] H.Andoh, M.Sawahashi,and F.Adachi, "Channel estimation using time-multiplexed pilot symbols for coherent Rake combining for DS-CDMA mobile radio", *IEICE Transactions on Communnications* vol. E81-B, July 1998, pp. 1365-1373

[22] S.Abeta, M.Sawahashi, and F.Adachi, "Performance comparison between time-multiplexed pilot channel and parallel pilot channel for coherent rake combining in DS-CDMA mobile radio", *IEICE Transactions on Communnications* vol. E81-B, July 1998, pp. 1417-1425

[23] S.Fukumoto, M. Sawahashi, and F.Adachi, "Matched filter-based RAKE combiner for wideband DS-CDMA mobile radio", *IEICE Transactions on Communnications* vol. E81-B, July 1998, pp. 1384-1391

[24] E.H.Dinan and B.Jabbari, "Spreading codes for direct sequence CDMA and wideband CDMA cellular networks", *IEEE Communications Magazine*, Sept. 1998 pp48-54

[25] R.C. Dixon, *Spread Spectrum Systems with Commercial Application*, Wiley,1994

[26] J.G.Proakis, *Digital Communication 3rd edition*, Mcgraw-Hill, Toronto,1995

[27] T.S.Rappaport, *Wireless Communications - Principles and Practices*, Prentice Hall, Toronto, 1996

[28] G.Aliftiras, *Recevier Implementations for a CDMA cellular System*, Mater's Thesis, Virginia Polytechnic Institute and State University, July 1996

[29] S.Parkvall, "User performance variability in DS-CDMA systems - long vs short spreading sequences", *IEEE Global Telecommunication Conference* vol. 2, Nov 1998, pp. 2543-2548

[30] H.S.Chang, Y.W.Park and Y.H.Lee, "DS-SS acquisition based on simultanous search and verification", *In 1998 IEEE Vehicular Technology Conference*, 1998,

[31] U.Cheng, "Performance of a class of parallel spread spectrum acquisition schemes in the the presence of data modulation", *IEEE Transaction on Communications*, Vol.38 pp. 596-604, May 1998,

[32] R.R.Rick, L.B.Milstein, "Parallel acquisition in mobile DS-CDMA systems", *IEEE Transaction on Communications*, Vol. 45, pp. 1466-1476 November 1997,

[33] W.Zha, S.D.Blostein, "Improved CDMA multiuser receivers robust to timing errors", *IEEE International Conference on Acoustics, Speech, and Signal Processing*, CD-ROM May 2001,

[34] Samina Chowdhury, Michael D. Zoltowski "Structured MMSE equalization for synchronous CDMA with sparse multipath channels", *IEEE International Conference on Acoustics, Speech, and Signal Processing* , CD-ROM May 2001,

[35] G.L.Stuber. *Principle of Miobile Communication*, Kluwer Academic, 1996

[36] W.C.Y.Lee, "Overview of cellular CDMA", *IEEE Transactions on Vehicular Technology* , Vol.40, No 2, 291- 302 May 1991

[37] R.L.Pickholtz, L.B.Milstein, D.L.Schilling, "Spread spectrum for mobile communications", *IEEE Transactions on Vehicular Technology*, Vol.40, No 2, 313-322 May 1991

[38] K.S.Gilhousen, I.M.Jacobs, R.Padovani, A.J.Viterbi, L.A.Weaver, C.E.Wheatly, "On capacity of a cellular CDMA systems", *IEEE Transactions on Vehicular Technology* , Vol.40, No 2, pp 303-312 May 1991

[39] W.R.Braun, "PN acquisition and tracking performance in DS/CDMA systems with symbol length spreading sequences", *IEEE Transactions on Communication* , Vol.45, No 12, pp 1595-1601 Nov 1997

[40] Y.H.Lee, S.J.Kim, "Sequence acquisition of DS-CDMA systems employing Gold sequences", *IEEE Transactions on Vechicular Technology* , Vol.495, No 6, pp 2397-2407 Nov 2000

[41] M.Z.Win, G.Chrisikos, N.R.Solleberger, "Performance of RAKE reception in dense multipath channel: implicaition of spreading bandwidth and selection diversity order", *IEEE Transactions on Selected Areas in Communication* , Vol.18, No 8, pp 1516-1525 Aug 2000

[42] J.Wang, J.Chen, "Performance of wideband CDMA sytems with complex spreading and imperfect channel estimation", *IEEE Transactions on Selected Areas in Communication* , Vol.18, No 8, pp 1516-1525 Aug 2000

[43] R.Price, P.E.Green, "A communication techniques for multipath channel", *Proceedings of the IRE* , pp 555-570 March 1958

[44] D.G.Brennan, "Linear diversity combining techniques", *Proceedings of the IRE* ,vol 47,pp 1075-1102 1958

[45] H.Holma,A.Toskala, *WCDMA based for UMTS: Radio Access for Third Generation Mobile Commuications*, John Wiley

[46] M.L.Moher,J.H.Lodge, "TCMP-a modulation and coding strategy for Rician fading channel", *IEEE Transactions on Selected Areas in Communication*, vol SAC-7,pp 1347-1355 Dec.1989

[47] J.K.Cavers, " An analysis of pilot symbol assisted modulation for Rayleigh fading channels", *IEEE Transactions on Selected Areas in Communication*, vol VT-40,pp 689-693 Nov.1991

[48] S.S.Sampei and T.Sunaga, " Rayleigh fading compensation for QAM in land mobile radio communications", *IEEE Transactions on Vehicular Technology*, vol VT-42,pp 137-147 May.1993

[49] F.Ling, " Coherent detection with reference-symbol based estimation for direct sequence CDMA uplink communication", IN *1993 Vehicular Technology Conference*, pp 400-403 New Jersey USA, May.1993

[50] S.Ariyavisitakull, " Signal and interference statistics of a CDMA system with feedback power control - part II", *IEEE Transaction on Communications* ,vol 42,pp 597-60 Feb/Mar./Apr. 1994

[51] S.Seo, T. dohi, F.Adachi, " SIR-based transmit power control of reverse link for coherent DS-CDMA mobile radio", *IEICE Transactions on Communications* ,vol E81-B,pp 1508-1516, July 1998

[52] Y.Honda and K.Jamal, " Channel estimation based on time-multiplexed pilot symbols ", IEICE Technical Report RCS96-70 ,August 1996

[53] S.Tantaratana, H. V.Poor, "Asymptotic relative efficiencies of Truncated Sequential Tests", *IEEE Transactions on Information Theory*, vol. IT-28, no. 6, pp911-923, 1982

[54] A.Wald, *A., Sequential Analysis* New York: Wiley, 1947

[55] H.Liu, M.D.Zoltowski, "Blind equalization in antenna array CDMA systems", *IEEE Transactions on Signal Processing*, Vol 45, No 1, Jan. 1997

[56] Qualcomm, *http://www.qualcomm.com/technology*

[57] 3GPP, *ftp://ftp.3gpp.org/specs/latest/*

[58] S.Moshavi, "Multi-user detection for DS-CDMA Communications", *IEEE Communications Magazine*, Oct. 1996

[59] S.Verdu, "Minimum probability of error for asynchronous gaussian multiple access channels", *IEEE Transactions on Information Theory*, vol.IT-32, no. 1, Jan. 1986, pp.85-96

[60] L.B.Milstein, "Wideband code division multiple access", *IEEE Transactions on Selected Areas in Communication*, vol 18,No 8, pp 1344-54 Aug. 2000

[61] F.Adachi, M.Sawahashi, " Wideband wireless access based on DS-CDMA", *IEICE Transactions on Communnications* ,vol E81-B,pp 1305-1316, July 1998

[62] S.Verdu, *Multiuser detection*, Cambridge University Press, 1998

[63] J.C.Liberti, T.S.Rappaport, *Smart antennas for wireless communications: IS-95 and Third Generation CDMA Applications*, Prentice Hall, 1999

[64] L.E. Miller, J.S.Lee, *CDMA engineering systems handbook*, Artech House Publisher, Oct. 1998

[65] A.J. Viterbi, *CDMA: Principles of Spread Spectrum Communications*, Addison-Wesley, 1995

[66] W.C.Jakes, *Microwave mobile communications*, Wiley-Interscience Publication, 1974

[67] J.D.Parsons, *The mobile radio propagation channel*, Halstead Press, 1992

[68] H.Suzuki, " A statistical model for urban radio propagation ", *IEEE Transactions on Communications*,vol 25, pp 673-680, 1977

[69] Wu et al., " On channel model parameters for microcellular CDMA systems", *IEEE Transactions on Vehichular Technology*,vol 45, pp 706-711, 1995

[70] A.F.Molisch, " Statistical properties of the rms delay spread of mobile radio channels with independent Rayleigh-fading paths", *IEEE Transactions on Vehichular Technology*,vol 45, pp 201-205, 1996

[71] A.Papoulis, *Probability, Random Variable and Stochastic Processes*, McGRAW-HALL, New York, 1991

[72] D.de Caen,"A lower bound on the probability of a union", *Discrete Mathematics*, 169(1997) 217-220

[73] O.Shin, K.B.Lee, "Utilization of multipaths for spread-Spectrum code acquisition in frequency-selective rayleigh fading channels", *IEEE Transaction on Communications*, Vol. 49, pp. 734-743 April 2001,

[74] A. Bhargave, R.J.P.Figueiredo, T.Eltoft, " A detection algorithm for the V-BLAST system", *In 2001 Global Telecommunication Conference*, CD-ROM

[75] Lei Wei, "Near optimum tree-search detection schemes for bit-synchronous multiuser CDMA systems over Gaussian and two-path Rayleigh-fading channels ", *IEEE Transaction on Communications*, Vol. 45, No 6, pp. 691-700 June 1997,

[76] Z. Xie, C.K. Rushforth, R.T.Short, T.K.Moon, " Joint signal detection and parameter estimation in multiuser communications", *IEEE Transaction on Communications*, Vol. 41, No 7, pp. 1208-1215, Augest 1997,

[77] M.Benthin, K.Kammeyer, " Influence of channel estimation on the performance of a coherent DS-CDMA system", *IEEE Transaction on Vehicular Technology*, Vol. 46, No 2, pp. 262-267, May 1997,

[78] G. Chen, X.Yu, " Adaptive channel estimation and dedicated pilot power adjustment based on the fading-rate measurement for a pilot-aided CDMA systems", *IEEE Journal on Selected Areas in Communications*, Vol. 19, No 1, pp. 132-138, January 2001,

[79] M.Benthin, K.Kammeyer, " Analysis of a simple successive interference cancellation scheme in DS/CDMA system,", *IEEE Journal on Selected Areas in Communications*, Vol. 12, No 5, pp. 796-807, June 1994,

[80] Wei Zha, Steven Blostein, "Soft-Decision Successive Interference Cancellation CDMA Receiver with Amplitude Averaging and Robust to Timing Errors", *In 2001 Global Telecommunication Conference*, CD-ROM